Faculty of Engineering

ENGINEERING PROJECT
ME4098

Performance Analysis of High Bypass Turbofan Engine

Zeki Çobanoğlu
150416035

Abstract

Over the 60 years, turbofan engines have undergone numerous advancements, emerging as the primary propulsion system utilized in both civilian airliners and military aircraft. Combining the strengths of turboprop engines, such as high propulsive efficiency and thrust, with those of turbojet engines, including high flight speed and altitude capabilities, turbofans have become indispensable. To meet the demands for increased thrust to propel wide-body airliners, enhance payload capacity and range, and bolster maneuverability for military aircraft, ongoing advancements in turbofan technology are imperative. These advancements aim to achieve larger thrust output, reduce noise and emissions, and enhance fuel efficiency. Accomplishing these objectives involves strategies such as augmenting the bypass ratio (BR), fan pressure ratio (FPR), overall pressure ratio (OPR), and turbine inlet temperature (TIT), as well as adopting innovative materials, manufacturing techniques, and cooling methods for turbines and combustion chambers. Such modifications have yielded enhancements in thermal, propulsive, and overall efficiencies, leading to reductions in thrust-specific fuel consumption (TSFC) and increases in specific thrust. This project undertakes a parametric investigation of a high bypass ratio turbofan engine, akin to the Trent 1000-A, a product of Rolls-Royce Aviation Company, with performance analysis conducted using GSP(Gas Turbine Simulation Program) and MATLAB codes.

Table of Contents

1 Introduction

Over the last sixty years, turbofan technology has undergone a profound evolution, spurred by the ever-growing demands for increased thrust, improved fuel efficiency, and reduced environmental impact in terms of emissions and noise levels. This evolution has been marked by significant advancements across key performance parameters, including bypass ratio, fan pressure ratio, overall pressure ratio, turbine inlet temperature, and the adoption of state-of-the-art materials and manufacturing methodologies. As a consequence, turbofan engines have not only propelled aircraft to unprecedented levels of performance. In this final year project, a parametric study of the Rolls-Royce Trent 1000-A is presented as a high bypass ratio turbofan engine.

The Rolls-Royce Trent 1000 stands as a British turbofan engine featuring a three-spool design, derived from earlier iterations within the Trent series. Renowned for its reliability and performance, the Trent 1000 notably propelled the Boeing 787 Dreamliner on commercial flights. The layout and the view of the engine are shown in **Figure 1** and **Figure 2** respectively.

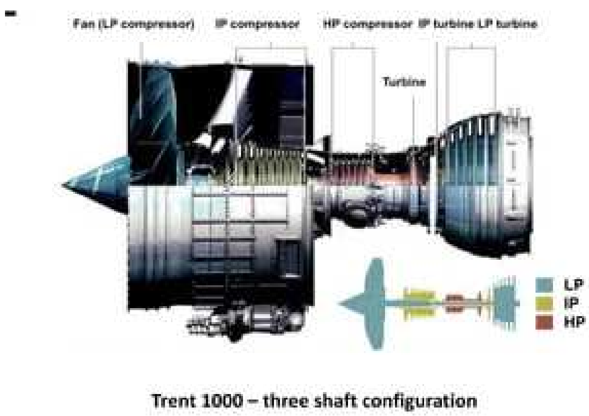

Figure 1:Layout of unmixed three-spool engine (Trent 1000)

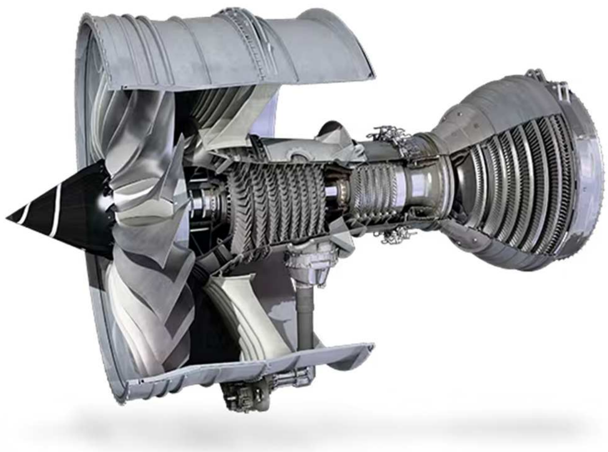

Figure 2:View of the unmixed three-spool engine (Trent 1000)

The three-spool engine is composed of low-pressure, intermediate-pressure, and high-pressure shafts running at different speeds(**N_1**, **N_2**, and **N_3**). The fan and the low-pressure turbine (LPT) compose the low-pressure shaft. The intermediate shaft is composed of an intermediate-pressure compressor (IPC) and an intermediate-pressure turbine (IPT). The high-pressure shaft is also composed of a high-pressure compressor (HPC) and a high-pressure turbine (HPT). Rolls-Royce was the first aero engine manufacturer to design, develop, and produce the three-spool turbofan engine. The Rolls-Royce RB211 was the first three-spool engine to enter service (1972). Later, several manufacturers developed and manufactured this type of engine. The layout of Rolls-Royce RB211 is shown in **Figure 3**.

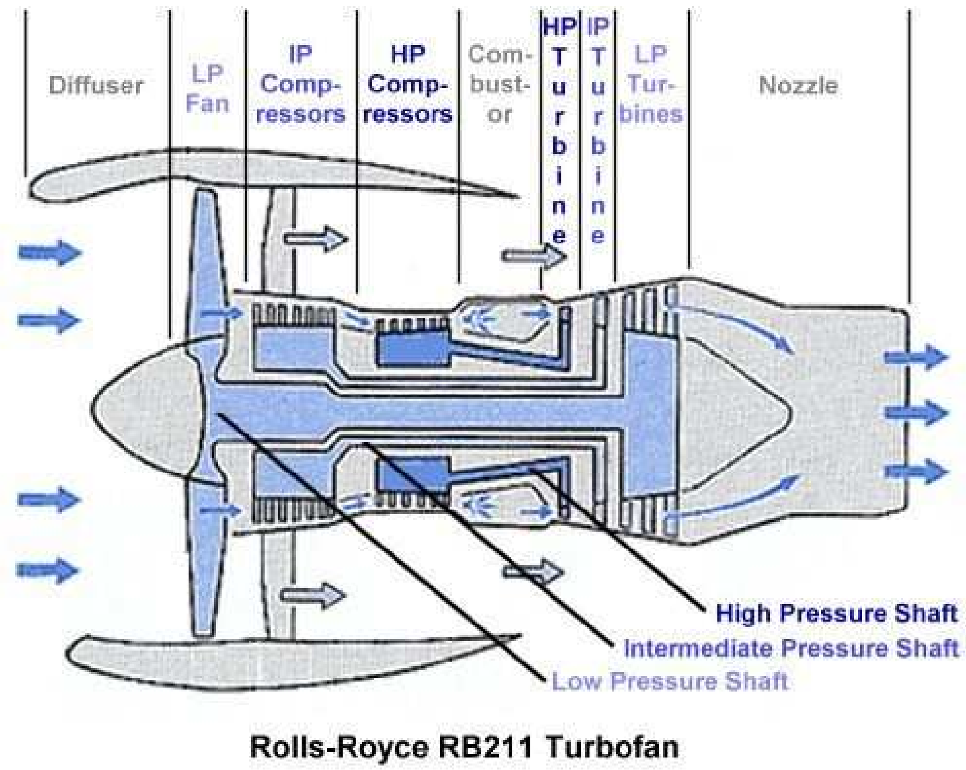

Figure 3:Layout of Rolls-Royce RB211

The graphs that represent TSFC(Thrust specific fuel consumption) and OPR(Overall pressure ratio) for Trent series engines by date of operation are shown in **Figure 4** and **Figure 5** respectively.

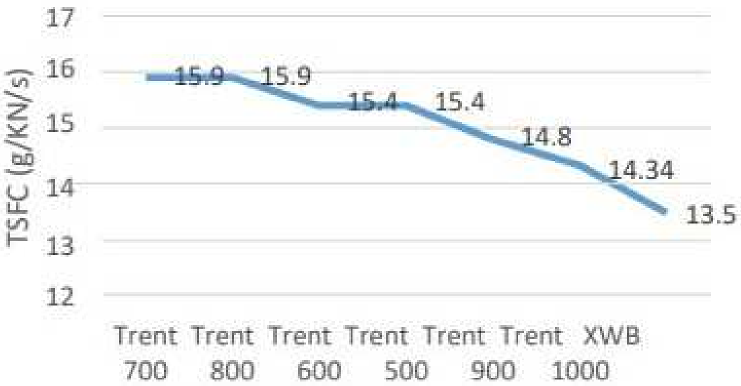

Figure 4:Development in TSFC for Trent engines arranged by date of operation

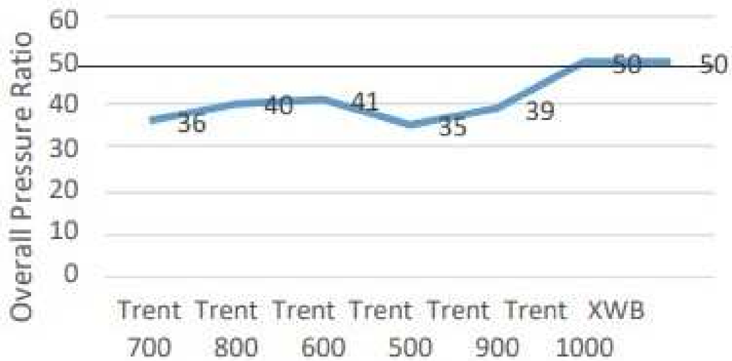

Figure 5:Development in OPR for Trent engines arranged by date of operation

1.1 Aims and Objectives

This project aims to determine the temperature, the pressure, and the entropy based on thermodynamic analysis in each section to make a parametric study and exergy analysis.

The objective of this project is to perform the parametric study by varying bypass ratio, pressure ratio, altitude, fuel eating value, mach number, ambient temperature, ambient pressure, and turbine inlet temperature(TIT) to get better thrust, thrust specific fuel consumption(TSFC), thermal efficiency, propulsive efficiency, overall efficiency and the second law efficiency; and make the exergy analysis for each operating conditions based on thermodynamics 2nd law.

2 Literature Review

Some of the related topics to the project are reviewed and summarized.

2.1 Basic Gas Turbine Operation

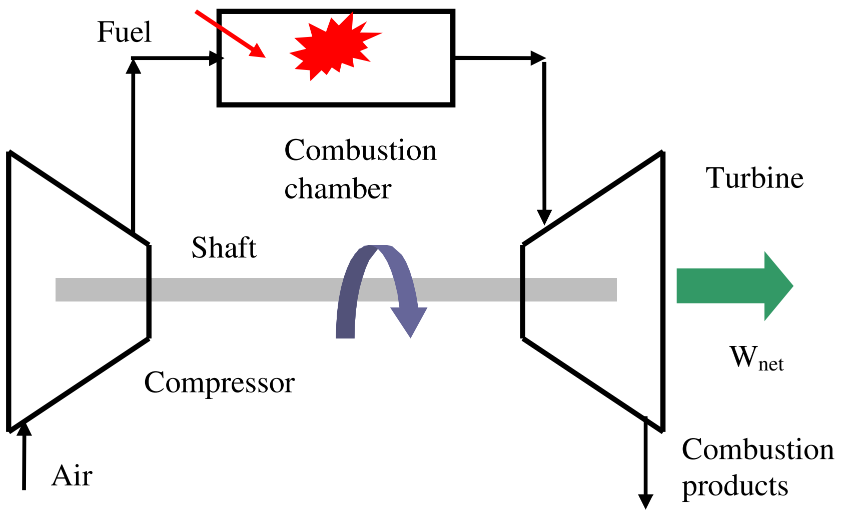

Figure 6: Schematic for an open gas-turbine cycle

-Fresh air enters the compressor at ambient temperature where its pressure and temperature are increased.

-The high pressure air enters the combustion chamber where the fuel is burned at constant pressure.

-The high temperature (and pressure) gas enters the turbine where it expands to ambient pressure and produces work.

2.2 Brayton Cycle

Brayton cycle is the ideal cycle for gas-turbine engines in which the working fluid undergoes a closed loop. That is the combustion and exhaust processes are modeled by constant-pressure heat addition and rejection, respectively.

The Brayton ideal cycle is made up of four internally reversible processes:

1-2	isentropic compression (in compressor)
2-3	const. pressure heat-addition (in combustion chamber)
3-4	isentropic expansion (in turbine)
4-1	const. pressure heat rejection (exhaust)

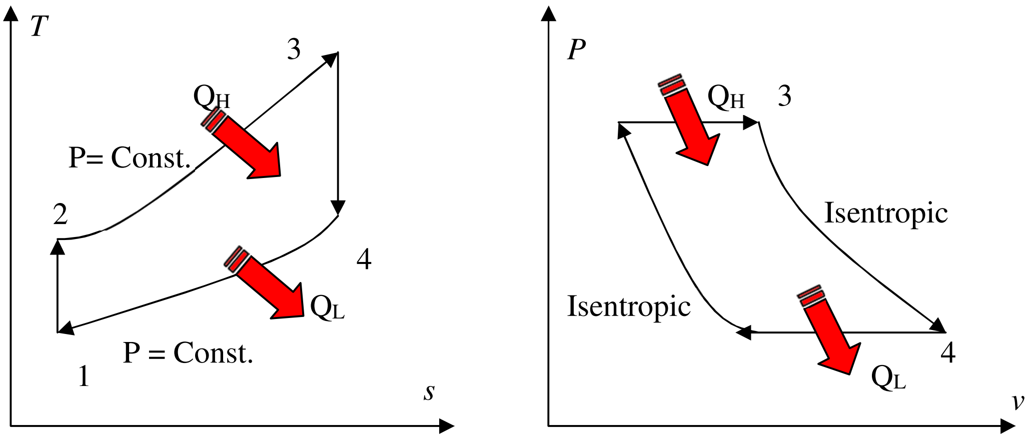

Figure 7: T-s and P-v diagrams for ideal Brayton cycle.

Thermal efficiency for the simple Brayton cycle is:

$$n_{Brayton} = 1 - \frac{q_{out}}{q_{in}} = 1 - \frac{(T_4 - T_1)}{(T_3 - T_2)} = 1 - \frac{T_1\left(\frac{T_4}{T_1} - 1\right)}{T_2\left(\frac{T_3}{T_2} - 1\right)}$$

$$\frac{T_2}{T_1} = \left(\frac{P_2}{P_1}\right)^{\frac{\gamma-1}{\gamma}} = \left(\frac{P_3}{P_4}\right)^{\frac{\gamma-1}{\gamma}} = \frac{T_3}{T_4}$$

Thus,

$$n_{Brayton} = 1 - \frac{1}{(r_P)^{\frac{\gamma-1}{\gamma}}}$$

$$r_P = \frac{P_2}{P_1} = \frac{P_3}{P_4}$$

Where where $\mathbf{r_P}$ is called the pressure ration and $\boldsymbol{\gamma} = \mathbf{c_p / c_v}$ is the specific heat ratio.

Specific heats can be represented by the specific heat ratio, which is

$$c_p = \frac{R}{\gamma - 1} \quad \left(\frac{kJ}{kg}\right)$$
$$c_v = \frac{R\gamma}{\gamma - 1} \quad \left(\frac{kJ}{kg}\right)$$
$$where\ R = ideal\ gas\ constant \quad \left(\frac{kJ}{kg}\right)$$

Under the cold-air-standard assumptions, the thermal efficiency of an ideal Brayton cycle depends on the pressure ratio of the gas turbine and the specific heat ratio of the working fluid. The thermal efficiency increases with both of these parameters, which is also the case for actual gas turbines. A plot of thermal efficiency versus the pressure ratio is given in **Figure 8** for **γ =1.4**, which is the specific-heat-ratio value of air at room temperature.

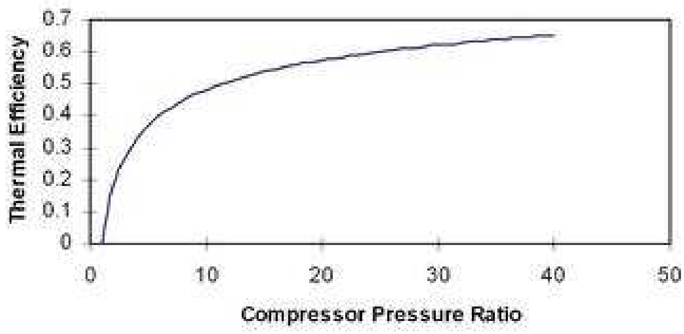

Figure 8:Thermal efficiency of the ideal Brayton cycle as a function of pressure ratio

The highest temperature in the cycle occurs at the end of the combustion process, and it is limited by the maximum temperature that the turbine blades can withstand. This also limits the pressure ratios that can be used in the cycle. The maximum temperature in the cycle $\mathbf{T_3}$ is limited by metallurgical conditions because the turbine blades cannot sustain temperatures above **1300 K**. Higher temperatures (up to **1600 K** can be obtained with ceramic turbine blades).

The air in gas turbines performs two important functions: It supplies the necessary oxidant for the combustion of the fuel, and it serves as a coolant to keep the temperature of various components within safe limits. The second function is accomplished by drawing in more air than is needed for the complete combustion of the fuel. In gas turbines, an air–fuel mass ratio of 50 or above is not uncommon. Therefore, in a cycle analysis, treating the combustion gases as air does not cause any appreciable error. Also, the mass flow rate through the turbine is greater than that through the compressor, the difference being equal to the mass flow rate of the fuel. Thus, assuming a constant mass flow rate throughout the cycle yields conservative results for open-loop gas-turbine engines.

The two major application areas of gas-turbine engines are aircraft propulsion and electric power generation. When it is used for aircraft propulsion, the gas turbine produces just enough power to drive the compressor and a small generator to power the auxiliary equipment. The high-velocity exhaust gases are responsible for producing the necessary thrust to propel the aircraft.

2.2.1 The Ideal Brayton Cycle For Gas Turbine Engines

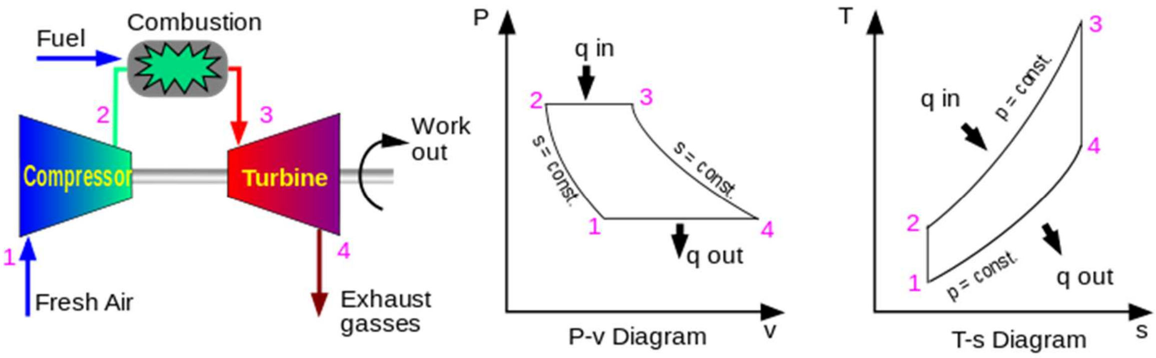

-1-2:Isentropic Compression
-2-3:Constant-Pressure Heat Addition(for combustion)
-3-4:Isentropic Expansion
-4-1:Constant-Pressure Heat Rejection(for exhaust)

2.2.2 Deviation of Actual Gas-Turbine Cycles from Idealized Ones

The actual gas-turbine cycle differs from the ideal Brayton cycle on several accounts. For one thing, some pressure drop during the heat-addition and heat-rejection processes is inevitable. More importantly, the actual work input to the compressor is more, and the actual work output from the turbine is less because of irreversibilities. The deviation of actual compressor and turbine behavior from the idealized isentropic behavior can be accurately accounted for by utilizing the isentropic efficiencies of the turbine and compressor as

$$n_{compressor} = \frac{w_s}{w_a} \cong \frac{h_{2s} - h_1}{h_{2a} - h_1}$$
$$n_{turbine} = \frac{w_a}{w_s} \cong \frac{h_3 - h_{4a}}{h_3 - h_{4s}}$$

where states **2a** and **4a** are the actual exit states of the compressor and the turbine, respectively, and **2s** and **4s** are the corresponding states for the isentropic case, as illustrated in **Figure 9.**

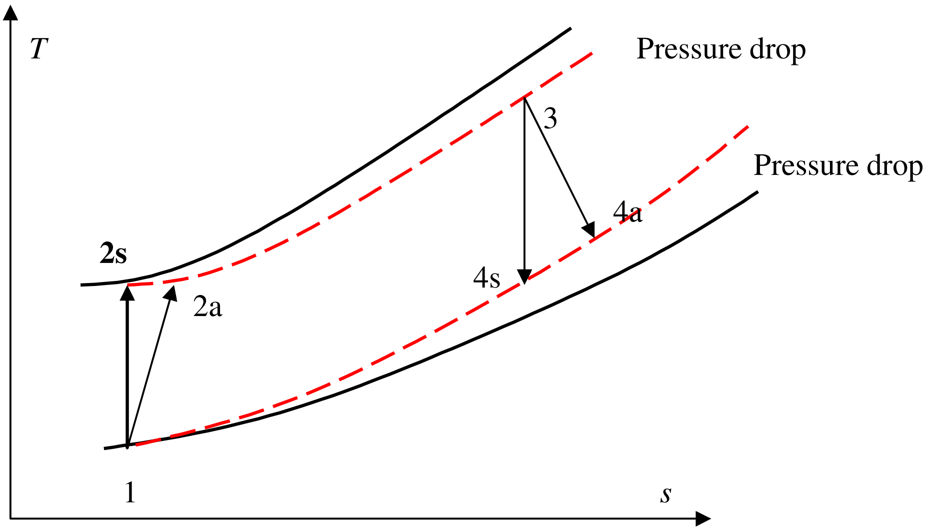

Figure 9: T-s diagram for the actual Brayton cycle.

2.2.3 Ideal Jet-Propulsion Cycles

Gas-turbine engines are extensively used to power aircraft due to their light weight, compact size, and high power-to-weight ratio. These engines operate on an open cycle known as a jet-propulsion cycle. The ideal jet-propulsion cycle differs from the simple ideal Brayton cycle because the gases are not expanded to the ambient pressure within the turbine. Instead, they are expanded to a pressure where the turbine produces just enough power to drive the compressor and auxiliary equipment, such as a small generator and hydraulic pumps. This means that the net work output of a jet-propulsion cycle is **zero**. After exiting the turbine at a relatively high pressure, the gases are accelerated through a nozzle to generate the thrust needed to propel the aircraft. Additionally, aircraft gas turbines typically operate at higher pressure ratios, often exceeding 40, and the fluid first passes through a diffuser where it slows down and its pressure increases before entering the compressor.

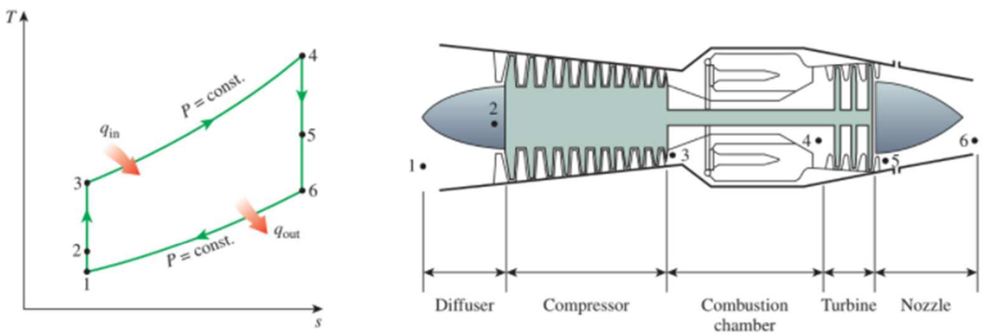

FIGURE 9–48
Basic components of a turbojet engine and the *T-s* diagram for the ideal turbojet cycle.

Figure 10:Basic components of a turbojet engine and the T-s diagram for the ideal turbojet engine

Aircraft achieve propulsion by accelerating a fluid in the direction opposite to their motion. This can be done by either slightly accelerating a large mass of fluid, as in propeller-driven engines, or by significantly accelerating a small mass of fluid, as in jet or turbojet engines. **Figure 10** illustrates a schematic of a turbojet engine and the T-s diagram of the ideal turbojet cycle. In the diffuser, the pressure of the air increases slightly as it decelerates. The air is then compressed by the compressor before being mixed with fuel in the combustion chamber. In the combustion chamber, the fuel-air mixture burns at constant pressure.

The high-pressure and high-temperature combustion gases partially expand in the turbine, producing enough power to drive the compressor and other equipment. Finally, the gases expand in a nozzle to the ambient pressure and leave the engine at a high velocity.In the ideal case, the turbine work is assumed to equal the compressor work. Also, the processes in the diffuser, the compressor, the turbine, and the nozzle are assumed to be isentropic. In the analysis of actual cycles, however, the irreversibilities associated with these devices should be considered. The effect of the irreversibilities is to reduce the thrust that can be obtained from a turbojet engine.

The thrust developed in a turbojet engine is the unbalanced force that is caused by the difference in the momentum of the low-velocity air entering the engine and the high-velocity exhaust gases leaving the engine, and it is determined from Newton's second law. The pressures at the inlet and the exit of a turbojet engine are identical (the ambient pressure); thus, the net thrust developed by the engine can be approximated by,

$$F \cong (\dot{m}V)_{exit} - (\dot{m}V)_{inlet} = \dot{m}(V_{exit} - V_{inlet}) \quad (kN)$$

where $\mathbf{V_{exit}}$ is the exit velocity of the exhaust gases and $\mathbf{V_{inlet}}$ is the inlet velocity of the air, both relative to the aircraft. Thus, for an aircraft cruising in still air, $\mathbf{V_{inlet}}$ is the aircraft velocity. In reality, the mass flow rates of the gases at the engine exit and the inlet are different, the difference being equal to the combustion rate of the fuel. However, the air–fuel mass ratio used in jet-propulsion engines is usually very high, making this difference very small. Thus, $\dot{m}$ is taken as the mass flow rate of air through the engine. For an aircraft cruising at a constant speed, the thrust is used to overcome air drag, and the net force acting on the body of the aircraft is zero. Commercial airplanes save fuel by flying at higher altitudes during long trips since air at higher altitudes is thinner and exerts a smaller drag force on aircraft.

The power developed from the thrust of the engine is called the propulsive power $\dot{W}_p$, which is the propulsive force (thrust) times the distance this force acts on the aircraft per unit time, that is, the thrust times the aircraft velocity

$$\dot{W}_P = FV_{aircraft} = \dot{m}(V_{exit} - V_{inlet})V_{aircraft} \quad (kW)$$

The net work developed by a turbojet engine is **zero**. Thus, we cannot define the efficiency of a turbojet engine in the same way as stationary gas-turbine engines. Instead, we should use the general definition of efficiency, which is the ratio of the desired output to the required input. The desired output in a turbojet engine is the power produced to propel the aircraft $\dot{W}_P$, and the required input is the heating value of the fuel $\dot{Q}_{in}$. The ratio of these two quantities is called the **overall efficiency** and is given by

$$n_{overall} = \frac{propulsive\ power}{energy\ input\ rate} = \frac{\dot{W}_P}{\dot{Q}_{in}}$$

Overall efficiency is a measure of how efficiently the thermal energy released during the combustion process is converted to propulsive energy. The remaining part of the energy released shows up as the kinetic energy of the exhaust gases relative to a fixed point on the ground and as an increase in the enthalpy of the gases leaving the engine. It is often convenient to break overall efficiency into two parts: **thermal efficiency** and **propulsive efficiency**, where

$$n_{thermal} = \frac{rate\ of\ production\ of\ kinetic\ energy}{energy\ input\ rate} = \frac{\left(\frac{\dot{m}_e u_e^2}{2} - \frac{\dot{m}_0 u_0^2}{2}\right)}{\dot{Q}_{in}}$$

$$n_{propulsive} = \frac{propulsive\ power}{rate\ of\ production\ of\ kinetic\ energy} = \frac{\dot{W}_P}{\left(\frac{\dot{m}_e u_e^2}{2} - \frac{\dot{m}_0 u_0^2}{2}\right)}$$

Thus,

$$n_{overall} = n_{thermal} * n_{propulsive}$$

Thermal efficiency of a jet engine is a measure of how effectively the engine converts the energy in the fuel into kinetic energy.

Propulsive efficiency of a jet engine is a measure of how effectively the engine converts the kinetic energy of the exhaust gases into useful thrust.

2.3 Modifications to Turbojet Engines

The first airplanes built were all propeller-driven, with propellers powered by engines essentially identical to automobile engines. The major breakthrough in commercial aviation occurred with the introduction of the turbojet engine in 1952. Both propeller-driven engines and jet-propulsion-driven engines have their own strengths and limitations, and several attempts have been made to combine the desirable characteristics of both in one engine. Two such modifications are the propjet engine and the turbofan engine.

The most widely used engine in aircraft propulsion is the turbofan (or fanjet) engine wherein a large fan driven by the turbine forces a considerable amount of air through a duct (cowl) surrounding the engine, as shown in **Figures 8** and **9**. The fan exhaust leaves the duct at a higher velocity, enhancing the total thrust of the engine significantly. A turbofan engine is based on the principle that for the same power, a large volume of slower-moving air.

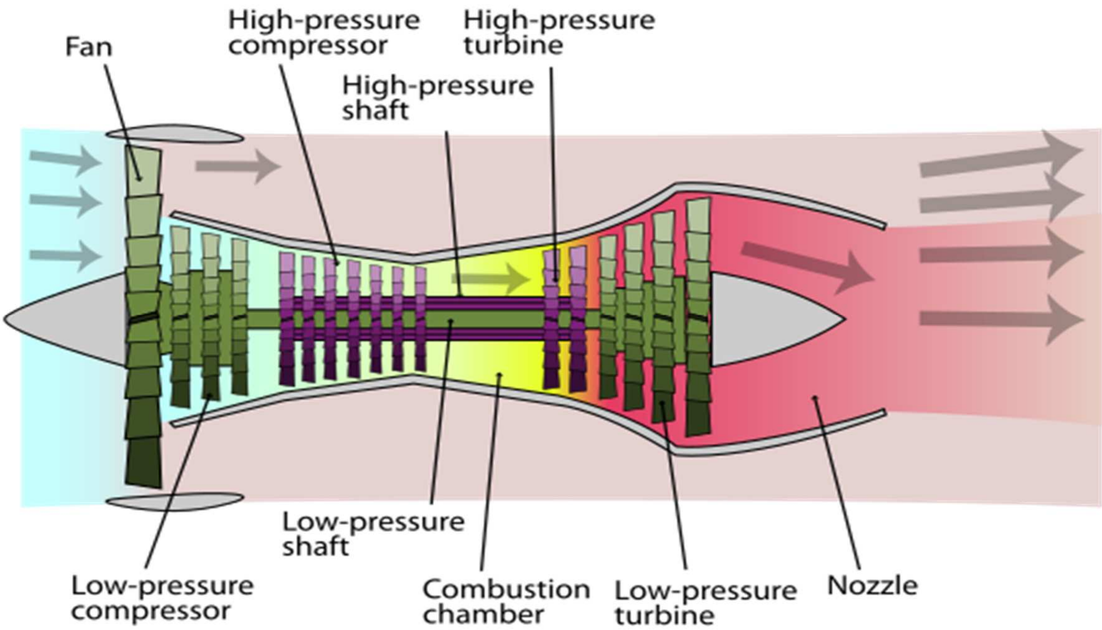

Figure 11: The schematic view of turbofan engine

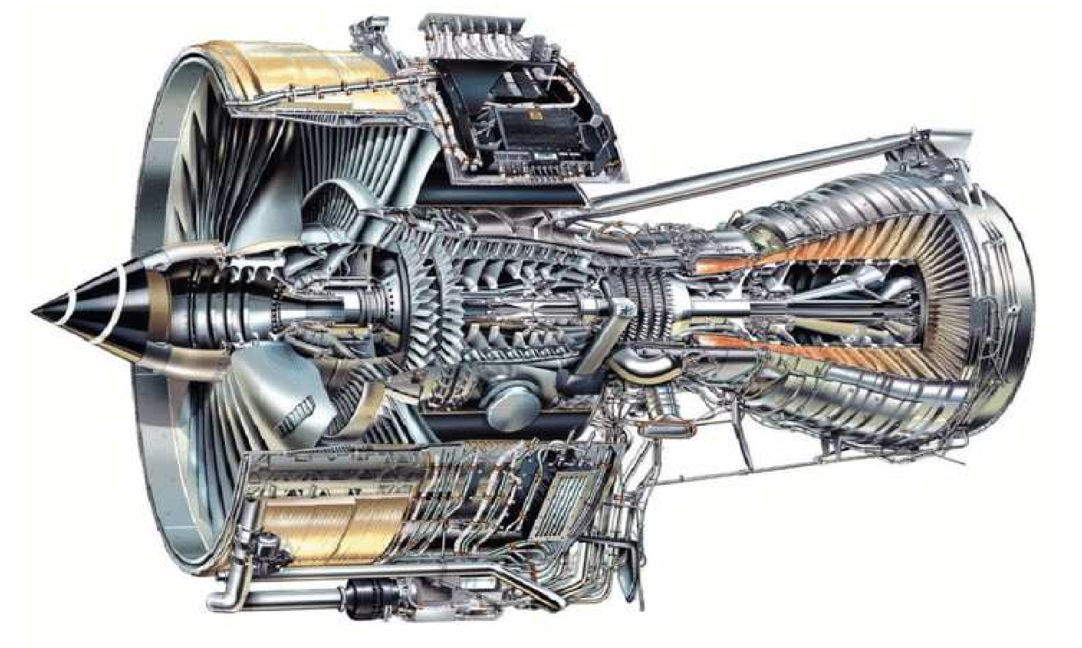

Figure 12:A view of three-shaft turbofan engine

The turbofan engine on an airplane can be distinguished from the less efficient turbojet engine by its fat cowling covering the large fan. All the thrust of a turbojet engine is due to the exhaust gases leaving the engine at about twice the speed of sound. In a turbofan engine, the high-speed exhaust gases are mixed with the lower-speed air, which results in a considerable reduction in noise.

New cooling techniques have resulted in considerable increases in efficiencies by allowing gas temperatures at the burner exit to reach over **1500C**, which is more than **100C** above the melting point of the turbine blade materials. Turbofan engines deserve most of the credit for the success of jumbo jets that weigh almost **400,000 kg** and are capable of carrying over **400 passengers** for up to a distance of **10,000 km** at speeds over **950 km/h** with less fuel per passenger mile.

2.4 Second-Law Analysis of Brayton Cycle

The ideal Brayton cycle is only internally reversible, and the cycle may involve irreversibilities external to the system. A second-law analysis of these cycles reveals where the largest irreversibilities occur and where to start improvements.

The exergy destruction for steady-flow systems can be expressed,in rate form,as

$$\dot{X}_{dest} = T_0 + X_{gen} = T_0\left(\dot{S}_{out} - \dot{S}_{in}\right) = T_0\left[\sum_{out} \dot{m}s - \sum_{in} \dot{m}s - \frac{\dot{Q}_{in}}{T_{b,in}} + \frac{\dot{Q}_{out}}{T_{b,out}}\right](kW)$$

or, on a unit–mass basis for a one-inlet, one-exit steady-flow device, as

$$x_{dest} = T_0 s_{gen} = T_0\left(s_e - s_i - \frac{q_{in}}{T_{b,in}} + \frac{q_{out}}{T_{b,out}}\right) \quad \left(\frac{kJ}{kg}\right)$$

where subscripts **i** and **e** denote the inlet and exit states, respectively.

The exergy destruction of a cycle is the sum of the exergy destructions of the processes that compose that cycle. The exergy destruction of a cycle can also be determined without tracing the individual processes by considering the entire cycle as a single process and using one of the relations above. Entropy is a property, and its value depends on the state only. For a cycle, reversible or actual, the initial and the final states are identical; thus se 5 si . Therefore, the exergy destruction of a cycle depends on the magnitude of the heat transfer with the high- and low-temperature reservoirs involved and on their temperatures. It can be expressed on a unit–mass basis as

$$x_{dest} = T_0\left(\sum \frac{q_{out}}{T_{b,out}} - \sum \frac{q_{in}}{T_{b,in}}\right) \quad \left(\frac{kJ}{kg}\right)$$

For a cycle that involves heat transfer only with a source at $\mathbf{T_H}$ and a sink at $\mathbf{T_L}$, the exergy destruction becomes

$$x_{dest} = T_0\left(\frac{q_{out}}{T_L} - \frac{q_{in}}{T_H}\right) \quad \left(\frac{kJ}{kg}\right)$$

The second law efficiency of the system can be determined by

$$\eta_{II} = \frac{\dot{X}_{recovered}}{\dot{X}_{expended}} = 1 - \frac{\dot{X}_{destroyed}}{\dot{X}_{expended}}$$

or in unit-mass basis,

$$\eta_{II} = \frac{x_{recovered}}{x_{expended}} = 1 - \frac{x_{destroyed}}{x_{expended}}$$

where

$$\dot{X}_{expended} = \left(1 - \frac{T_L}{T_H}\right)\dot{Q}_{in}$$

$$x_{expended} = x_{heat,in} = \left(1 - \frac{T_L}{T_H}\right)q_{in}$$

$$\dot{Q}_{in} = heat\ input\ rate$$

$$q_{in} = heat\ input\ in\ unit\ mass\ basis$$

The exergies of a fluid stream φ at any state can be determined from

$$\varphi = (h - h_0) - T_0(s - s_0) + \frac{V^2}{2} + gz \quad \left(\frac{kJ}{kg}\right)$$

where subscript "**0**" denotes the state of the surroundings.

2.5 Turbofan Engines

Turbofan engine was designed to avoid the unwanted properties of subsonic flight efficiency of turbojet engines.

An obvious way to improve turbojet engine efficiency is to raise the burner temperature to improve Carnot efficiency and fit the nozzle and larger compressor. This process increases the thrust, but the exhaust gases exit the engine with a high velocity which consumes additional engine power.

Due to the above-given reasons, the jet engine consumes a high amount of fuel. These engines have slow speed and low efficiency. Therefore, scientists designed the turbofan to avoid extra fuel consumption and improve fuel economy.

Working principle and components of turboshaft engines as a turbojet engine(or as a gas turbine engine) will be reviewed and summarized.

2.5.1 Turbofan Engine Working Principle

Any gas turbine operates with intake, compression, expansion, and exhaust cycle. As a fundamental of the gas turbine working principle, in each gas turbine type, the compressor first compresses the air and this air is then driven through the combustion engine. Fuel is continuously burned for high temperature and high-pressure gas processing. What a gas turbine is doing is expanding the gas generated by the combustor into the turbine and thus generating the rotary energy that is used by the compressor on the preceding stage. There is an output shaft for the remaining energy

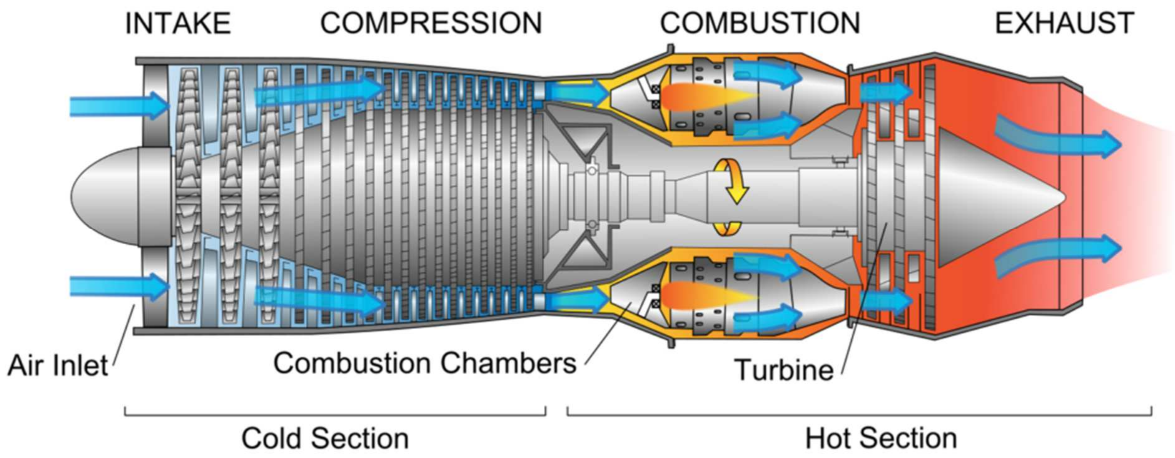

Figure 13:General Turbojet Engine

Turbofan engines can be connected to the front of a turbojet engine with a duct fan. The fan then creates an extra push, helps the engine to cool and reduces the engine noise output.

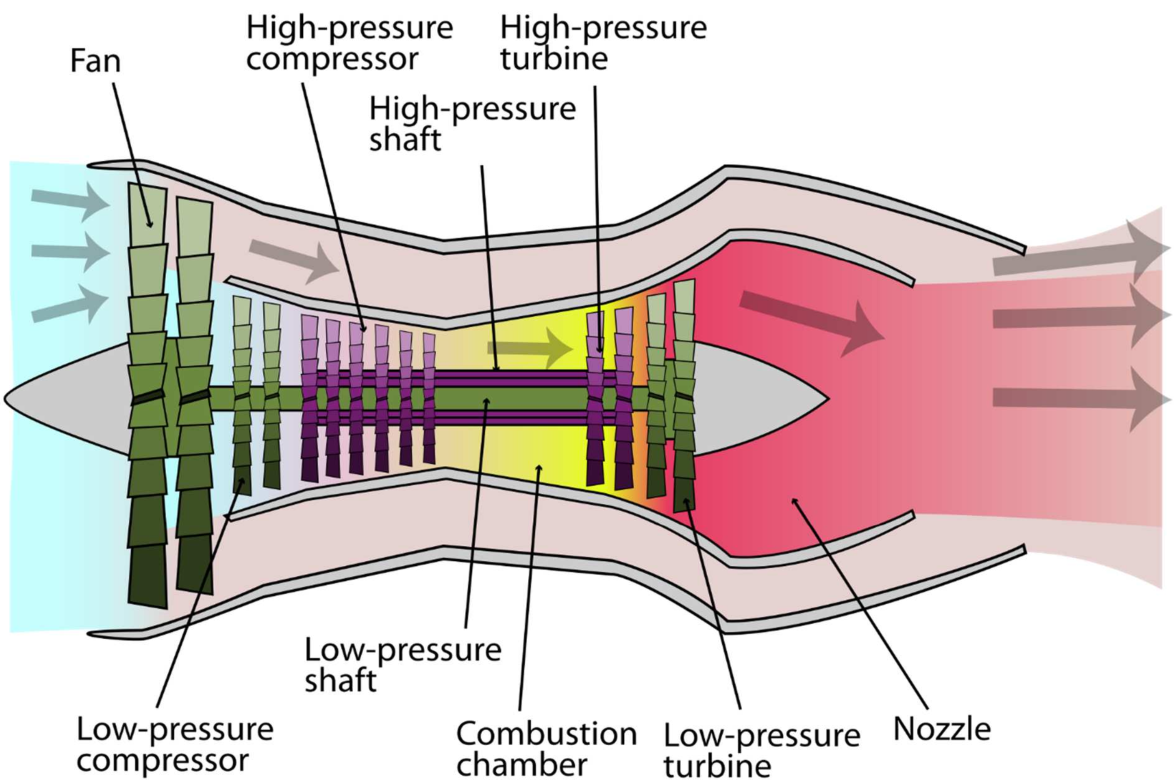

Figure 14:General Turbofan Engine

A turbofan engine works in the following way:

- Firstly, the air is sucked inside the engine via a fan, and air divides into two various paths.
- Some part of the air enters the engine core where combustion takes place while the remaining part of the air (bypass air) moves outside of the engine core by a duct.
- After suction, the air enters into a low-pressure compressor which increases the pressure of the air according to the requirements and sends it into a high-pressure compressor.
- When the low compressed air comes into the high-pressure compressor, it further compresses the air up to very high pressure and also high increases its temperature.
- The high-pressure compressor makes the air temperature so high that when it touches the fuel in the combustion chamber, the combustion process starts itself.
- After combustion of the air-fuel mixture, the combusted gas enters into the low-pressure and high-pressure turbine.
- After entering the turbine, the hot gases expand into the turbine and strike the turbine blades. The turbine blades extract enough power from the combusted mixture to move the low-pressure compressor and fan. The remaining power of the combusted mixture is sent toward the exhaust nozzle.
- When the exhaust gases enter the nozzle, the nozzle converts their pressure energy into speed and converts them into very high-speed gases.
- When high-speed gases are discharged from the nozzle into the atmosphere, they generate thrust, which moves the airplane forward.
- The speed of the air flowing by the fan is slightly faster than the speed of the air flowing free. This flow of air is known as the bypass or fan airflow.

2.5.2 Turbofan Engine Components

The most common components of turbofan engines(shown in **Figure 14**) are given below:

1. Fan
2. Compressor
3. Turbine
4. Shaft
5. Combustion chamber
6. Nozzle

1.Fan

This part helps the engine to generate thrust.

A fan is the first component of turbofans. Air flows through the engine's two parts. Some portion of the air directs to the core of the engine, where ignition occurs. The remaining air (referred to as "bypass air") flows through a ducted fan on the external side of the engine's core. This bypass air creates additional thrust, cools the engine, and calms it down by removing the engine exhaust gases. In the latest fanjet, maximum engine thrust is created by bypass air.

2.Compressor

The main objective of the compressor is to increase the pressure and temperature of the air.

A turbofan engine uses two compressors (low-pressure compressor and high-pressure compressor) for air compression. These are centrifugal compressors. This centrifugal compressor has a series of rotating blades shaped like an airfoil to compress and accelerate the air. The major parts of the centrifugal compressor are the impeller, inlet port, diffuser, and discharge port.As air passes across the compressor, the impeller blades of the compressor become smaller during this process. They add energy into the air and compress it. Due to this process, the pressure and temperature inside the combustion chamber increase. The compressor has a series of fixed or stator blades. These stator blades receive high-velocity air by the impeller and convert this velocity into air pressure.

3.Combustion Chamber

A combustion chamber is a place inside the engine where the combustion takes place. When the air leaves the compressor and arrives inside the combustion chamber, it mixes with the fuel and ignites.It sounds simple,but in reality,it is a highly complex procedure. This is because the burner must continue providing stable burning of the air-fuel mixture while the air flows by the burner at a very high speed.

4.Turbine

As the combusted air leaves the combustion chamber, it enters the turbine. A turbine is a series of aerodynamic blades that are very similar to compressor blades. As high-velocity hot air runs through the blades of the turbine, they absorb additional energy from the air, causing the turbine to rotate completely and rotates the engine shaft connected with it.

The turbine shaft is also connected to the fan and compressor. As the turbine spins, the compressor and fans at the front of the turbofan engine continue to suck in more air and quickly mix with the fuel and burn.

The turbines require an additional fan (as shown in the above diagram), which results in more giant turbines and larger temperature and pressure drops, which results in smaller nozzles. This signifies that the core escape velocity will decrease.

5.Nozzle

The nozzle is the last part of the fanjet engine.This component of the engine is vital because it generates thrust by expelling exhaust gases into the atmosphere with high speed, which helps the airplane move forward.

This process works according to Newton's third law. According to this law, each action has an equal but opposite direction reaction. Therefore, when the nozzle expels the air at high speed, the air also exerts an equal but opposite directional force and moves the aircraft forward.

2.6 Fuel Consumption

To move an airplane through the air, a propulsion system is used to generate thrust. The amount of thrust an engine generates is important. But due to the main objective of this project the amount of fuel used to generate that thrust is more important.Engineers use an efficiency factor, called **thrust specific fuel consumption** rather than using only ‘’fuel consumption’’ to characterize an engine's fuel efficiency. "Thrust specific fuel consumption" is quite a mouthful, so engineers usually just call it the engine's **TSFC**.

The fuel consumption of **TSFC** is "how much fuel the engine burns each hour." The specific of **TSFC** is a scientific term meaning "divided by mass or weight." In this case, specific means "per pound (Newton) of thrust." The thrust of **TSFC** is included to indicate that we are talking about gas turbine engines. There is a corresponding brake specific fuel consumption (**BSFC**) for engines that produce shaft power. Gathering all the terms together, **TSFC** is the mass of fuel burned by an engine in one hour divided by the thrust that the engine produces. The units of this efficiency factor are mass per time divided by force (in English units, pounds mass per hour per pound; in metric units, kilograms per hour per Newton).

Mathematically, **TSFC** is a ratio of the engine fuel mass flow rate $\dot{\boldsymbol{m}}_{\boldsymbol{f}}$ to the amount of thrust **F** produced by burning the fuel:

$$TSFC = \frac{\dot{m}_f}{FN} \quad \left(\frac{kg}{N * hr}\right)$$

If we divide both numerator and denominator by the engine airflow $\dot{\boldsymbol{m}}_{\boldsymbol{0}}$, we obtain another form of the equation in terms of the air to fuel ratio **AF**, and the specific thrust **SFN**.

$$TSFC = \frac{1}{(AF) * SFN} \quad \left(\frac{kg}{N * hr}\right)$$

$$\boldsymbol{Low\,TSFC = High\,Efficiency}$$

$$\boldsymbol{High\,TSFC = Low\,Efficiency}$$

2.7 Specific Thrust

Another part of the literature studies was to study the specific thrust. Studies that have been made (both numerically and analytically) shows that fan pressure ratio is highly dependent on specific thrust, **SFN**. It also worth to mention that the determination of an optimum $\mathbf{FPR_{op}}$ is very important as this value together with **TIT**, **BPR** and **OPR** will ensure minimum **SFC**.Specific thrust can be formulated as

$$SFN = \frac{FN}{\dot{m}_0} \quad \left(\frac{N * s}{kg}\right)$$

Where

$$\dot{m}_0 = total\ mass\ flow\ rate$$

2.8 Conceptual Design Tools

Today with the current technology, other more newly developed programs as **MATLAB** and **Simulink** are being more considered when it comes to engine design, mainly because of the current requirements in system development. Such advanced programs in software modelling with more suitable graphical interfaces make it easier to control the whole conceptual design process of an engine. Engine parameters can easily be assessed with these tools.

GSP(Gas Turbine Simulation Program) stands as a versatile modeling tool with the ability to simulate virtually any configuration of a gas turbine engine, accommodating external loads such as water brakes, pumps, and generators. Its foundation lies in 0D modeling, where thermodynamic cycles are represented in an averaged manner across component interfaces. Through a process of component model stacking, GSP constructs the thermodynamic cycle of the targeted engine based on input configurations, typically derived from the engine's design or established reference points. Essential information for configuring the cycle, such as turbine and compressor maps, is readily accessible from manufacturers or various online sources.

Beyond its role as a performance predictor, GSP excels in conducting parameter sensitivity analyses. These include assessments of ambient condition effects during flight, installation losses, impacts of engine malfunctions (including control system failures), and evaluations of component deterioration. Analysis input relies on the model configuration, allowing users to specify parameters like fuel flow to predict generated power, or vice versa. Simulation output is presented in a table within the component property window, offering data on gas conditions (temperatures, pressures, mass flows, areas, speeds, etc.) and gas composition (with access to gas species through a comprehensive thermo-chemical gas properties model). The results of simulations can be exported as tab-separated files for further custom analysis, such as comparing simulation data with measurements from operating equipment.

3 Methodology

3.1 Design Constraints and Assumptions

-Steady operating conditions exist.

-Besides thermodynamic modelling in GSP,the working fluid(air) is assumed as an ideal gas.

-Specific heats are not constant.

-Bleed flows are neglected.

-Potential energy changes are negligible.

-Kinetic energy changes are essential,so they are taken into account.

3.2 Engine Schematic

The main objective is to model the turbofan engine and determine the specific heat ratio, temperature, pressure, and entropy based on thermodynamic analysis at every section from 1 to 14 as shown in **Figure 15** for a three-shaft turbofan engine, and to make a performance and exergy analysis of the engine using the given input data in the following **Table 1** and **Table 2**.

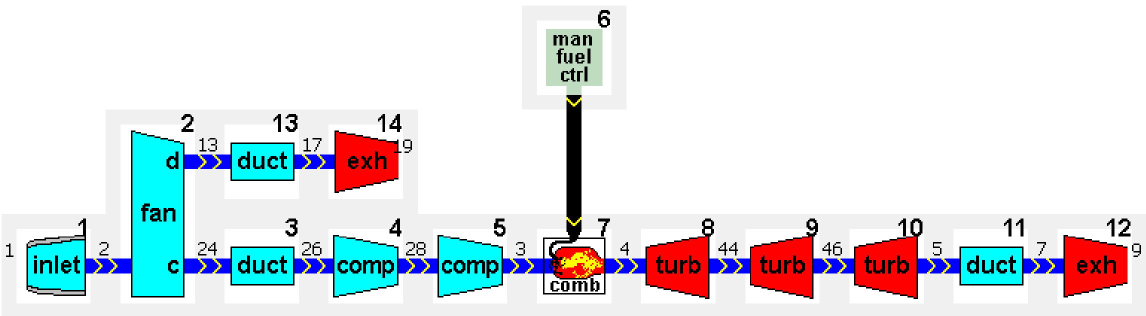

Figure 15:Three-shaft turbofan engine schematic

3.3 Thermodynamic Analysis

-Ambient conditions

$$P_1 = Ambient\ pressure$$

$$T_1 = Ambient\ temperature$$

$$P_{01} = Total\ ambient\ pressure$$

$$T_{01} = Total\ ambient\ temperature$$

$$M = Flight\ mach\ number$$

$$P_{01} = P_1\left(1 + \frac{\gamma - 1}{2} * M^2\right)^{\frac{\gamma}{\gamma-1}}$$

$$T_{01} = T_1\left(1 + \frac{\gamma - 1}{2} * M^2\right)$$

-Inlet

$$P_{02} = n_{int} * P_{01}$$

$$T_{02} = T_{01}$$

-Fan

$$P_{03} = \pi_{fan} * P_{02}$$

$$T_{03} = T_{02}\left(1 + \frac{\pi_{fan}{}^{\frac{\gamma-1}{\gamma}} - 1}{n_{fan}}\right)$$

-Cold core duct

$$P_{04} = \pi_{ccd} * P_{03}$$

$$T_{04} = T_{03}$$

-IPC(Intermediate pressure compressor)

$$P_{05} = \pi_{ipc} * P_{04}$$

$$T_{05} = T_{04}\left(1 + \frac{\pi_{ipc}{}^{\frac{\gamma-1}{\gamma}} - 1}{n_{ipc}}\right)$$

-HPC(High pressure compressor)

$$P_{06} = \pi_{hpc} * P_{05}$$

$$T_{06} = T_{05}\left(1 + \frac{\pi_{hpc}^{\frac{\gamma-1}{\gamma}} - 1}{n_{hpc}}\right)$$

-Combustor

$$\dot{m}_f = mass\ flow\ rate\ of\ fuel$$

$$\dot{m}_a = mass\ flow\ rate\ of\ air$$

$$\dot{m}_c = mass\ flow\ rate\ of\ air\ in\ the\ core$$

$$f = fuel\ air\ ratio$$

$$b = bypass\ ratio$$

$$P_{07} = n_{cc} * P_{06}$$

$$f = \frac{\dot{m}_f}{\dot{m}_c} = \frac{\dot{m}_f}{(1-b)\dot{m}_a}$$

$$T_{07} = \frac{c_{p,a}T_{06} + n_{cc}fQ}{(1+f)c_{p,g}}$$

-HPT

$$T_{08} = T_{07} - \frac{c_{p,a}(T_{08} - T_{07})}{(1+f)n_{hpt,mech}c_{p,g}}$$

$$P_{08} = P_{07}\left(1 - \frac{1 - \frac{T_{08}}{T_{07}}}{n_{hpt}}\right)^{\frac{\gamma}{\gamma-1}}$$

-IPT(Intermediate pressure turbine)

$$T_{09} = T_{08} - \frac{c_{p,a}(T_{09} - T_{08})}{(1+f)n_{ipt,mech}c_{p,g}}$$

$$P_{09} = P_{08}\left(1 - \frac{1 - \frac{T_{09}}{T_{08}}}{n_{ipt}}\right)^{\frac{\gamma}{\gamma-1}}$$

-LPT(Low pressure turbine)

$$T_{010} = T_{09} - \frac{c_{p,a}(T_{010} - T_{09})}{(1+f)n_{lpt,mech}c_{p,g}}$$

$$P_{010} = P_{09}\left(1 - \frac{1 - \frac{T_{010}}{T_{09}}}{n_{lpt}}\right)^{\frac{\gamma}{\gamma-1}}$$

-Hot core duct

$$P_{011} = \pi_{hcd} * P_{010}$$

$$T_{011} = T_{010}$$

-Hot nozzle

$$P_{012} = \pi_{hn} * P_{011}$$

$$T_{012} = T_{011}$$

Checking whether the hot nozzle is choked or not

$$P_c = P_{012}\left(1 - \frac{1}{n_{hn}} * \frac{\gamma - 1}{\gamma + 1}\right)^{\frac{\gamma}{\gamma-1}}$$

$$if\ P_c > P_1\ then\ nozzle\ is\ choked$$

$$P_{13} = P_c$$

$$T_{13} = T_{012} * \frac{2}{\gamma + 1}$$

$$V_{13} = a_{13} = \sqrt{\gamma R T_{13}}$$

$$if\ P_c < P_1\ then\ nozzle\ is\ unchoked$$

$$P_{13} = P_1$$

$$T_{13} = T_{012} - n_{hn}\left[T_{010}\left(1 - \left(\frac{P_1}{P_{012}}\right)\right)\right]^{\frac{\gamma}{\gamma-1}}$$

$$V_{13} = \sqrt{2c_p(T_{012} - T_{13})}$$

-Cold nozzle

Similar to the Hot nozzle sequence getting P_{14}, T_{14}, *and* V_{14}.

Height	**3.485 m**
Company	**Rolls-Royce**
Application	**Boeing 787 Dreamliner**
Certified(EASA)	**07 August 2007**
Description	**Three-shaft High BPR Turbofan Engine**
Weight(Dry)	**5936 kg**
Overall length	**4.738 m**
Fan diameter	**2.85 m**
Presence of FADEC	**Yes**
Max. take-off thrust	**307.8 kN**
Max. continuous thrust	**287.6 kN**
OPR(Overall pressure ratio)	**50**
Fuel flow rate(take-off)	**2.867 kg/s**
Fuel flow rate(cruise)	**1.116 kg/s**
Bypass ratio	**10**
Total air mass flow rate(take-off)	**1210 kg/s**
Fuel heating value	**43031 kJ/kg**
Compressor stages	**1 Fan, 8 IPC, 6 HPC**
Turbine stages	**6 LPT, 1 IPT, 1 HPT**

Table 1:Turbofan engine specifications

The analysis is performed at the following operating points or conditions:

-Take-Off M0.25 at sea level

-Cruise M0.85 at 12000 m

Performance analysis of High Bypass Turbofan Engine Trent 1000-A was performed for take-off and cruise conditions with the input data in **Table 2** and **Table 3**.

Parameters	Take-off	Cruise
Height	**0 m**	**12000 m**
Mach number	**0.25**	**0.85**
π_{fan}	**1.54**	**1.54**
π_{ipc}	**9.61**	**9.61**
π_{hpc}	**3.38**	**3.38**
TIT	**1750 K**	**1500 K**
$\dot{m}_a$	**1210 kg/s**	**600 kg/s**
$\dot{m}_f$	**2.855 kg/s**	**1.1439 kg/s**
Thrust force	**307.8 kN**	**72.802 kN**
Specific thrust	**0.2089 kN*s/kg**	**0.1213 kN*s/kg**
TSFC	**0.0375 kg/s*kN**	**0.05657 kg/s*kN**
Hot jet velocity	**532.3 m/s**	**484.3 m/s**
Cold jet velocity	**264.2 m/s**	**300.2 m/s**

Table 2:Input data of the turbofan engine

Inlet	**0.98**
Fan	**0.93**
IPC	**0.91**
HPC	**0.91**
C.C	**0.99**
HPT	**0.93**
IPT	**0.93**
LPT	**0.93**
Bypass duct	**0.97**
Cold core duct	**0.97**
Hot core duct	**0.98**
Cold exhaust nozzle	**0.95**
Hot exhaust nozzle	**0.95**

Table 3:Engine Modules Efficiencies(Pressure ratios of ducts included)

3.4 Engine Components

Engine components with key datas in GSP environment are shown below.

Inlet

$$Design\ mass\ flow: 1210\frac{kg}{s}\ (Take\ off), 600\frac{kg}{s}\ (Cruise)$$

$$Pressure\ ratio = 0.980$$

Fan

$$Core\ side\ design\ efficiency: 0.930$$

$$Duct\ side\ design\ efficieny: 0.930$$

$$Core\ side\ design\ pressure\ ratio: 1.54$$

$$Duct\ side\ design\ pressure\ ratio: 1.54$$

$$Design\ bypass\ ratio: 10.000$$

$$Design\ rotor\ speed: 2300rpm(Shaft\ 1)$$

$$shaft\ nr: 1$$

IPC

$$Design\ efficiency: 0.910$$

$$Design\ pressure\ ratio: 9.61$$

$$Design\ rotor\ speed: 6000rpm(Shaft\ 2)$$

$$shaft\ nr: 2$$

HPC

$$Design\ efficiency: 0.910$$

$$Design\ pressure\ ratio: 3.38$$

$$Design\ rotor\ speed: 12000rpm(Shaft\ 3)$$

$$shaft\ nr: 3$$

Combustor

$$Design\ combustion\ efficiency: 0.99$$

$$Design\ point\ rel. pressure\ loss: 0.01$$

$$T_{exit}: 1750K(Take\ off), 1500K(Cruise)$$

$$Fuel: Jet\ A/A1, JP\ 8, Avtur$$

$$Fuel\ lower\ heating\ value: 43031.000\,\frac{kJ}{kg}$$

HPT

$$Design\ efficiency: 0.930$$

$$spool\ mech.\ efficiency: 0.999$$

$$Design\ rotor\ speed: 12000 rpm (Shaft\ 3)$$

$$shaft\ nr: 3$$

IPT

$$Design\ efficiency: 0.930$$

$$spool\ mech.\ efficiency: 0.999$$

$$Design\ rotor\ speed: 6000 rpm (Shaft\ 2)$$

$$shaft\ nr: 2$$

LPT

$$Design\ efficiency: 0.930$$

$$spool\ mech.\ efficiency: 0.999$$

$$Design\ rotor\ speed: 2300 rpm (Shaft\ 1)$$

$$shaft\ nr: 1$$

Ducts

$$bypass\ duct\ rel.\ total\ pressure\ loss: 0.030$$

$$cold\ core\ duct\ rel.\ total\ pressure\ loss: 0.030$$

$$hot\ core\ duct\ rel.\ total\ pressure\ loss: 0.020$$

Hot nozzle

$$Velocity\ coefficient\ CV: 0.975$$

$$Thrust\ coefficient\ CX: 1.000$$

Cold nozzle

$$Velocity\ coefficient\ CV: 0.975$$

$$Thrust\ coefficient\ CX: 1.000$$

4 Results

After performing the analysis to obtain total temperature, total pressure, entropy, and specific heat ratio at every section, an analytical study and modeling using GSP and MATLAB were performed to generate performance curves of the engine at takeoff and cruise conditions as follows;

4.1 Take-off condition(0.25M at sea level)

Station No.	Total Temperature (K)	Total Pressure (bar)	Entropy (kJ/kg*K)	Specific Heat Ratio
1	291.75	1.05828	6.82989	1.40014
2	291.75	1.03711	6.83568	1.40014
3	332.91	1.59715	6.84441	1.398817
4	332.91	1.54924	6.85316	1.398817
5	655.49	14.88816	6.89982	1.369393
6	926.62	50.32199	6.92907	1.341981
7	1750.00	49.81877	7.83872	1.284516
8	1525.52	25.57909	7.85311	1.290748
9	1268.08	10.64123	7.87250	1.301391
10	900.42	2.22085	7.91018	1.326321
11	900.42	2.17644	7.91598	1.326321
12	900.42	2.10596	7.91018	1.338205
13	332.91	1.54924	6.85316	1.398817
14	332.91	1.5152	6.84441	1.40012

Table 4: Temperatures, pressures, entropies, and specific heat ratios at engine sections during take-off

At take-off condition, the thermal, propulsive, and overall efficiencies are calculated as follows:

$$\eta_{thermal} = 0.43809 \cong 0.438$$

$$\eta_{propulsive} = 0.41517 \cong 0.415$$

$$\eta_{overall} = 0.18188 \cong 0.182$$

4.2 Specific Heat Ratio(Take-off)

The temperatures with specific heat ratios during the take-off condition are shown below.

Station No.	Temperature (K)	Specific heat ratio
1	291.75	1.40014
2	291.75	1.40014
3	332.91	1.398817
4	332.91	1.398817
5	655.49	1.369393
6	926.62	1.341981
7	1750.00	1.284516
8	1525.52	1.290748
9	1268.08	1.301391
10	900.42	1.326321
11	900.42	1.326321
12	778.02	1.338205
13	332.91	1.398817
14	296.78	1.40012

Table 5:Temperatures and specific heat ratios at engine sections during take-off

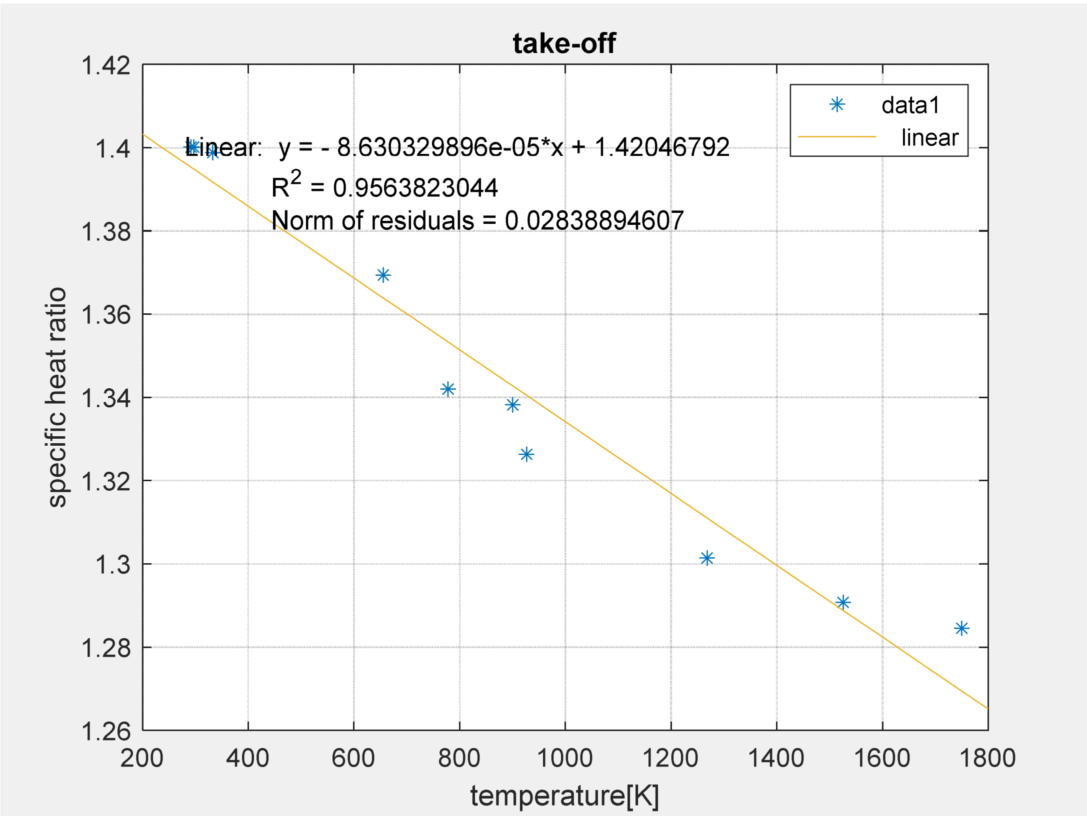

Figure 16:Linear regression curve for take-off condition

Applying linear regression analysis using MATLAB on the data given in **Table 5**, the equation of the line shown in **Figure 16** is:

$$y = -8.630329896e - 05x + 1.42046792$$

or

$$\gamma(T) = (-8.630329896 * 10^{-5})T + 1.42046792$$

$$where\ \boldsymbol{T}\ is\ in\ \boldsymbol{K}$$

Therefore,the specific heat can be determined as

$$c_p(T) = \frac{R\gamma(T)}{\gamma(T) - 1}$$

where

$$R = 0.28705 \frac{kJ}{kg * K}$$

T-s diagram of Take-off condition is shown in **Figure 17**.

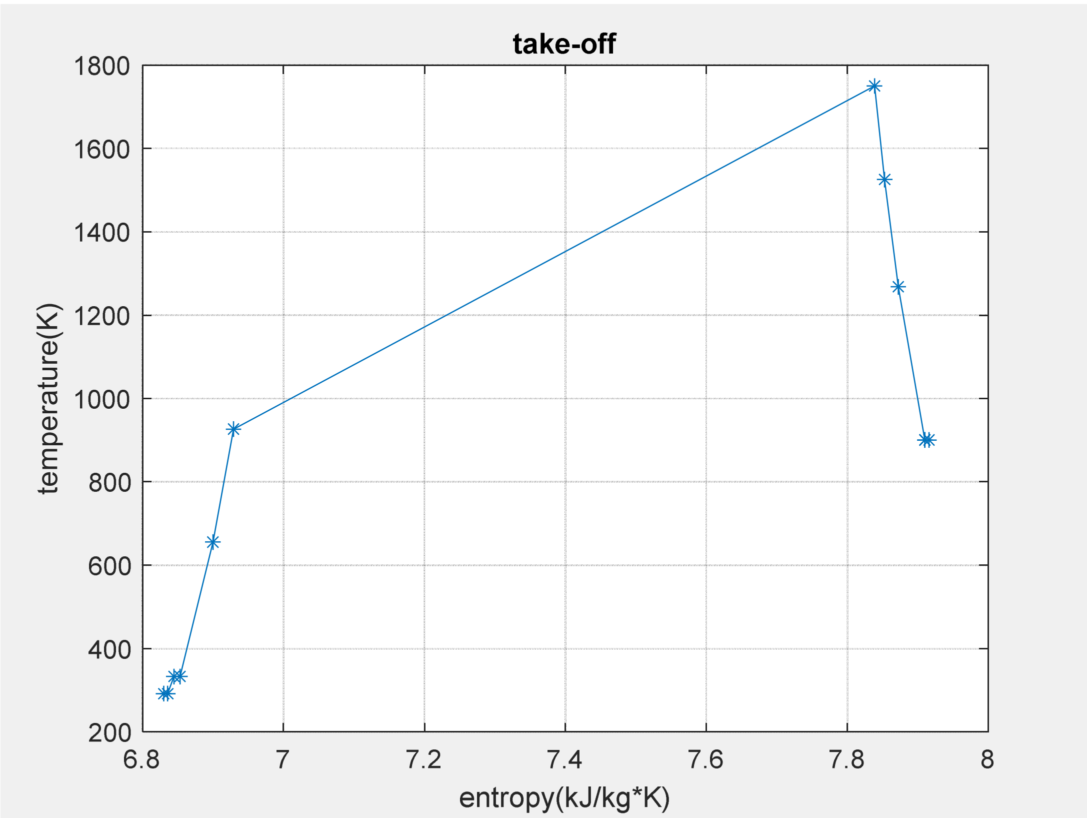

Figure 17:T-s diagram of Take-off condition

4.3 Second Law Analysis of Take-off Condition

4.3.1 Flow Exergies at Take-Off Condition

The ambient conditions during take-off is shown below.

$$T_0 = 288.15\ K, P_0 = 1.01325\ bar, s_0 = 6.82989\ \frac{kJ}{kg * K}$$

The exergies of the fluid streams at each section are shown in **Table 6**.

Station No.	Exergy (kJ/kg)
1	3.6465927
2	1.9782042
3	41.301954
4	38.780642
5	362.96524
6	652.65230
7	1390.88709
8	1098.28250
9	777.00501
10	340.52836
11	338.85709
12	340.52836
13	38.780642
14	41.301954

Table 6:Exergies of fluid stream at engine sections during take-off

4.3.2 Second-Law Efficiencies at Take-Off Condition

The second law efficiency, or the exergy efficiency, of the components of the engine is shown in **Table 7**.

Components	**Second-Law Efficiency**
Inlet	**0.542**
Fan	**0.950**
IPC	**0.975**
HPC	**0.975**
Combustor	**0.668**
HPT	**0.986**
IPT	**0.983**
LPT	**0.975**
Bypass duct	**0.939**
Cold core duct	**0.939**
Hot core duct	**0.995**
Cold exhaust nozzle	**0.879**
Hot exhaust nozzle	**0.414**

Table 7:Second-law efficiencies of engine components

At take-off condition, the second law efficiency of the engine is calculated as follows:

$$\eta_{\mathrm{II}} = 0.47640 \cong 0.476$$

4.4 2D Performance Analysis(Take-off)

4.4.1 Turbine Inlet Temperature(TIT or T_7) Effect

TIT(Turbine inlet temperature) vs FN(Thrust)

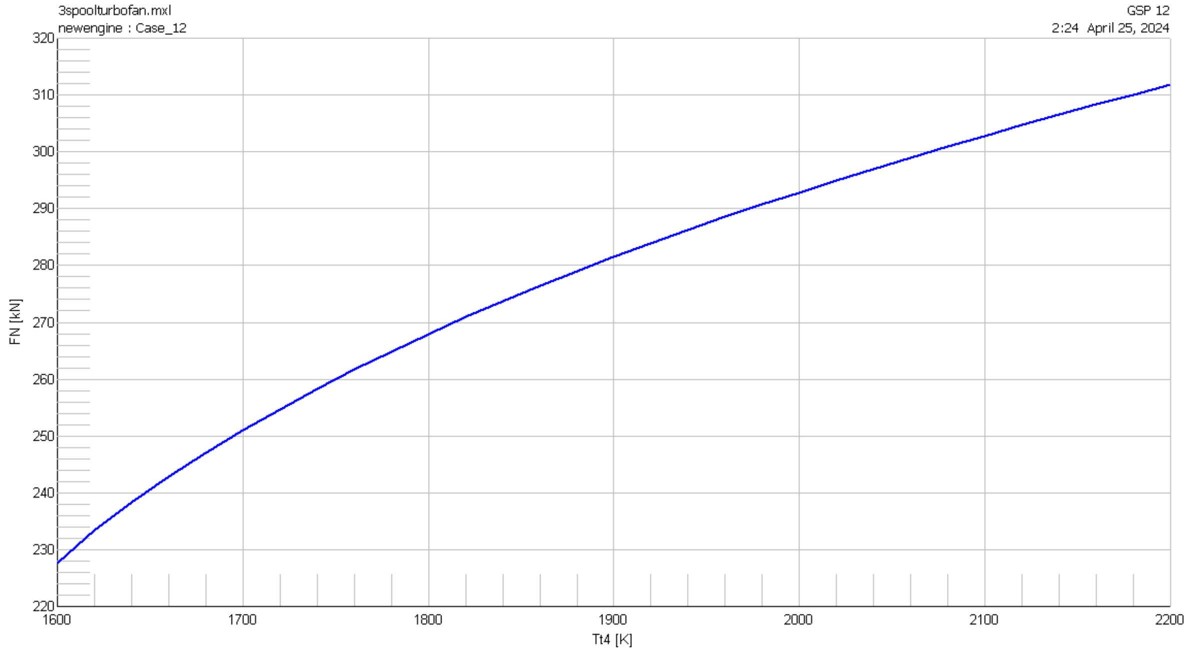

Figure 18:TIT vs FN

TIT(Turbine inlet temperature) vs TSFC(Thrust specific fuel consumption)

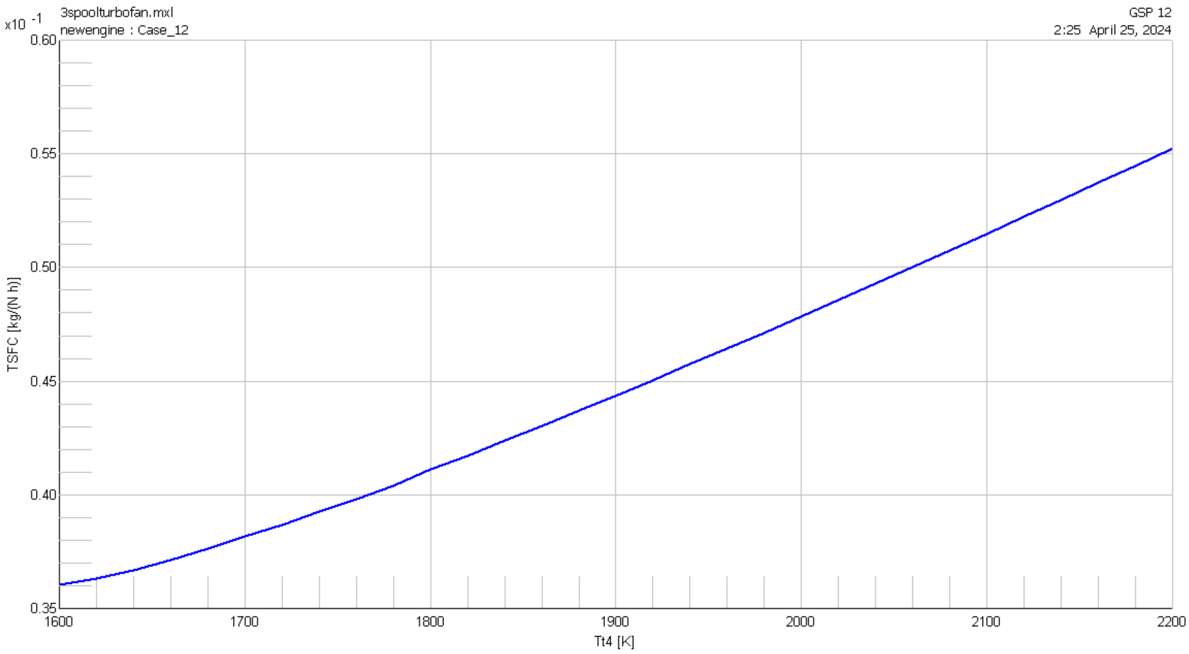

Figure 19:TIT vs TSFC

TIT(Turbine inlet temperature) vs ETA_t(Thermal efficiency)

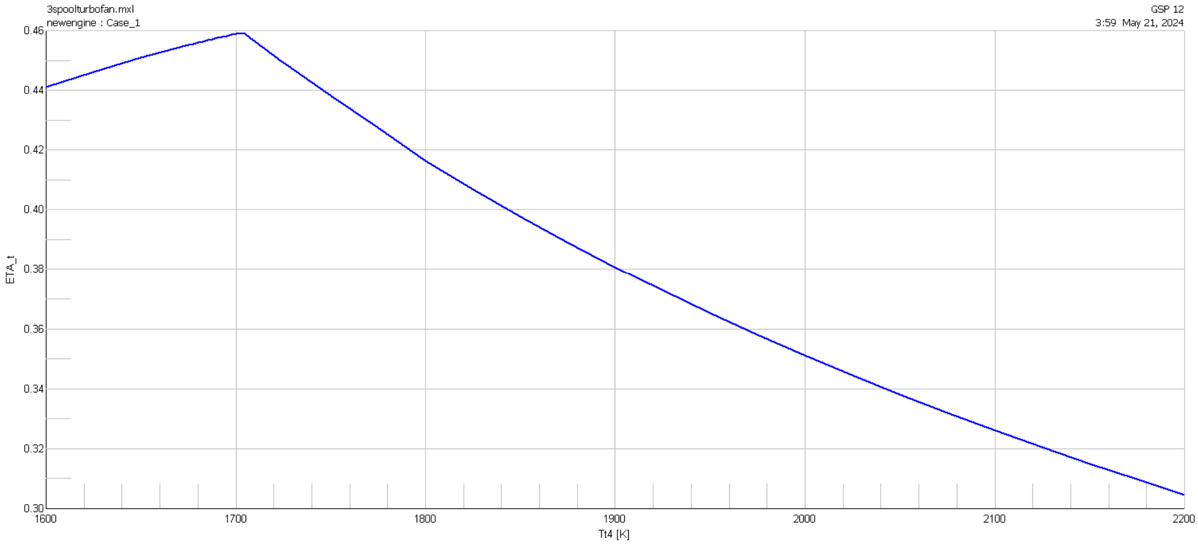

Figure 20:TIT vs ETA_t

TIT(Turbine inlet temperature) vs ETA_p(Propulsive efficiency)

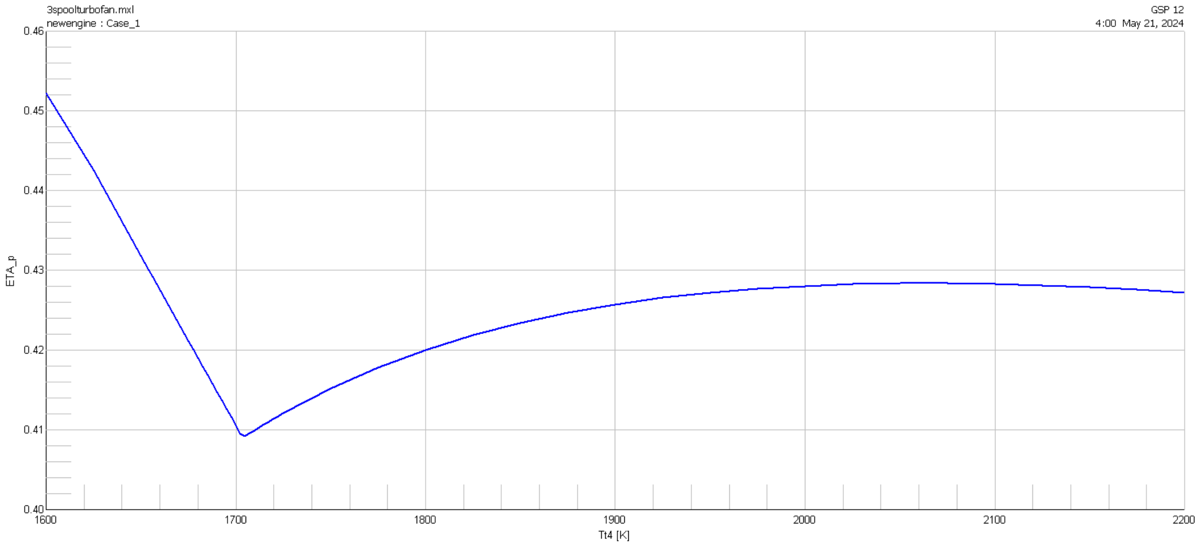

Figure 21:TIT vs ETA_p

TIT(Turbine inlet temperature) vs ETA_o(Overall efficiency)

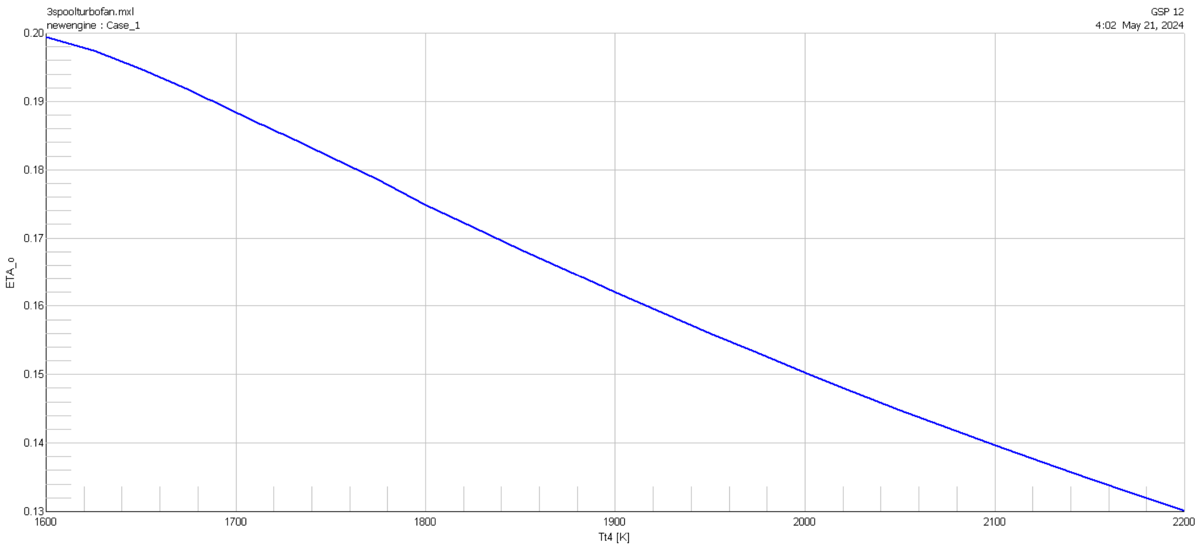

Figure 22:TIT vs ETA_o

TIT(Turbine inlet temperature) vs ETA_II(Second law efficiency)

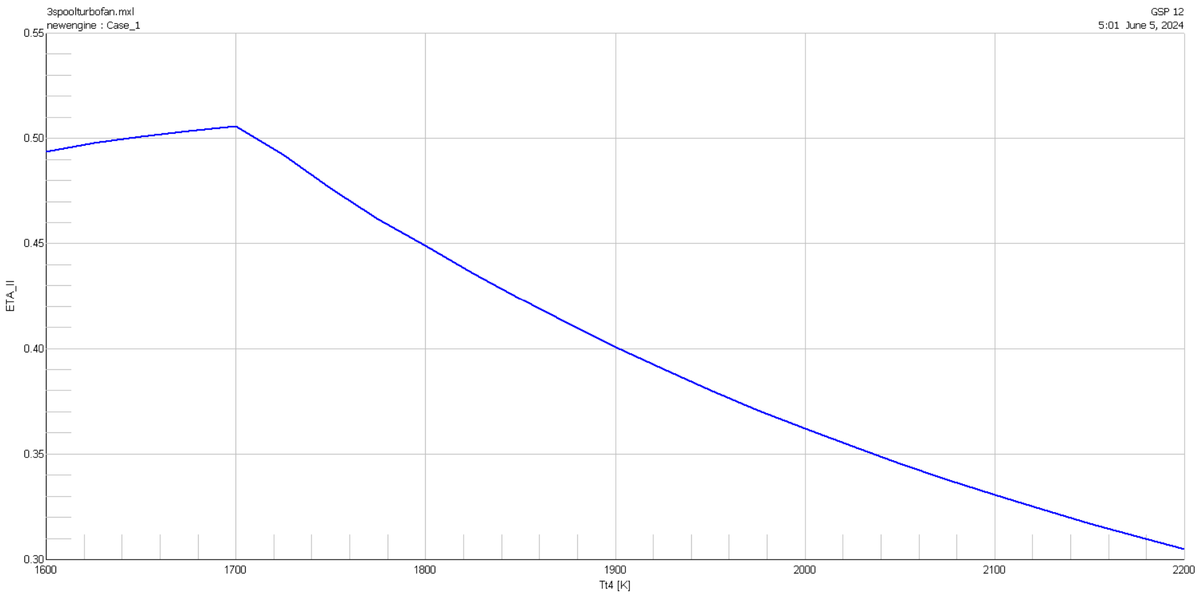

Figure 23:TIT vs ETA_II

4.4.2 Intermediate Compressor Pressure Ratio(π_{IPC}) Effect

π_{IPC}(Intermediate compressor pressure ratio) vs FN(Thrust)

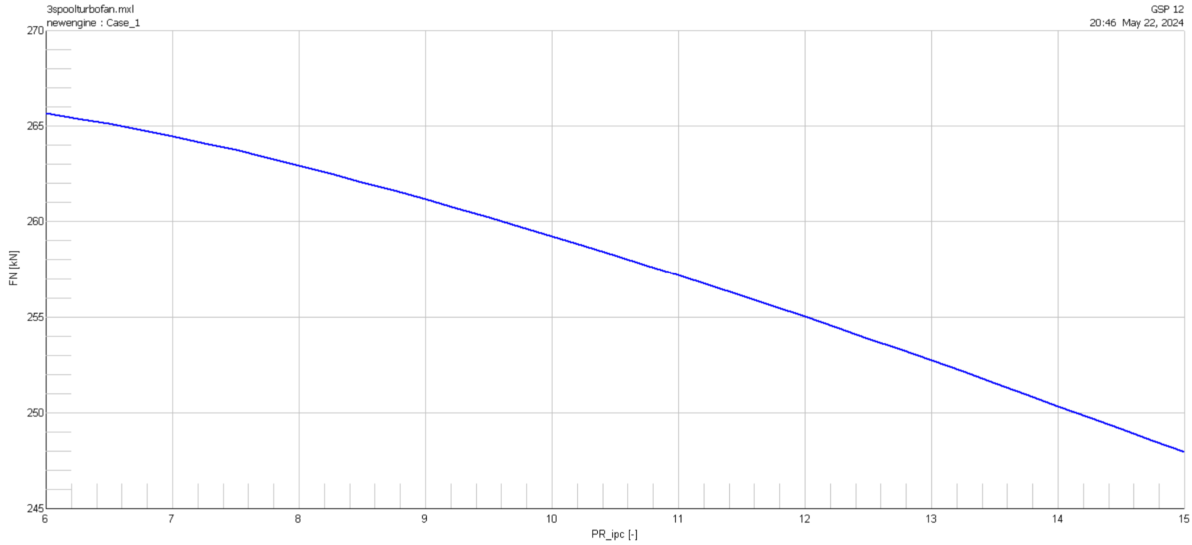

Figure 24: π_{IPC} vs FN

π_{IPC}(Intermediate compressor pressure ratio) vs TSFC(Thrust specific fuel consumption)

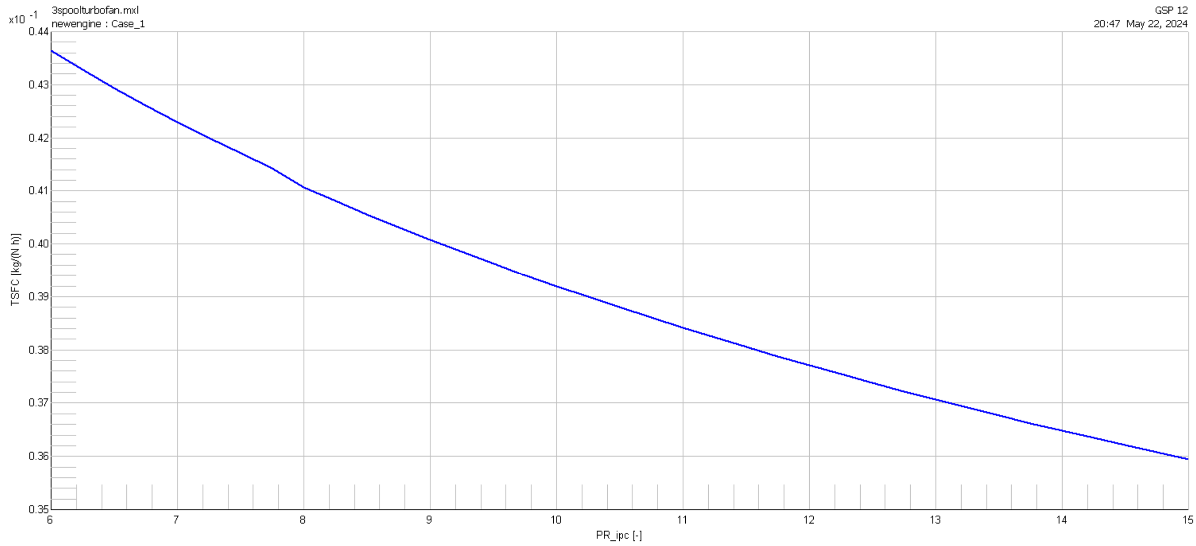

Figure 25: π_{IPC} vs TSFC

π_{IPC}(Intermediate compressor pressure ratio) vs ETA_t(Thermal efficiency)

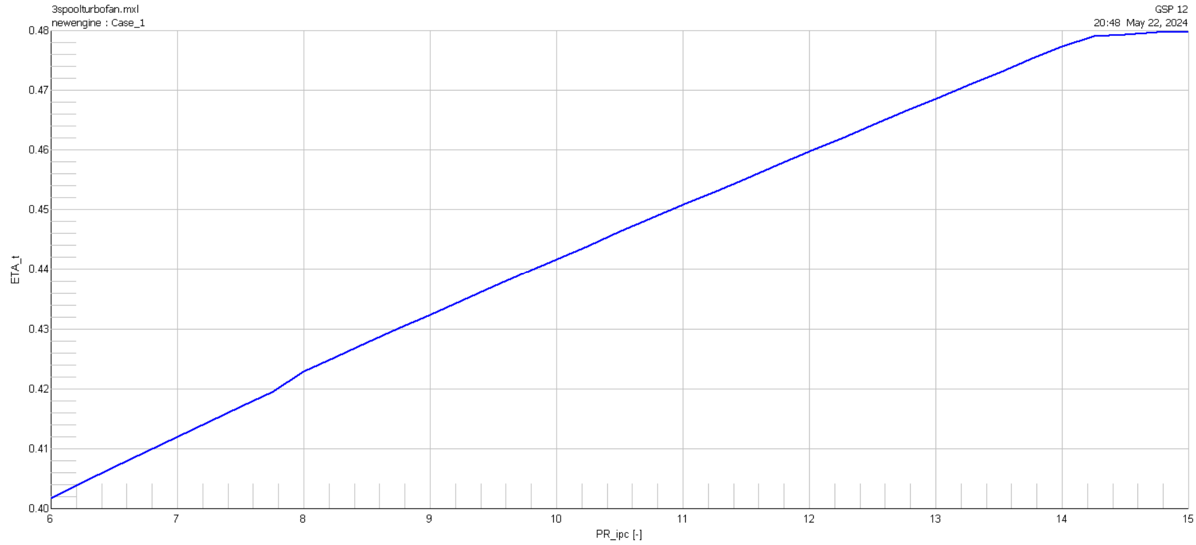

Figure 26: π_{IPC} vs ETA_t

π_{IPC}(Intermediate compressor pressure ratio) vs ETA_p(Propulsive efficiency)

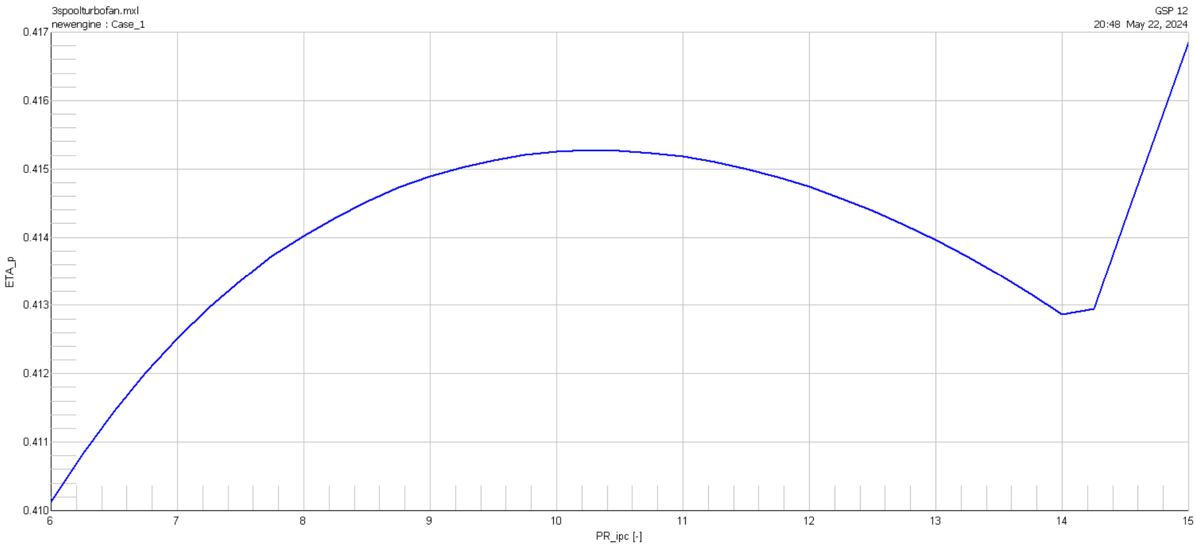

Figure 27: π_{IPC} vs ETA_p

π_{IPC}(Intermediate compressor pressure ratio) vs ETA_o(Overall efficiency)

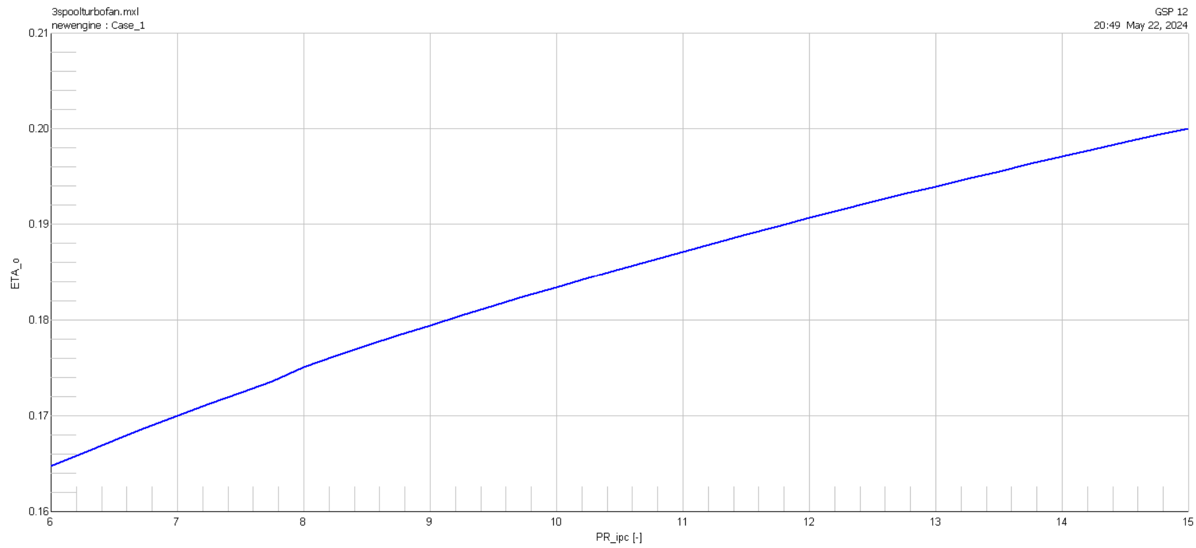

Figure 28: π_{IPC} vs ETA_o

π_{IPC}(Intermediate compressor pressure ratio) vs ETA_II(Second law efficiency)

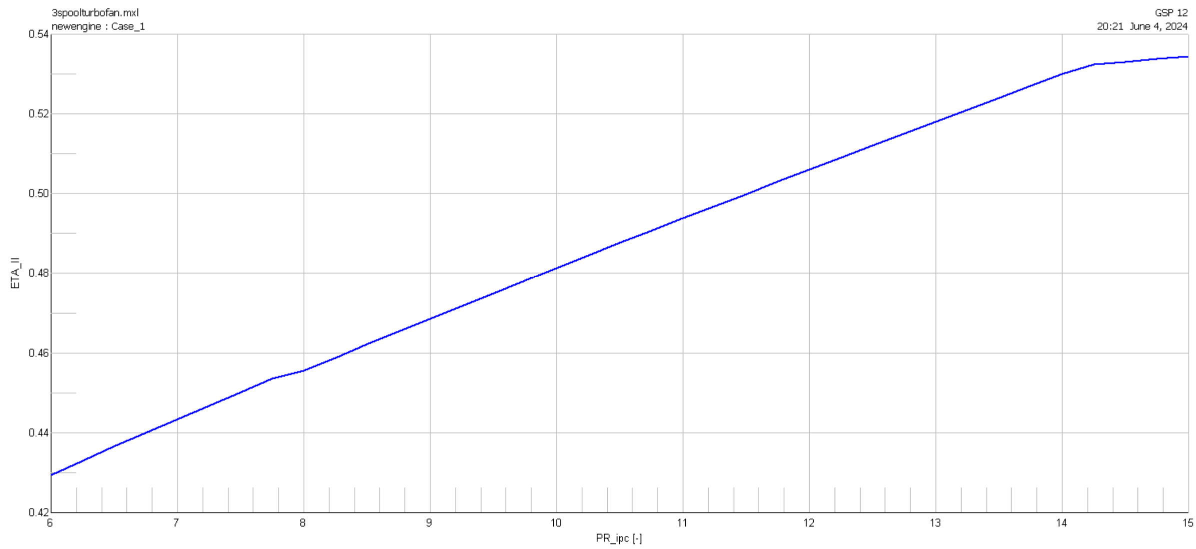

Figure 29: π_{IPC} vs ETA_II

4.4.3 High Compressor Pressure Ratio(π_{HPC}) Effect

π_{HPC} (High compressor pressure ratio) vs FN(Thrust)

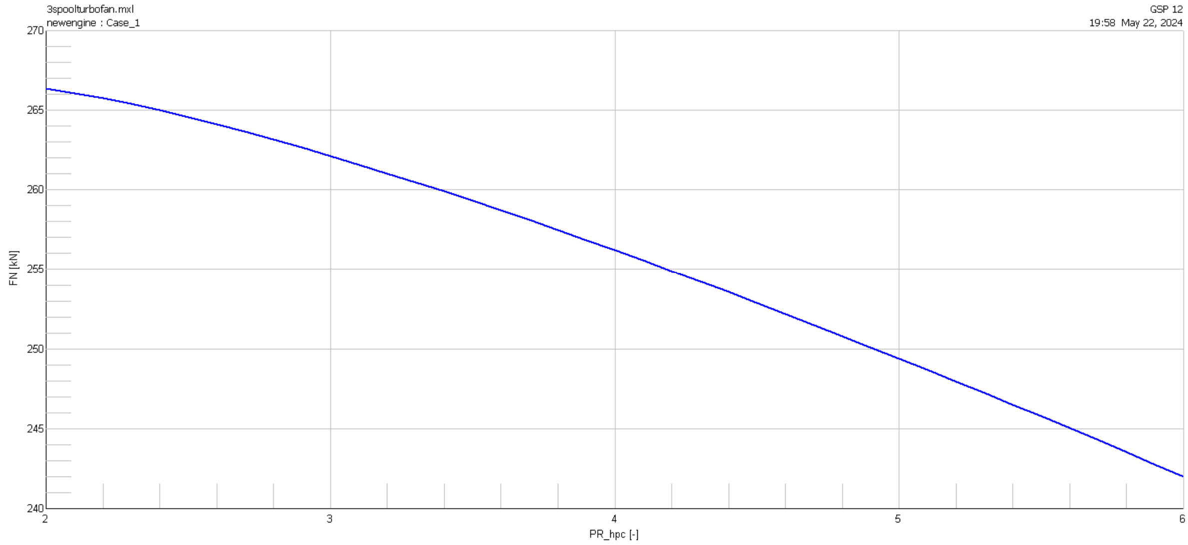

Figure 30: π_{HPC} vs FN

π_{HPC} (High compressor pressure ratio) vs TSFC(Thrust specific fuel consumption)

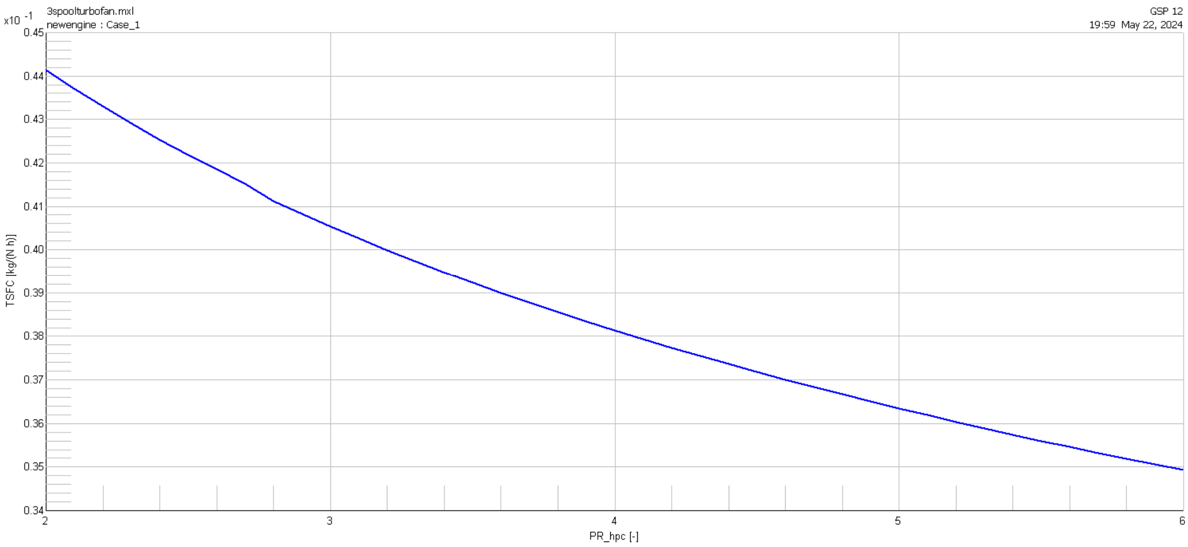

Figure 31: π_{HPC} vs TSFC

π_{HPC} (High compressor pressure ratio) vs ETA_t(Thermal efficiency)

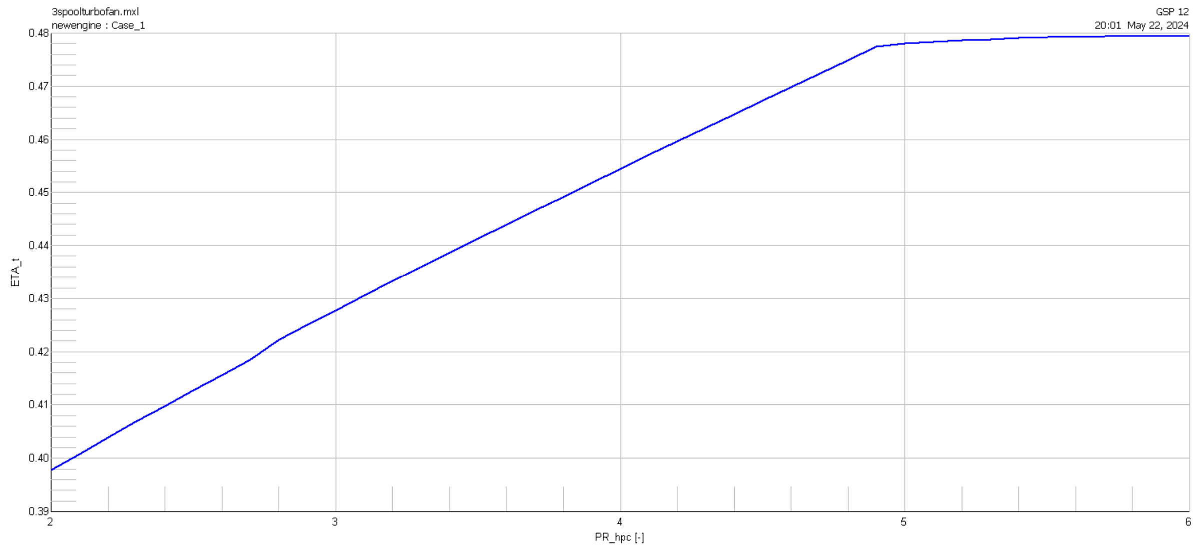

Figure 32: π_{HPC} vs ETA_t

π_{HPC} (High compressor pressure ratio) vs ETA_p(Propulsive efficiency)

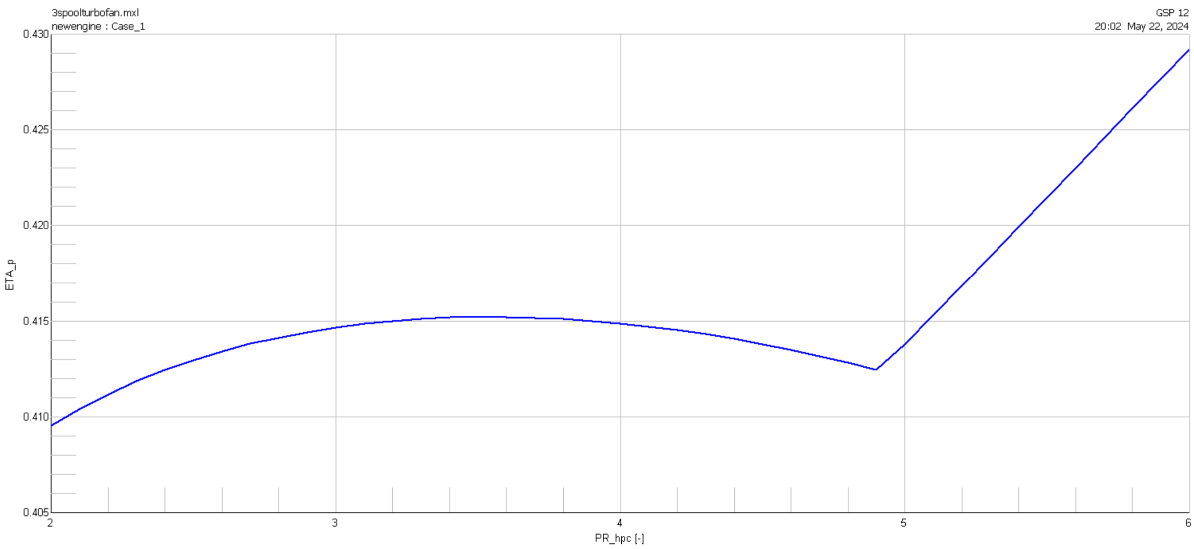

Figure 33: π_{HPC} vs ETA_p

π_{HPC} (High compressor pressure ratio) vs ETA_o(Overall efficiency)

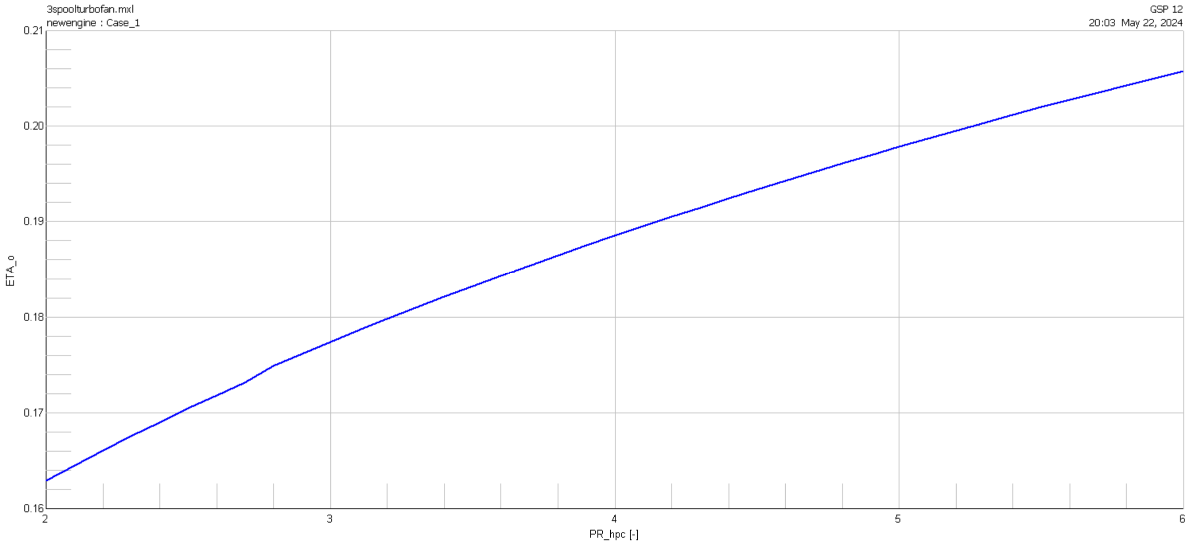

Figure 34: π_{HPC} vs ETA_o

π_{HPC} (High compressor pressure ratio) vs ETA_II(Second law efficiency)

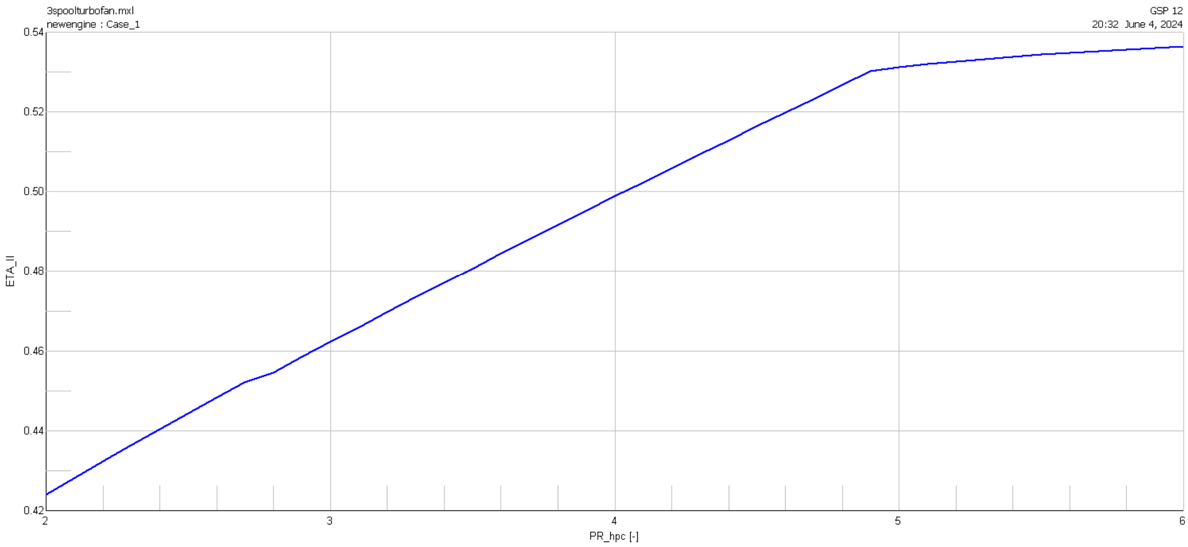

Figure 35: π_{HPC} vs ETA_II

4.4.4 Fan Pressure Ratio(π_{fan}) Effect

π_{fan} (Fan pressure ratio) vs FN(Thrust) vs TIT(Turbine inlet temperature)

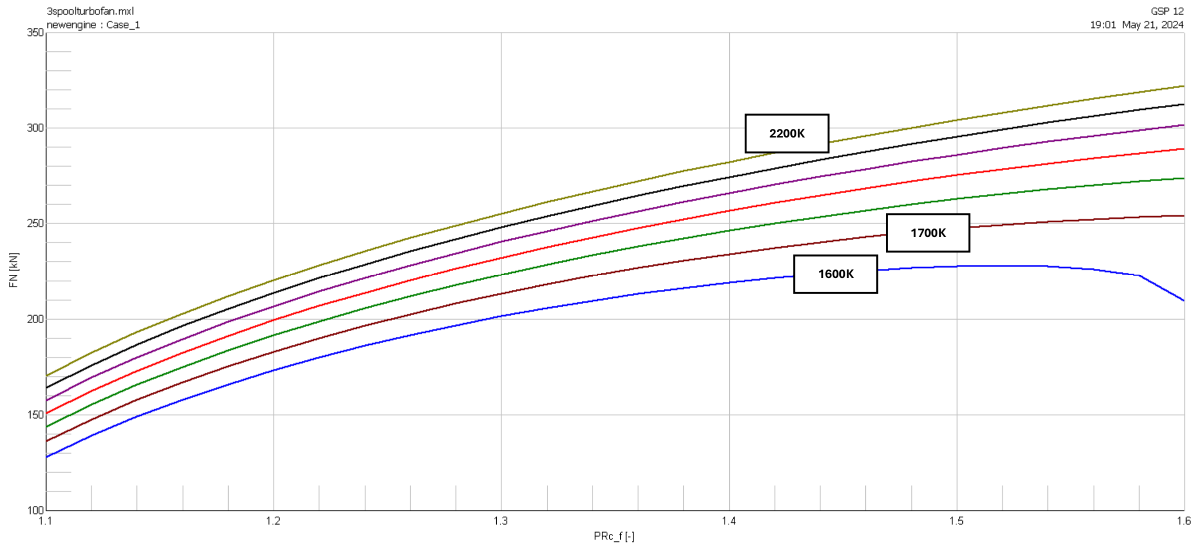

Figure 36: π_{fan} vs FN vs TIT

π_{fan} (Fan pressure ratio) vs TSFC(Thrust specific fuel consumption) vs TIT(Turbine inlet temperature)

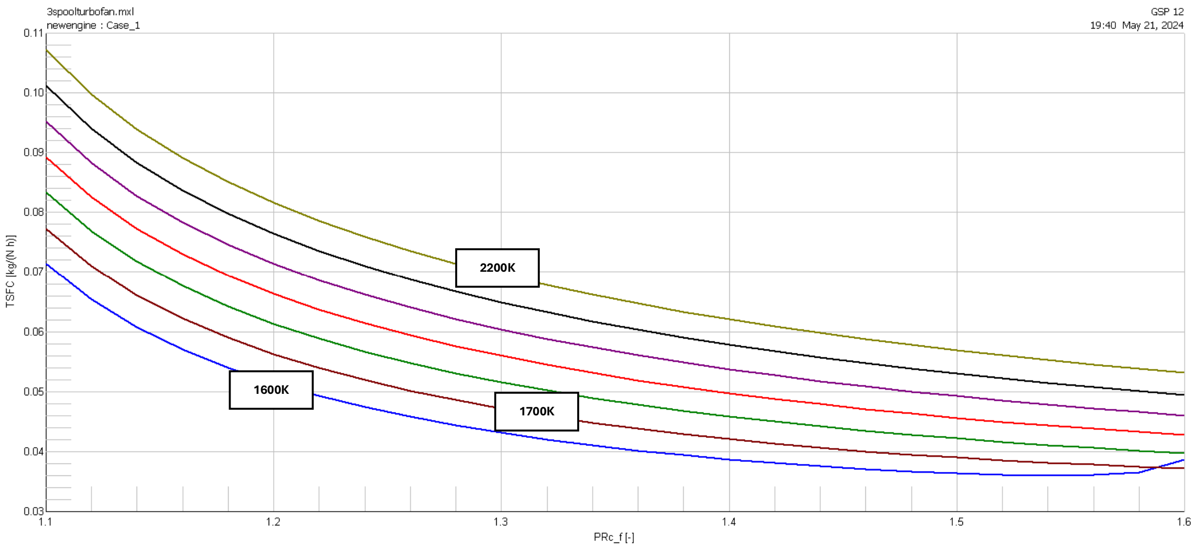

Figure 37: π_{fan} vs TSFC vs TIT

π_{fan} (Fan pressure ratio) vs ETA_t(Thermal efficiency) vs TIT(Turbine inlet temperature)

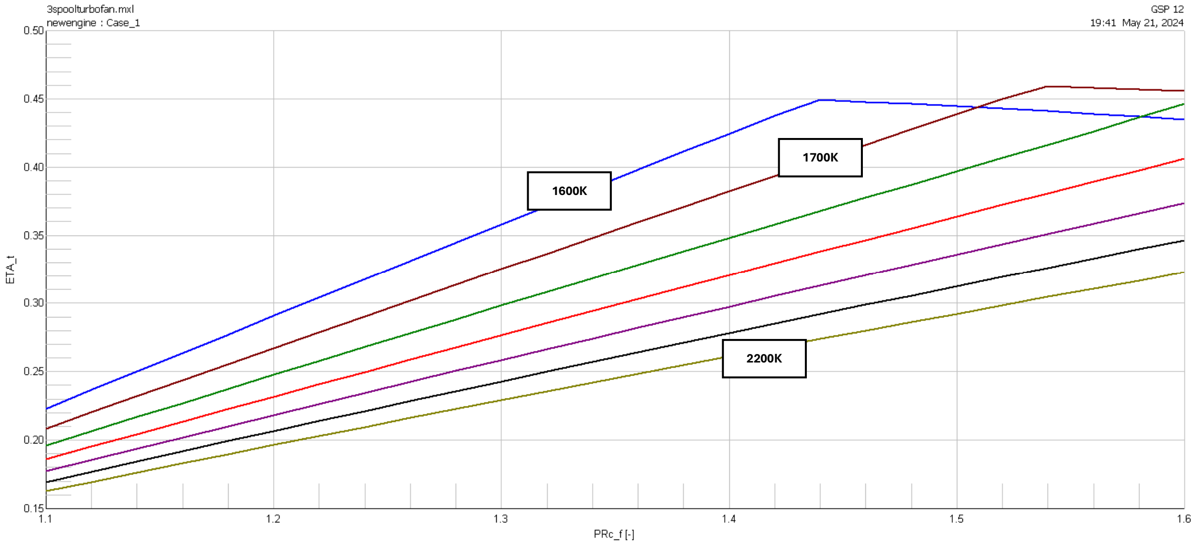

Figure 38: π_{fan} vs ETA_t vs TIT

π_{fan} (Fan pressure ratio) vs ETA_p(Propulsive efficiency) vs TIT(Turbine inlet temperature)

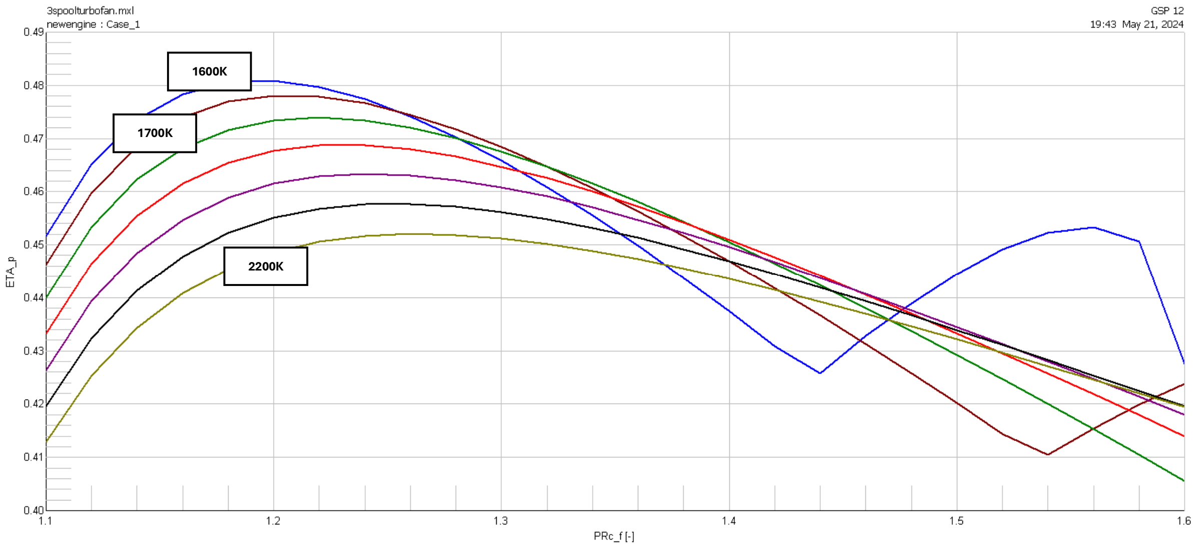

Figure 39: π_{fan} vs ETA_p vs TIT

π_{fan} (Fan pressure ratio) vs ETA_o(Overall efficiency) vs TIT(Turbine inlet temperature)

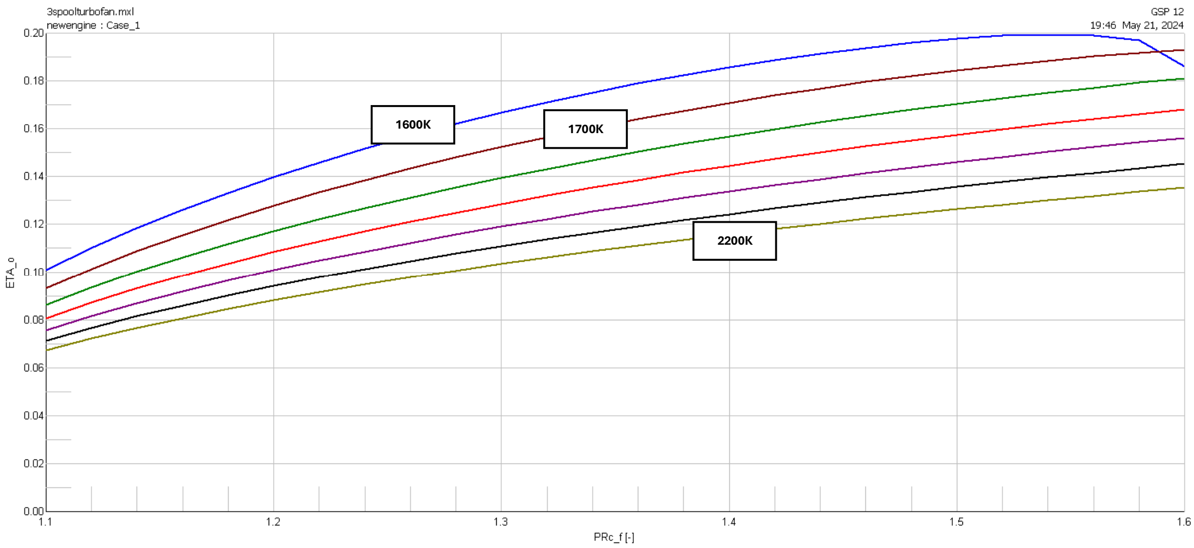

Figure 40: π_{fan} vs ETA_o vs TIT

π_{fan} (Fan pressure ratio) vs ETA_II(Second law efficiency) vs TIT(Turbine inlet temperature)

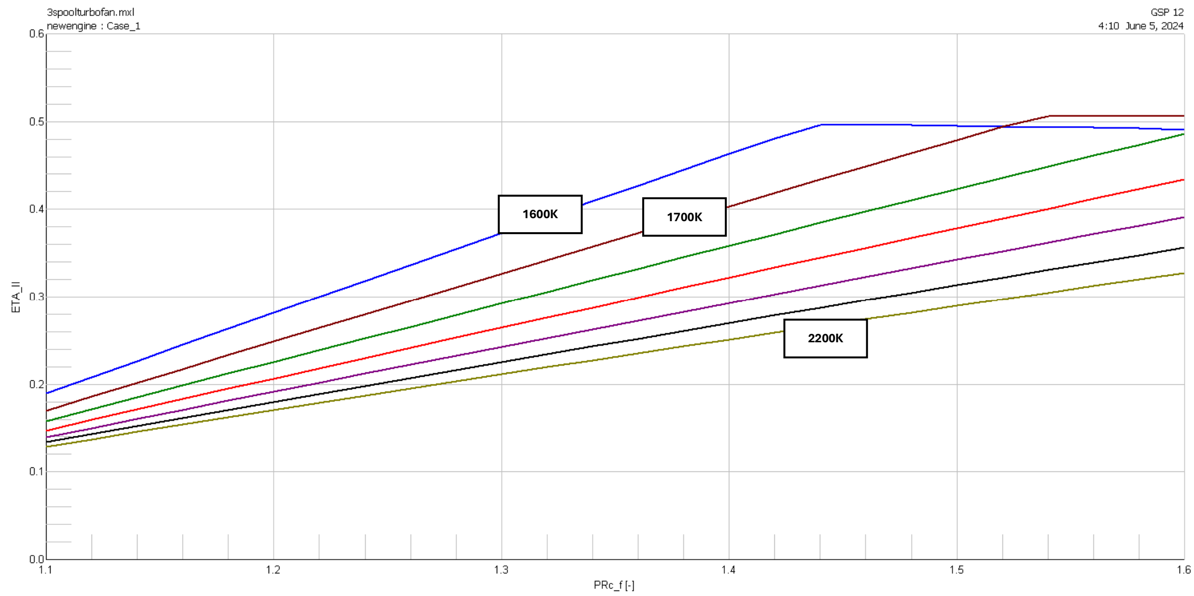

Figure 41: π_{fan} vs ETA_II vs TIT

4.4.5 OPR(Overall Pressure Ratio) Effect

OPR(Overall pressure ratio) vs SFN(Specific thrust)

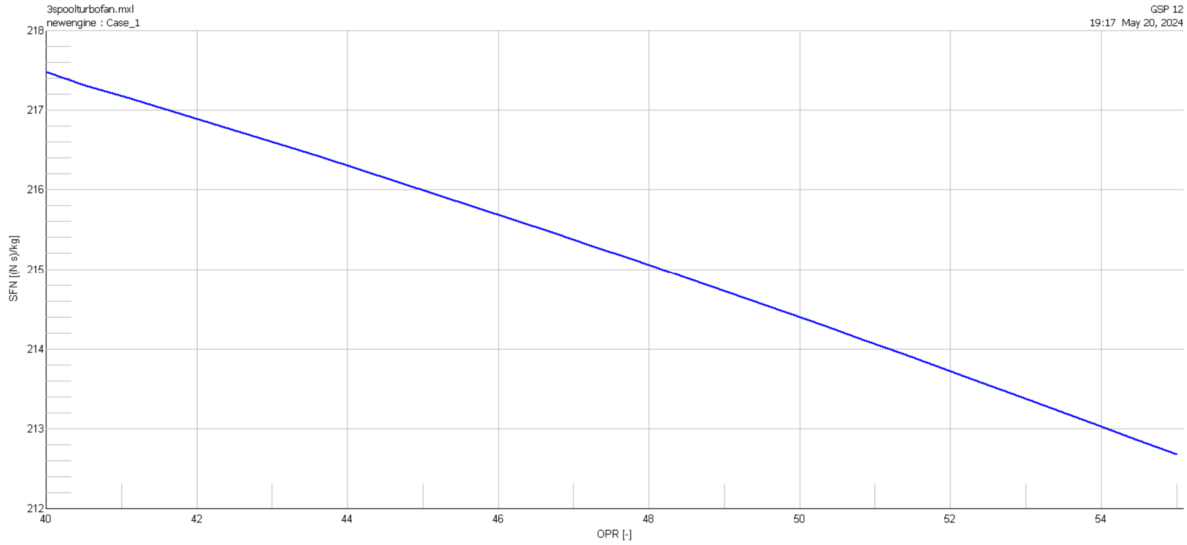

Figure 42:OPR vs SFN

OPR(Overall pressure ratio) vs TSFC(Thrust specific fuel consumption)

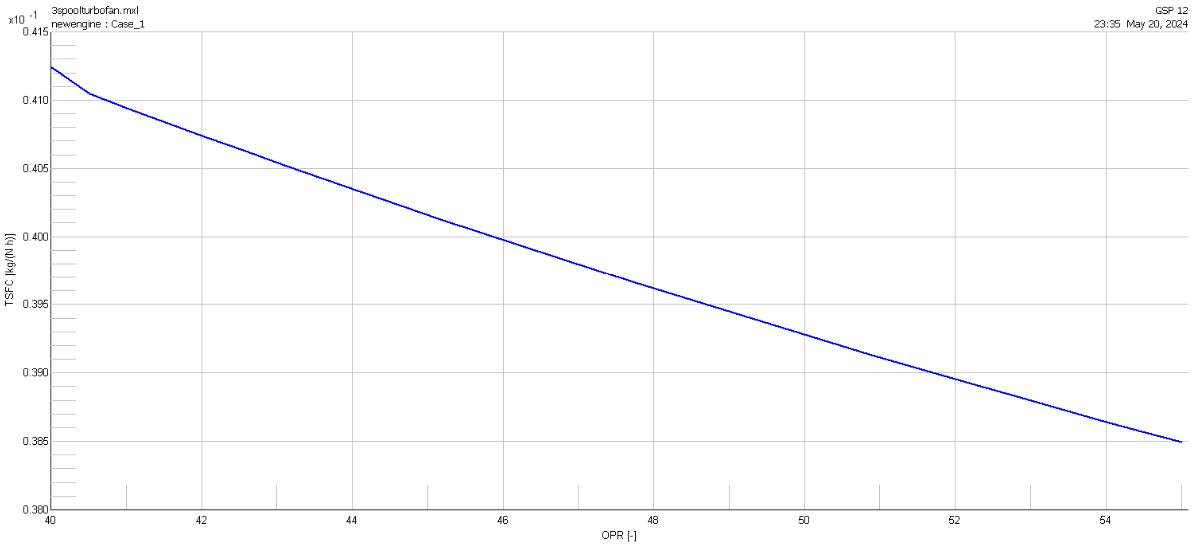

Figure 43:OPR vs TSFC

OPR(Overall pressure ratio) vs ETA_t(Thermal efficiency)

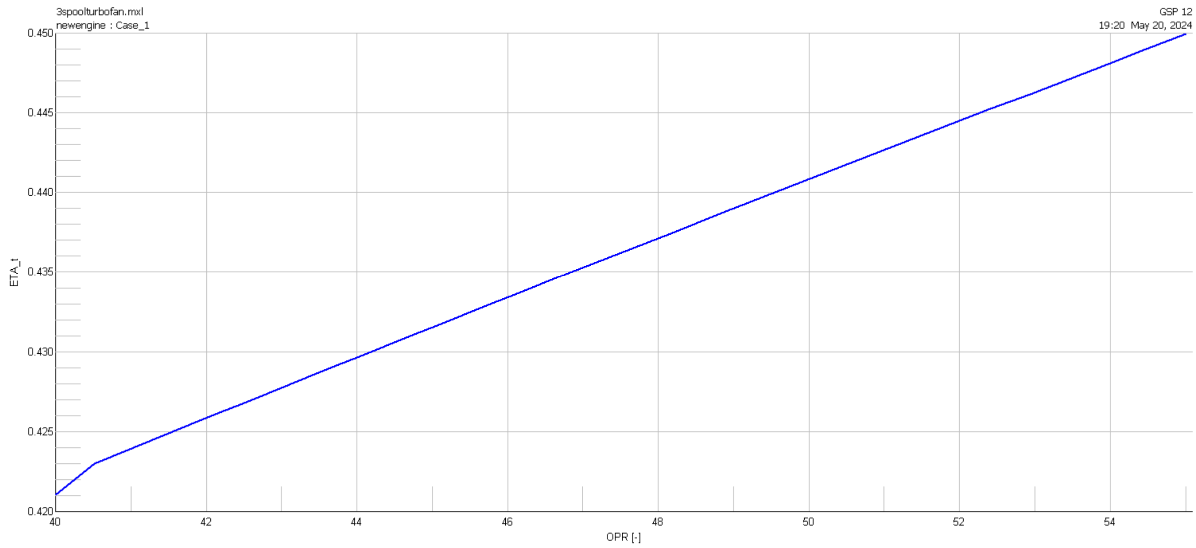

Figure 44:OPR vs ETA_t

OPR(Overall pressure ratio) vs ETA_p(Propulsive efficiency)

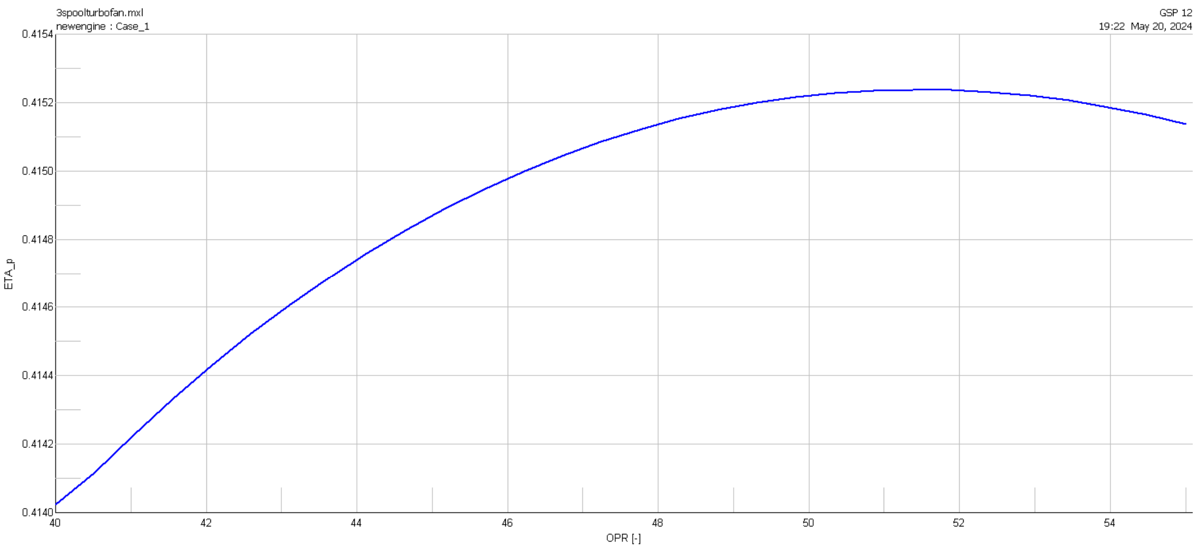

Figure 45:OPR vs ETA_p

OPR(Overall pressure ratio) vs ETA_o(Overall efficiency)

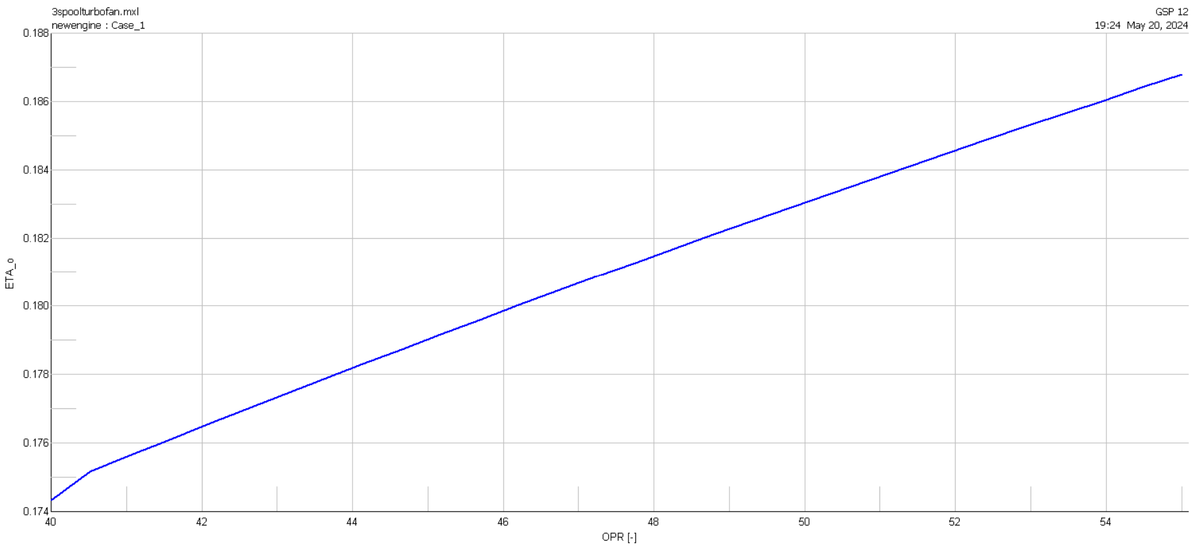

Figure 46:OPR vs ETA_o

OPR(Overall pressure ratio) vs ETA_II(Second law efficiency)

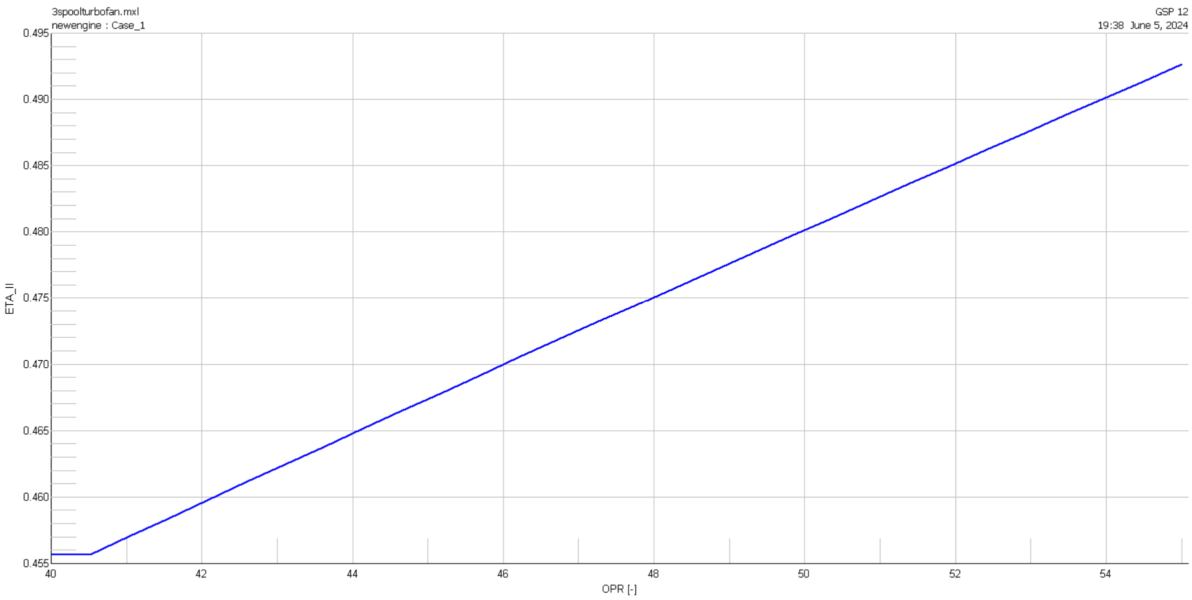

Figure 47:OPR vs ETA_II

4.4.6 BPR(Fan Bypass Ratio) Effect

BPR(Bypass ratio) vs SFN(Specific thrust)

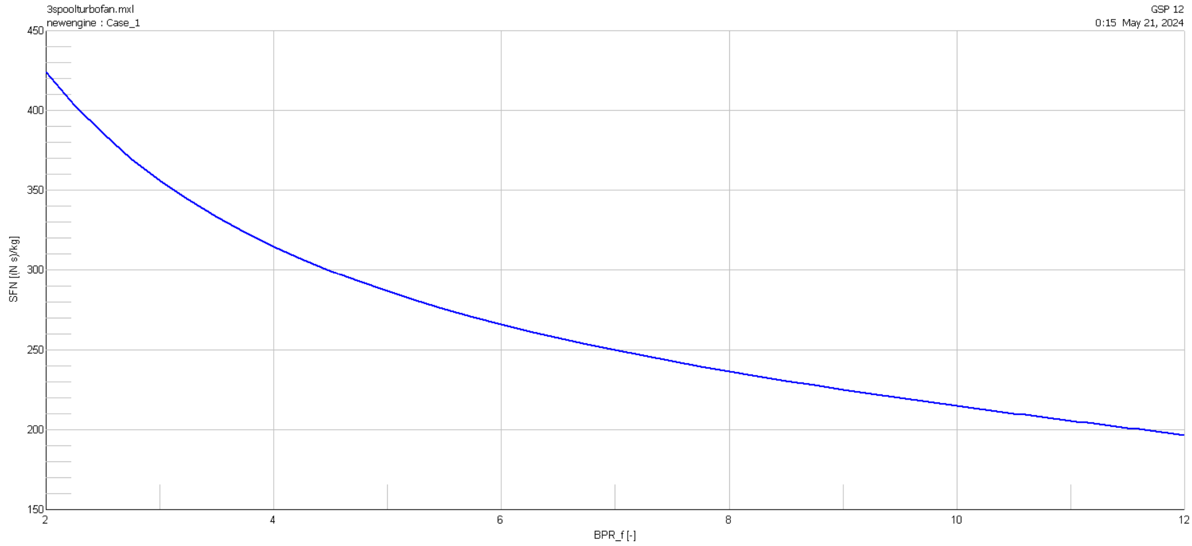

Figure 48:BPR vs SFN

BPR(Bypass ratio) vs TSFC(Thrust specific fuel consumption)

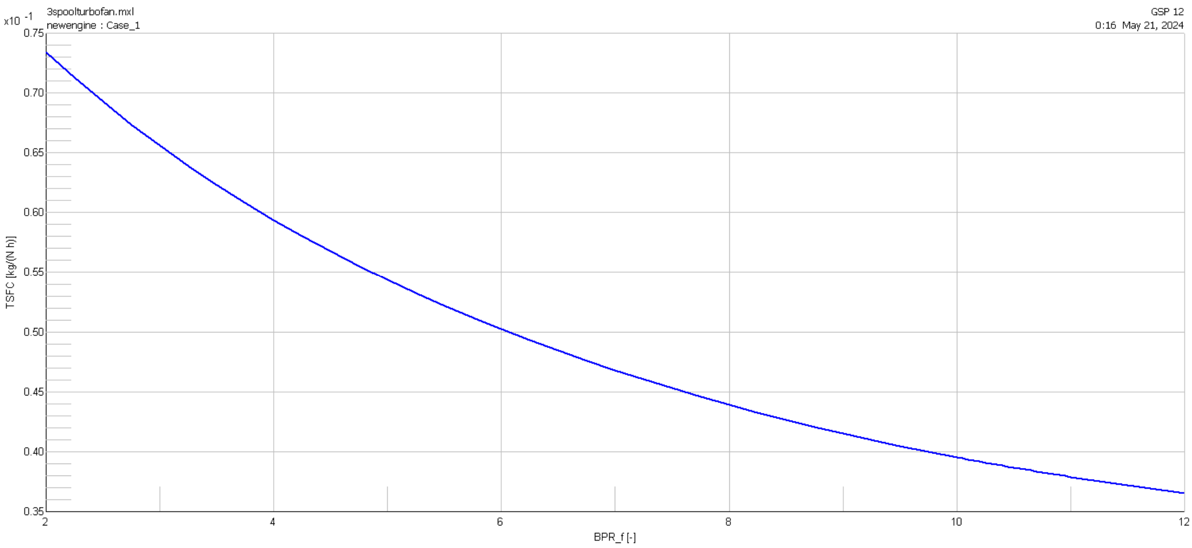

Figure 49:BPR vs TSFC

BPR(Bypass ratio) vs ETA_t(Thermal efficiency)

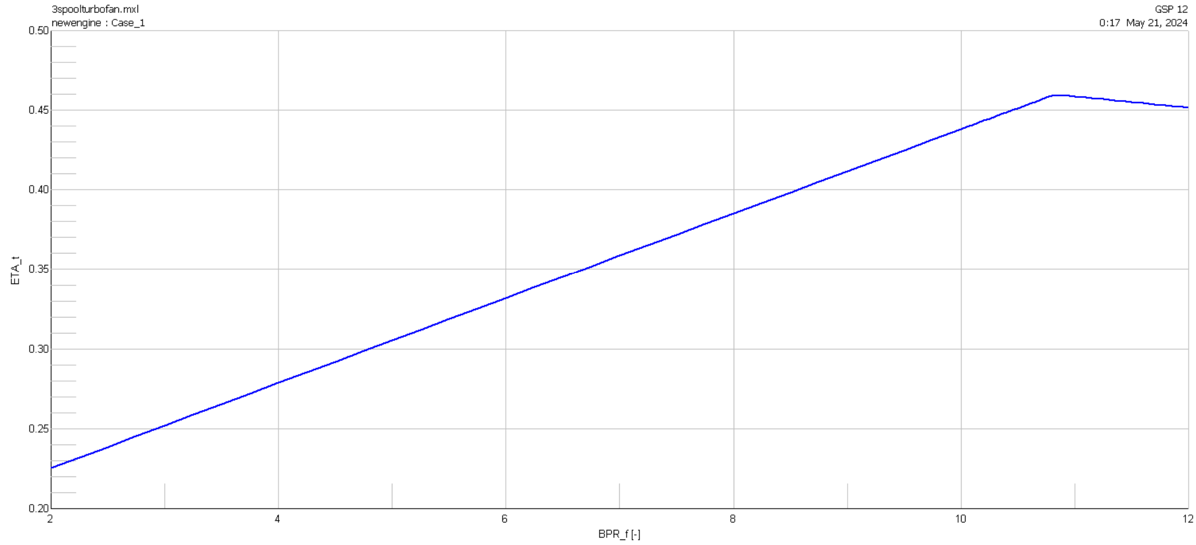

Figure 50:BPR vs ETA_t

BPR(Bypass ratio) vs ETA_p(Propulsive efficiency)

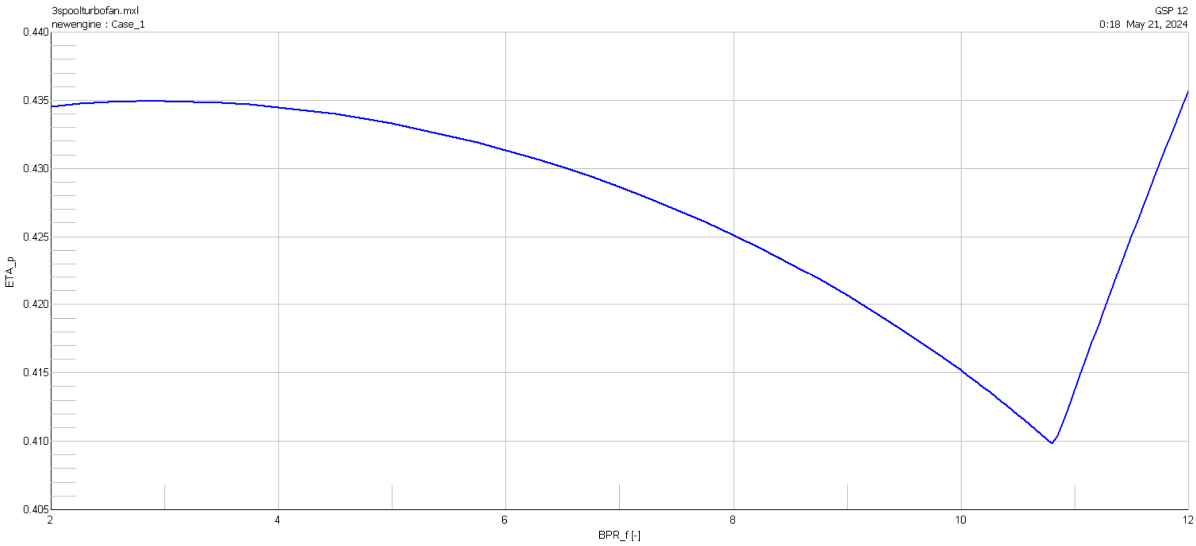

Figure 51:BPR vs ETA_p

BPR(Bypass ratio) vs ETA_o(Overall efficiency)

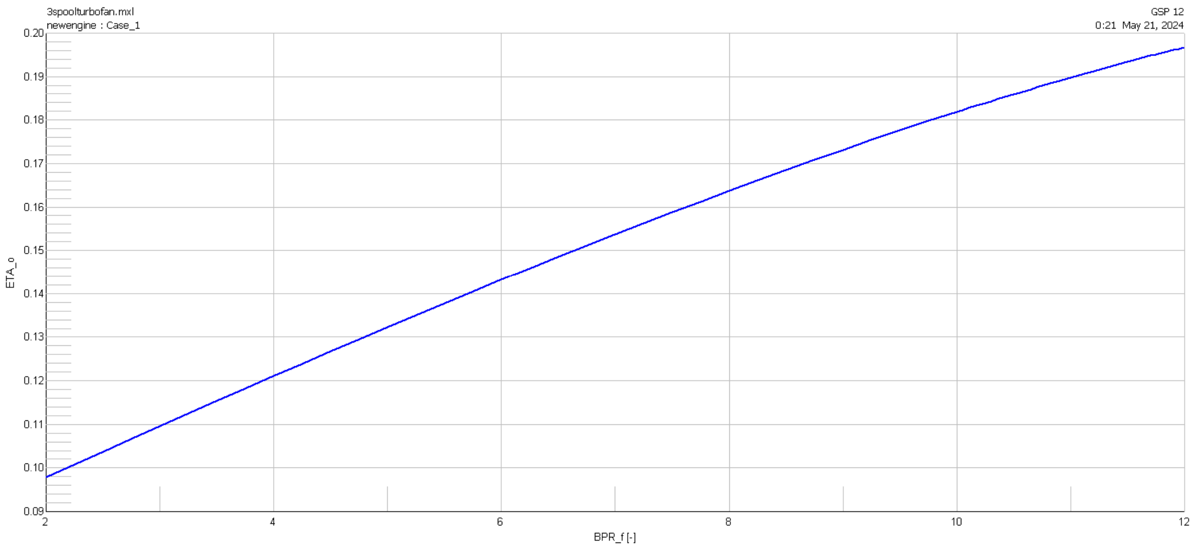

Figure 52:BPR vs ETA_o

BPR(Bypass ratio) vs ETA_II(Second law efficiency)

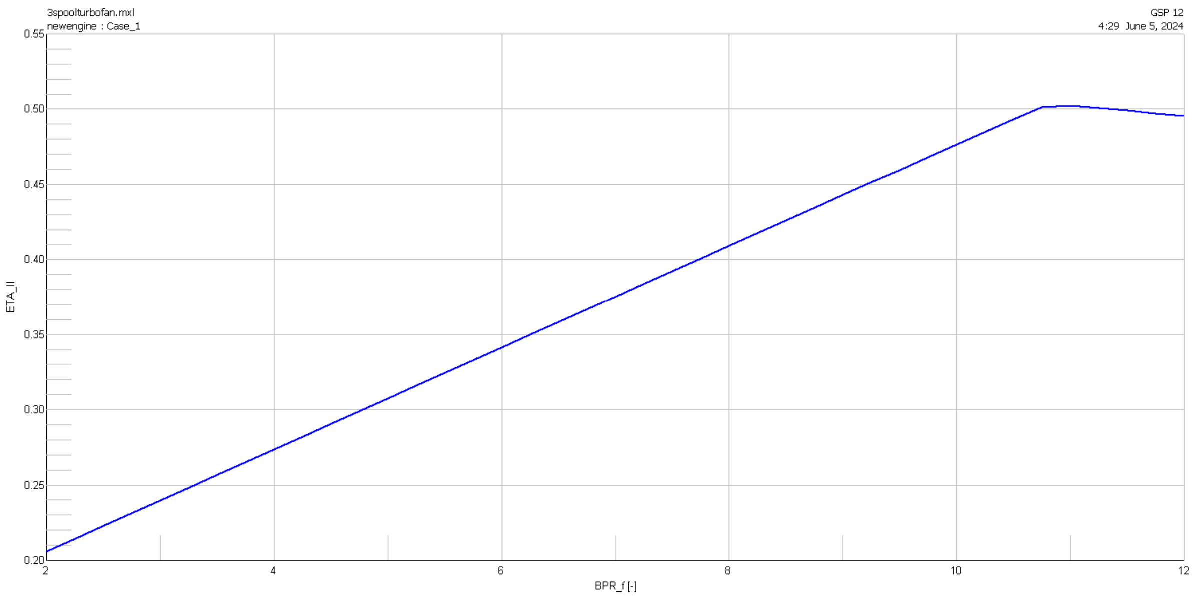

Figure 53:BPR vs ETA_II

4.5 Performance Analysis Report(Take-off)

4.5.1 TIT(Turbine Inlet Temperature)

The performance analysis was performed between temperatures of **1600K** and **2200K**. According to the results of the analysis,

-**FN(Thrust)** increases when **TIT** increases.

-**TSFC(Thrust specific fuel consumption)** increases when **TIT** increases

-$\boldsymbol{n_{thermal}}$**(Thermal efficiency)** increases when **TIT** increases up to about **1700K**. After **1700K**, $\boldsymbol{n_{thermal}}$ decreases when **TIT** increases.

-$\boldsymbol{n_{propulsive}}$**(Propulsive efficiency)** decreases with increasing **TIT** up to about **1700K**. After 1**700K**, $\boldsymbol{n_{propulsive}}$ increases with increasing **TIT**.

-$\boldsymbol{n_{overall}}$**(Overall efficiency)** decreases when **TIT** increases.

-$\boldsymbol{n_{II}}$**(Second-law efficiency)** increases with increasing **TIT** up to about **1700K**. After **1700K**, $\boldsymbol{n_{II}}$ decreases with increasing **TIT**.

4.5.2 π_{IPC}(Intermediate compressor pressure ratio)

The performance analysis was performed between pressure ratios of **6** and **15**. According to the results of the analysis,

-**FN(Thrust)** decreases when π_{IPC} increases.

-**TSFC(Thrust specific fuel consumption)** decreases when π_{IPC} increases.

-$\boldsymbol{n_{thermal}}$**(Thermal efficiency)** increases when π_{IPC} increases up to about **14.3**. After **14.3**, $\boldsymbol{n_{thermal}}$ remains approximately constant in the increase of π_{IPC}.

-The change in $\boldsymbol{n_{propulsive}}$**(Propulsive efficiency)** due to the increase in π_{IPC} is quite small; it is almost constant. Nevertheless, if we examine it, $\boldsymbol{n_{propulsive}}$ increases when π_{IPC} increases up to about **10**. $\boldsymbol{n_{propulsive}}$ decreases when π_{IPC} is between **10** and **14** and continues to increase after **14**.

-$\boldsymbol{n_{overall}}$**(Overall efficiency)** increases when π_{IPC} increases.

-$\boldsymbol{n_{II}}$**(Second-law efficiency)** increases when π_{IPC} increases up to about **14.3**. After **14.3**, $\boldsymbol{n_{II}}$ increases very slightly in the increase of π_{IPC}.

4.5.3 π_{HPC}(High compressor pressure ratio)

The performance analysis was performed between pressure ratios of **2** and **6**. According to the results of the analysis,

-**FN(Thrust)** decreases when π_{HPC} increases.

-**TSFC(Thrust specific fuel consumption)** decreases when π_{HPC} increases.

-$n_{thermal}$**(Thermal efficiency)** increases when π_{HPC} increases up to about **4.9**. After **4.9**, $n_{thermal}$ remains approximately constant in the increase of π_{HPC}.

-$n_{propulsive}$**(Propulsive efficiency)** increases when π_{HPC} increases up to **3.5**. $n_{propulsive}$ decreases when π_{HPC} is between **3.5** and **4.9** and continues to increase after **4.9**.

-$n_{overall}$**(Overall efficiency)** increases when π_{HPC} increases.

-n_{II}**(Second-law efficiency)** increases when π_{HPC} increases up to about **4.9**. After **4.9**, n_{II} increases very slightly in the increase of π_{HPC}.

4.5.4 π_{fan}(Fan pressure ratio)

The performance analysis was performed between pressure ratios of **1.1** and **1.6** with **7** different **TIT(Turbine inlet temperature)** values of **1600K 1700K 1800K 1900K 2000K 2100K 2200K**.According to the results of the analysis,

-**FN(Thrust)** increases when π_{fan} increases. **FN** is highest when **TIT is 2200K**

-**TSFC(Thrust specific fuel consumption)** decreases when π_{fan} increases. **TSFC** is lowest when **TIT** is **1600K**.

-When **TIT** is at **1600K** and π_{fan} increases until about **1.44**, $n_{thermal}$**(Thermal efficiency)** increases.After **1.44**, $n_{thermal}$ begins to decrease with increasing π_{fan}.Similarly, when **TIT** is at **1700K** and π_{fan} increases until about **1.54**, $n_{thermal}$ increases.After **1.54**, $n_{thermal}$ begins to decrease with increasing π_{fan}. It can be concluded that at higher **TIT** values, the break occurs at higher π_{fan} values and $n_{thermal}$ increases up to higher π_{fan} values, but again, the highest $n_{thermal}$ values are seen when **TIT** is **1600K**.

-The variation and characteristic of $n_{propulsive}$**(Propulsive efficiency)** with increasing π_{fan} for each **TIT** value is somewhat complex, but generally speaking, $n_{propulsive}$ increases with increasing π_{fan} for each **TIT** value up to about **1.2**. After **1.2**, $n_{propulsive}$ tends to decrease. $n_{propulsive}$ is highest when **TIT** is **1600K**.

-For each **TIT** value, $n_{overall}$**(Overall efficiency)** increases as π_{fan} increases. $n_{overall}$ is highest when **TIT** is **1600K**.

-When **TIT** is at **1600K** and π_{fan} increases until about **1.44**, n_{II}**(Second-law efficiency)** increases.After **1.44**, n_{II} begins to decrease with increasing π_{fan}.Similarly, when **TIT** is at **1700K** and π_{fan} increases until about **1.54**, n_{II} increases.After **1.54**, n_{II} begins to decrease with increasing π_{fan}. It can be concluded that at higher **TIT** values, the break occurs at higher π_{fan} values and n_{II} increases up to higher π_{fan} values, but again, the highest n_{II} values are seen when **TIT** is **1600K**.

4.5.5 OPR(Overall pressure ratio)

The performance analysis was performed between pressure ratios of about **40** and **55**. According to the results of the analysis,

-**SFN(Specific thrust)** decreases when **OPR** increases.

-**TSFC(Thrust specific fuel consumption)** decreases when **OPR** increases.

-$n_{thermal}$**(Thermal efficiency)** increases when **OPR** increases.

-The change in $n_{propulsive}$**(Propulsive efficiency)** due to the increase in **OPR** is quite small; it is almost constant. Nevertheless, if we examine it, $n_{propulsive}$ increases when **OPR** increases up to about **51**. After **51**, $n_{propulsive}$ starts to decrease with increasing **OPR**.

-$n_{overall}$**(Overall efficiency)** increases when **OPR** increases.

-n_{II}**(Second-law efficiency)** increases when **OPR** increases.

4.5.6 BPR(Bypass ratio)

The performance analysis was performed between bypass ratios of **2** and **12**. According to the results of the analysis,

-**SFN(Specific thrust)** decreases when **BPR** increases.

-**TSFC(Thrust specific fuel consumption)** decreases when **BPR** increases.

-$n_{thermal}$**(Thermal efficiency)** increases when **BPR** increases up to about **10.8**. After **10.8**, $n_{thermal}$ decreases with increasing **BPR**.

-$n_{propulsive}$**(Propulsive efficiency)** decreases when **BPR** increases up to about **10.8**. After **10.8**, $n_{propulsive}$ increases with increasing **BPR**.

-$n_{overall}$**(Overall efficiency)** increases when **BPR** increases.

-n_{II}**(Second-law efficiency)** increases when **BPR** increases up to about **10.8**. After **10.8**, n_{II} decreases with increasing **BPR**.

4.6 Cruise condition(0.85M at 12000m)

Station No.	Total Temperature (K)	Total Pressure (bar)	Entropy (kJ/kg*K)	Specific Heat Ratio
1	247.96	0.31002	7.01927	1.400917
2	247.96	0.30382	7.02486	1.400917
3	283.01	0.46789	7.03360	1.40034
4	283.01	0.45385	7.04234	1.40034
5	561.23	4.36151	7.08881	1.380114
6	799.94	14.7419	7.11794	1.353659
7	1500.00	14.59449	7.96966	1.295557
8	1299.60	7.43742	7.98425	1.303199
9	1071.31	3.06669	8.00391	1.316155
10	744.49	0.61784	8.04289	1.344988
11	744.49	0.60548	8.04870	1.344988
12	744.49	0.58561	8.04289	1.357087
13	283.01	0.45385	7.04234	1.40034
14	283.01	0.4385	7.03360	1.40267

Table 8:Temperatures, pressures, entropies, and specific heat ratios at engine sections during cruise

At cruise condition, the thermal, propulsive, and overall efficiencies are calculated as follows:

$$\eta_{thermal} = 0.44205 \cong 0.442$$

$$\eta_{propulsive} = 0.84768 \cong 0.848$$

$$\eta_{overall} = 0.37472 \cong 0.375$$

4.7 Specific Heat Ratio(Cruise)

The temperatures with specific heat ratios during the cruise condition are shown below.

Station No.	Temperature (K)	Specific heat ratio
1	247.96	1.400917
2	247.96	1.400917
3	283.01	1.40034
4	283.01	1.40034
5	561.23	1.380114
6	799.94	1.353659
7	1500.00	1.295557
8	1299.60	1.303199
9	1071.31	1.316155
10	744.49	1.344988
11	744.49	1.344988
12	638.41	1.357087
13	283.01	1.40034
14	238.09	1.40267

Table 9:Temperatures and specific heat ratios at engine sections during cruise

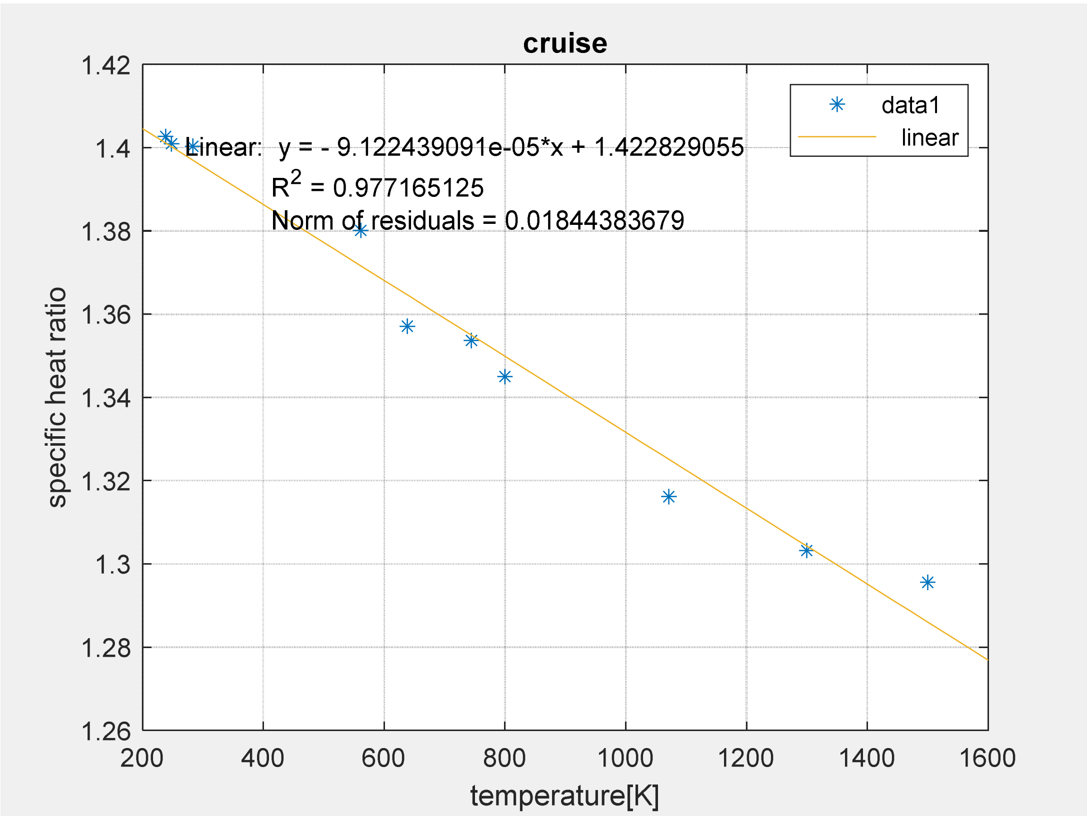

Figure 53:Linear regression curve for cruise condition

Applying linear regression analysis using MATLAB on the data given in **Table 9**, the equation of the line shown in **Figure 53** is:

$$y = -9.122439091e - 05x + 1.422829055$$

or

$$\gamma(T) = (-9.122439091 * 10^{-5})T + 1.422829055$$

$$where\ \boldsymbol{T}\ is\ in\ \boldsymbol{K}$$

Therefore,the specific heat can be determined as

$$c_p(T) = \frac{R\gamma(T)}{\gamma(T) - 1}$$

where

$$R = 0.28705 \frac{kJ}{kg * K}$$

T-s diagram of Cruise condition is shown in **Figure 54**.

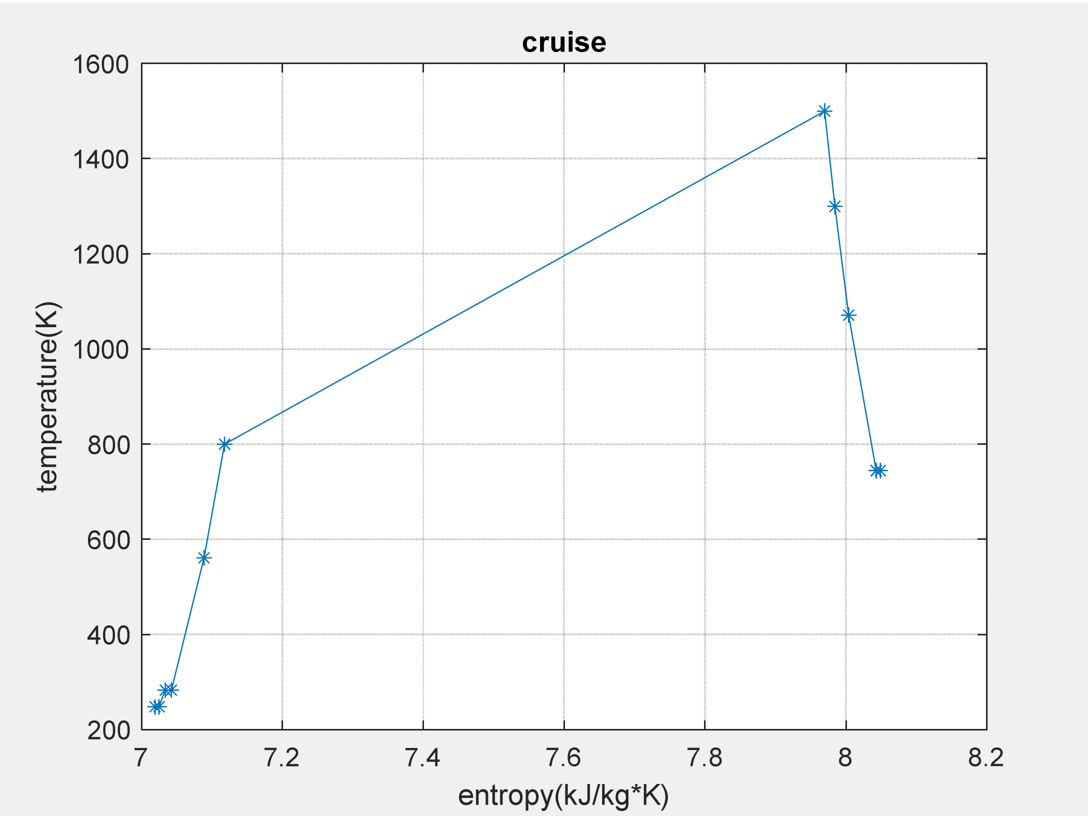

Figure 54:T-s diagram of Cruise condition

4.8 Second Law Analysis of Cruise Condition

4.8.1 Flow Exergies at Cruise Condition

The ambient conditions during cruise is shown below.

$$T_0 = 216.65\ K, P_0 = 0.1933\ bar, s_0 = 7.01927\ \frac{kJ}{kg * K}$$

The exergies of the fluid streams at each section are shown in **Table 6**.

Station No.	**Exergy (kJ/kg)**
1	**149.08479**
2	**147.87371**
3	**181.28106**
4	**179.38754**
5	**456.92183**
6	**708.53382**
7	**1349.44815**
8	**1098.47618**
9	**823.55935**
10	**447.26004**
11	**446.00131**
12	**447.26004**
13	**179.38754**
14	**181.28106**

Table 10:Exergies of fluid stream at engine sections during cruise

4.8.2 Second-Law Efficiencies at Cruise Condition

The second law efficiency, or the exergy efficiency, of the components of the engine is shown in **Table 7**.

Components	Second-Law Efficiency
Inlet	**0.992**
Fan	**0.950**
IPC	**0.979**
HPC	**0.984**
Combustor	**0.717**
HPT	**0.987**
IPT	**0.984**
LPT	**0.978**
Bypass duct	**0.989**
Cold core duct	**0.989**
Hot core duct	**0.997**
Cold exhaust nozzle	**0.249**
Hot exhaust nozzle	**0.262**

Table 11:Second-law efficiencies of engine components

At cruise condition, the second law efficiency of the engine is calculated as follows:

$$\eta_{\mathrm{II}} = 0.26529 \cong 0.265$$

4.9 2D Performance Analysis(Cruise)

4.9.1 Turbine Inlet Temperature(TIT or T_7) Effect

TIT(Turbine inlet temperature) vs Thrust

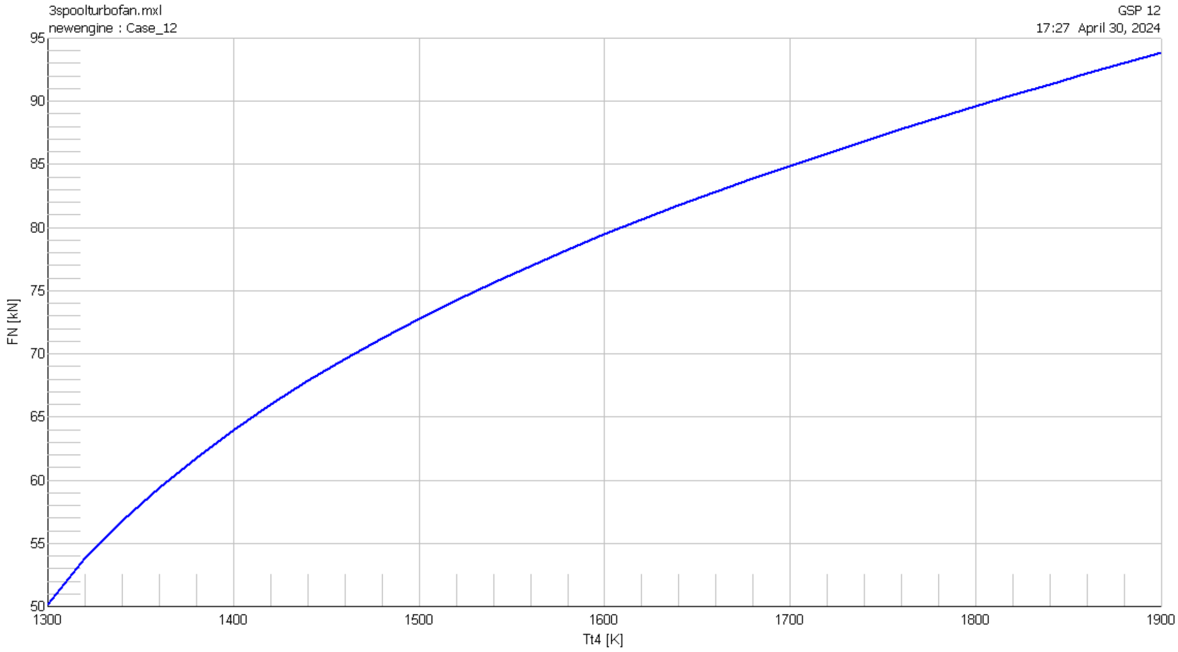

Figure 55:TIT vs Thrust

TIT(Turbine inlet temperature) vs TSFC(Thrust specific fuel consumption)

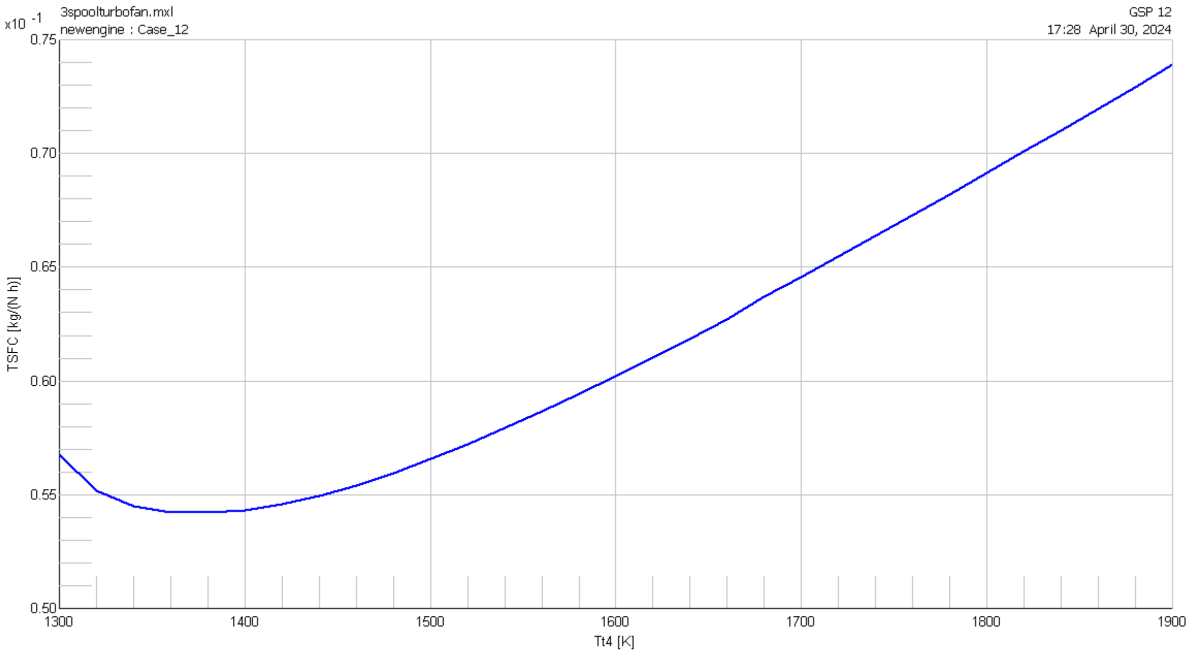

Figure 56:TIT vs TSFC

TIT(Turbine inlet temperature) vs ETA_t(Thermal efficiency)

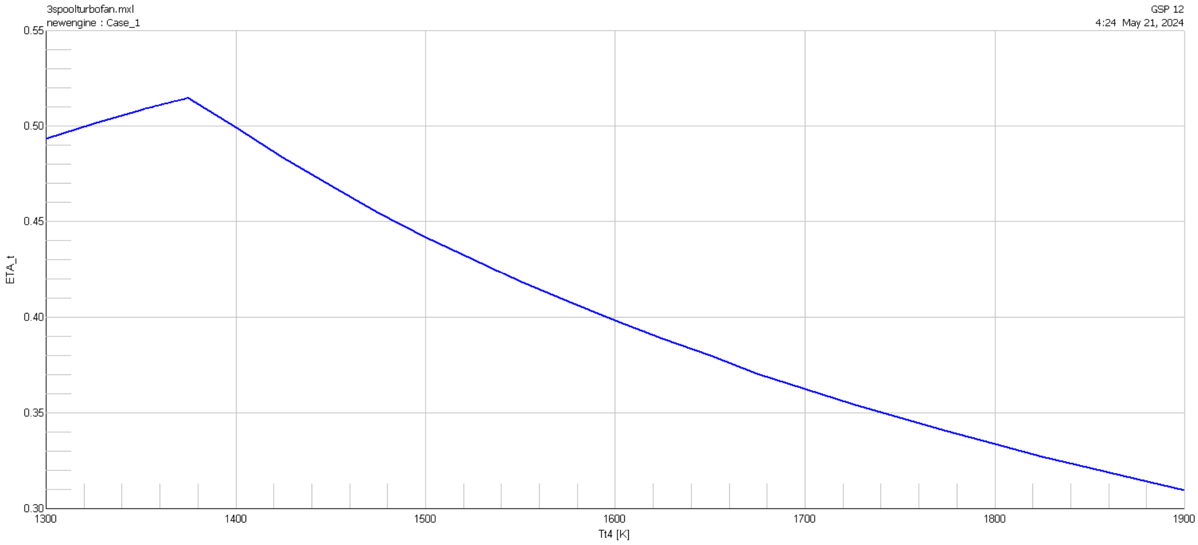

Figure 57:TIT vs ETA_t

TIT(Turbine inlet temperature) vs ETA_p(Propulsive efficiency)

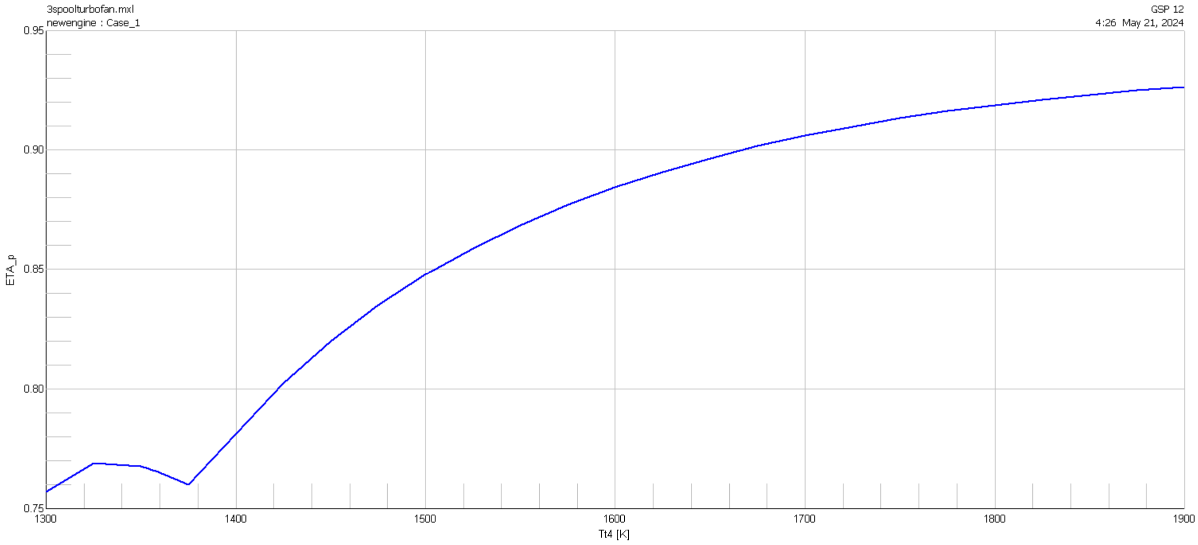

Figure 58:TIT vs ETA_p

TIT(Turbine inlet temperature) vs ETA_o(Overall efficiency)

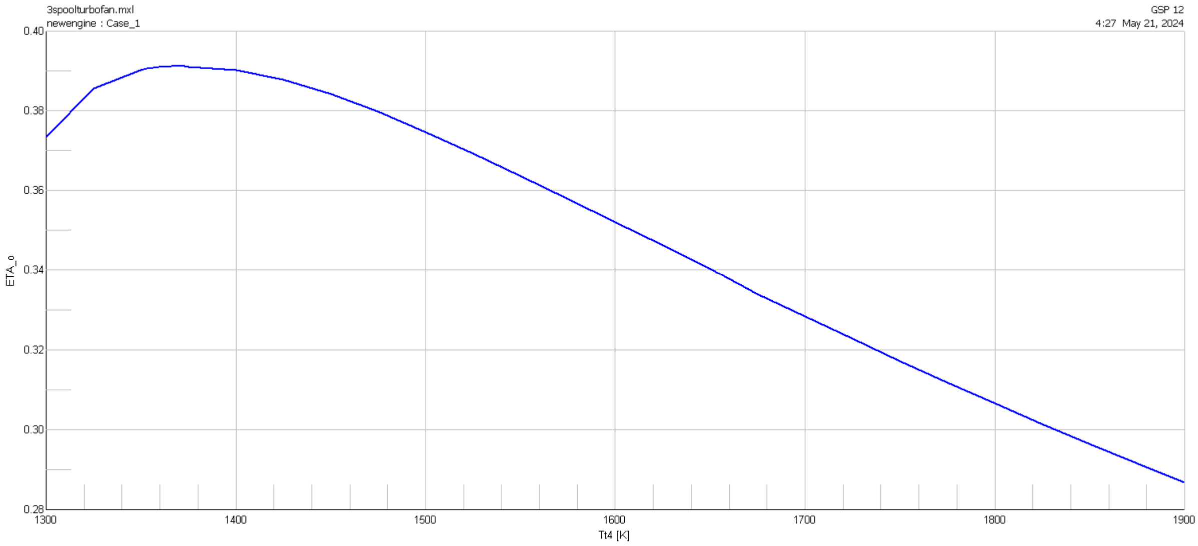

Figure 59:TIT vs ETA_o

TIT(Turbine inlet temperature) vs ETA_II(Second law efficiency)

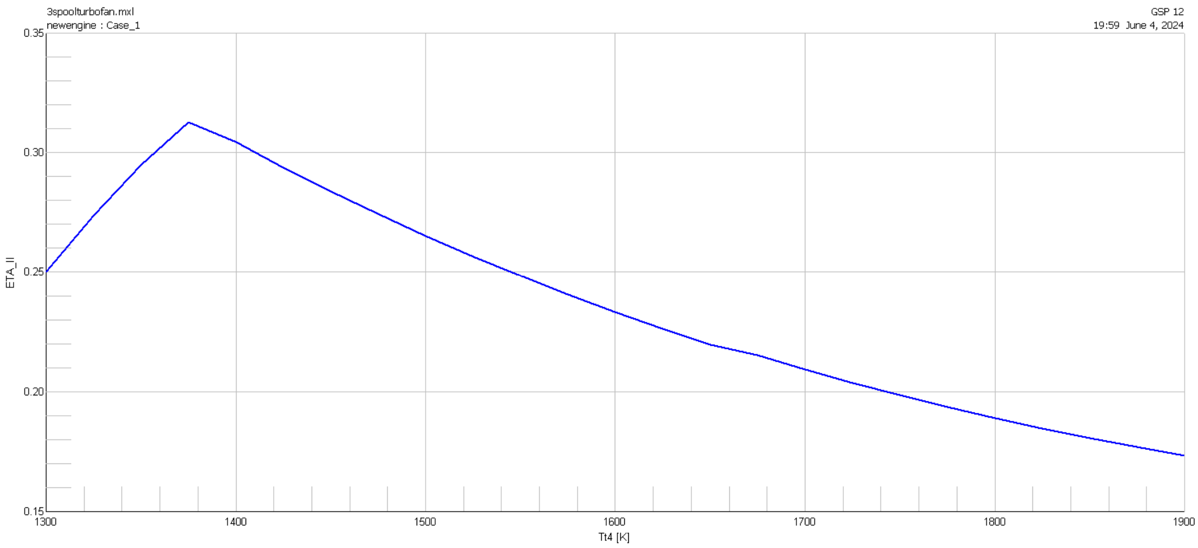

Figure 60:TIT vs ETA_II

4.9.2 Intermediate Compressor Pressure Ratio(π_{IPC}) Effect

π_{IPC}(Intermediate compressor pressure ratio) vs FN(Thrust)

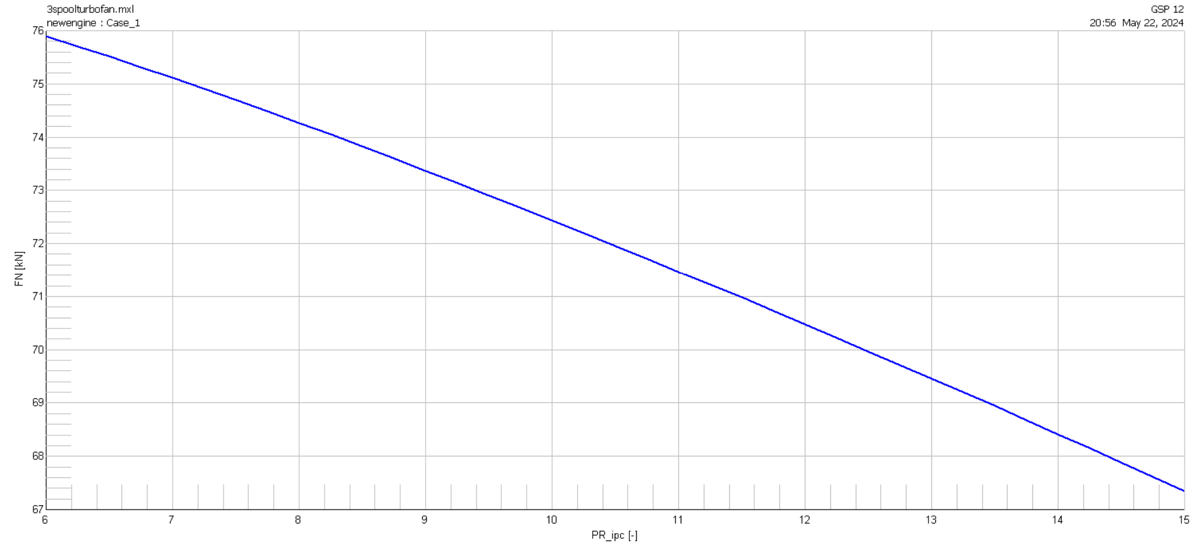

Figure 61: π_{IPC} vs FN

π_{IPC}(Intermediate compressor pressure ratio) vs TSFC(Thrust specific fuel consumption)

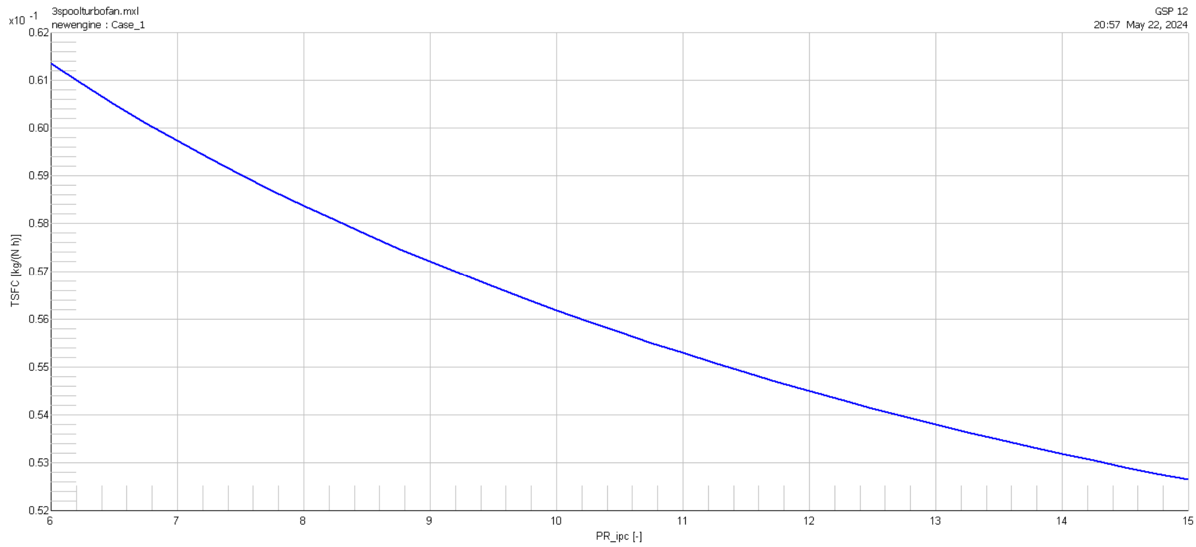

Figure 62: π_{IPC} vs TSFC

π_{IPC}(Intermediate compressor pressure ratio) vs ETA_t(Thermal efficiency)

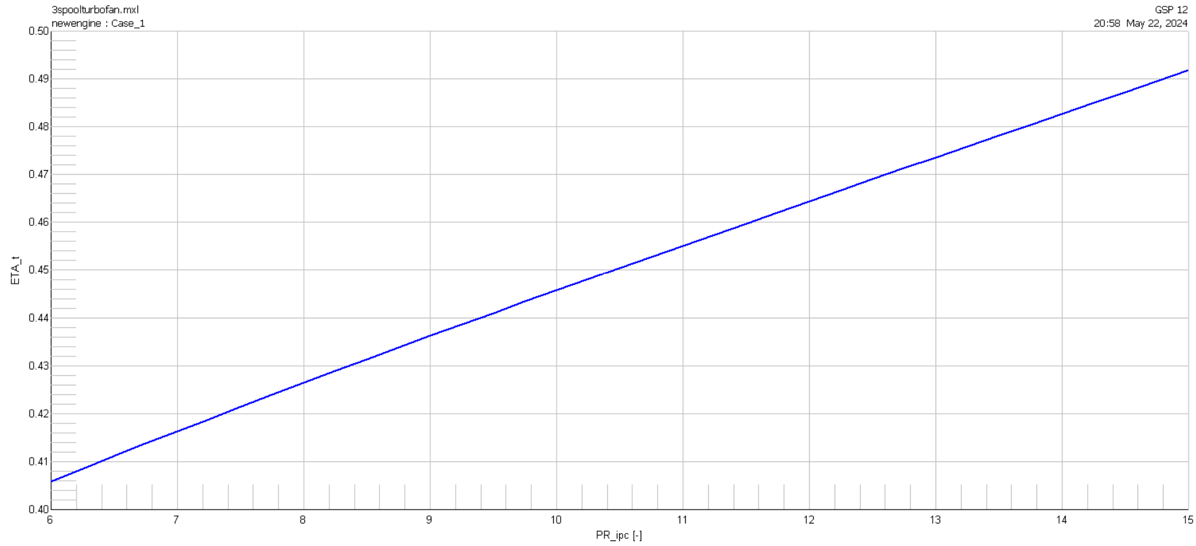

Figure 63: π_{IPC} vs ETA_t

π_{IPC}(Intermediate compressor pressure ratio) vs ETA_p(Propulsive efficiency)

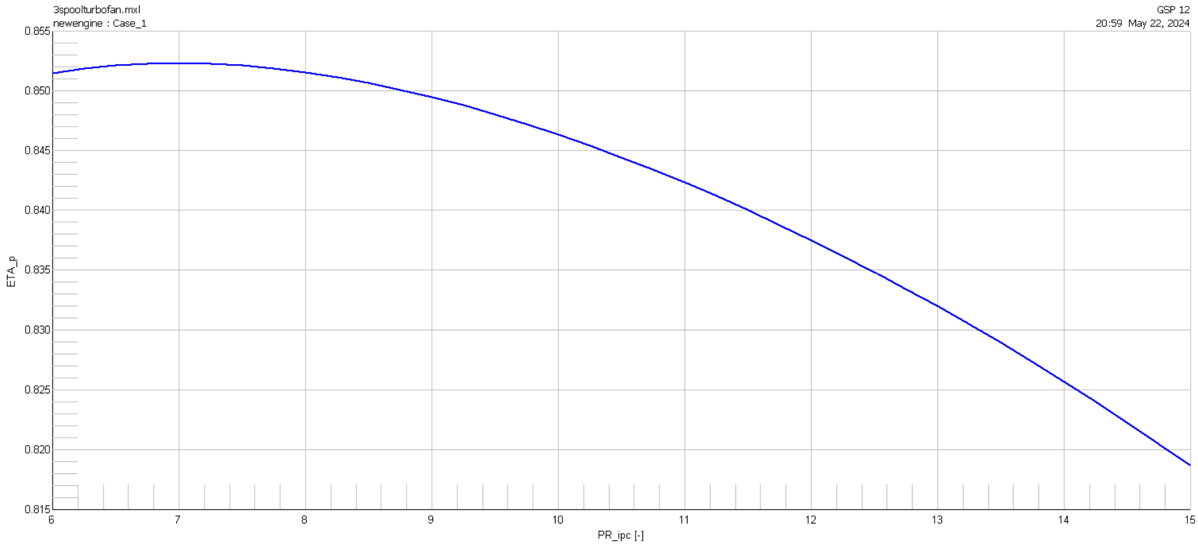

Figure 64: π_{IPC} vs ETA_p

π_{IPC}(Intermediate compressor pressure ratio) vs ETA_o(Overall efficiency)

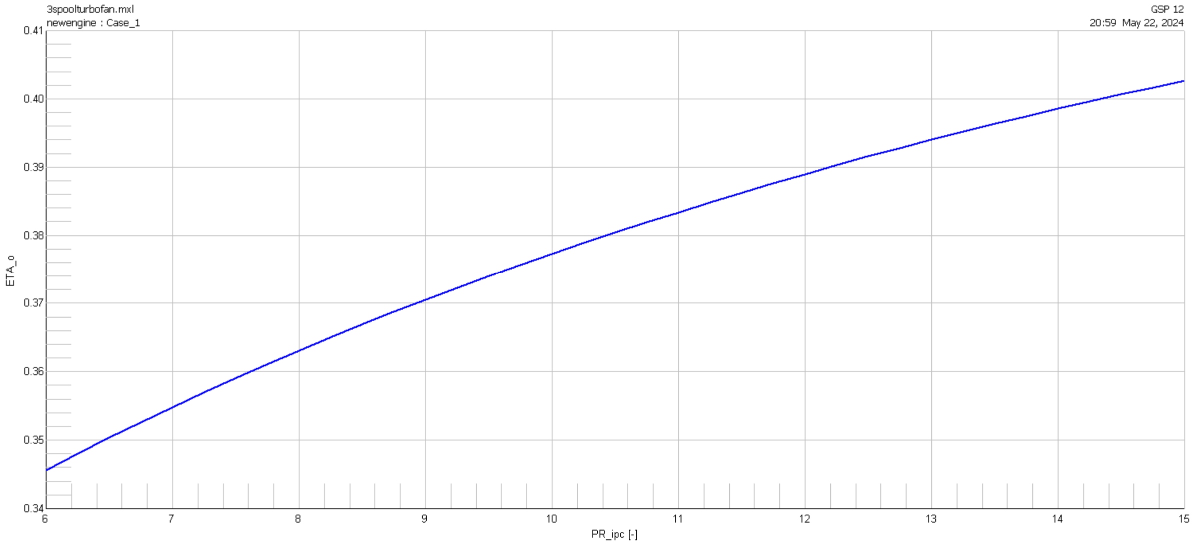

Figure 65: π_{IPC} vs ETA_o

π_{IPC}(Intermediate compressor pressure ratio) vs ETA_II(Second law efficiency)

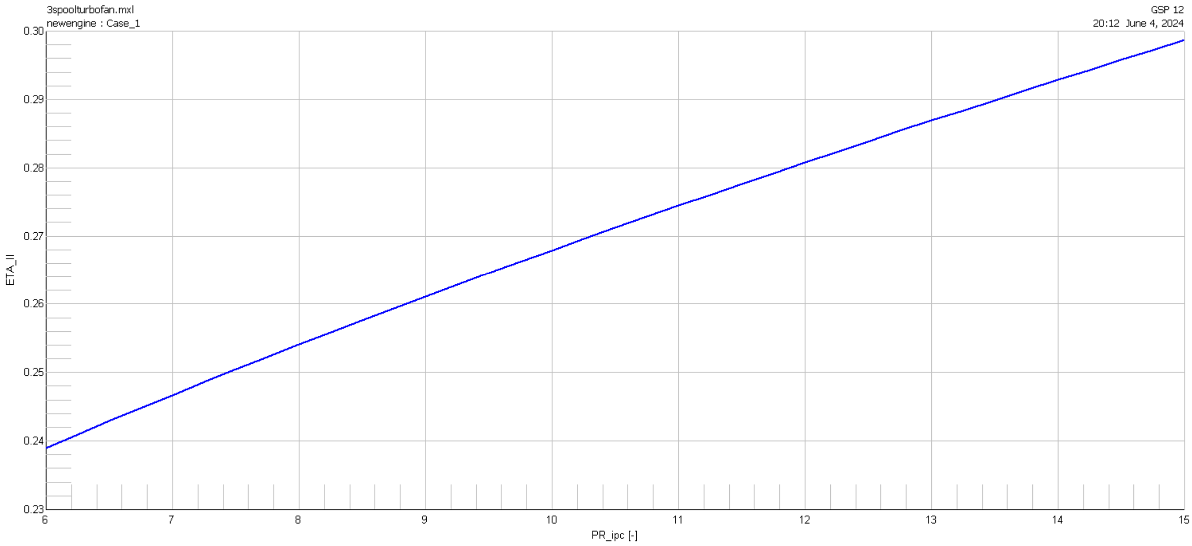

Figure 66: π_{IPC} vs ETA_II

4.9.3 High Compressor Pressure Ratio(π_{HPC}) Effect

π_{HPC} (High compressor pressure ratio) vs FN(Thrust)

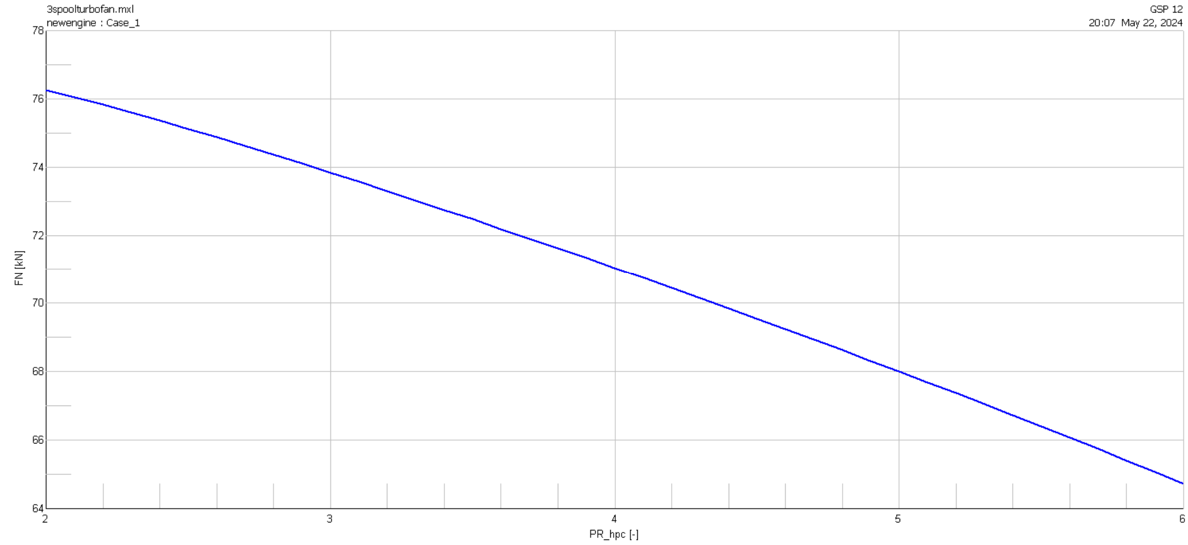

Figure 67: π_{HPC} vs FN

π_{HPC} (High compressor pressure ratio) vs TSFC(Thrust specific fuel consumption)

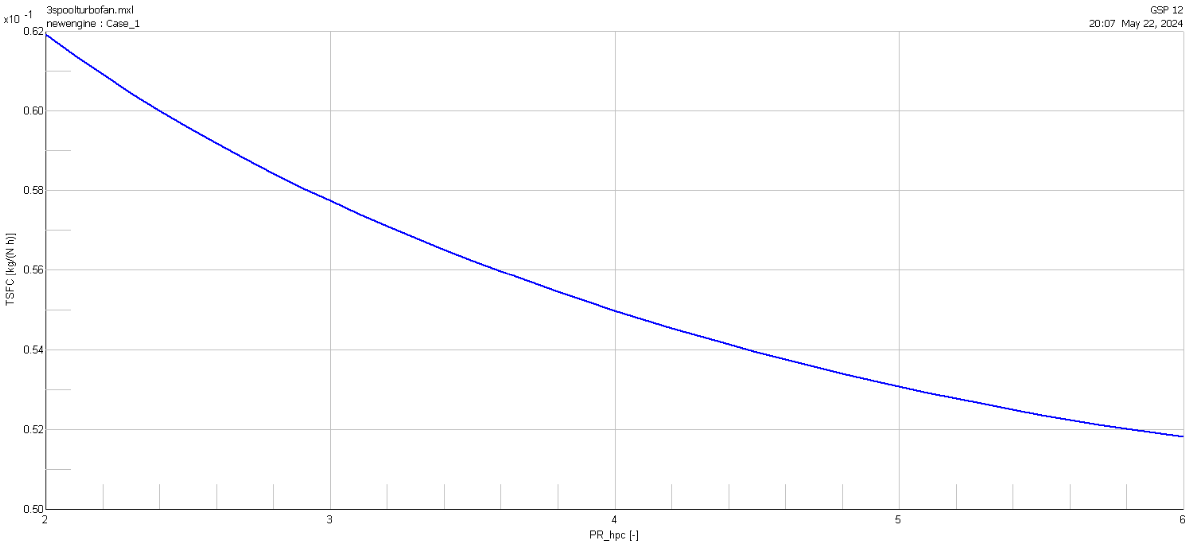

Figure 68: π_{HPC} vs TSFC

π_{HPC} (High compressor pressure ratio) vs ETA_t(Thermal efficiency)

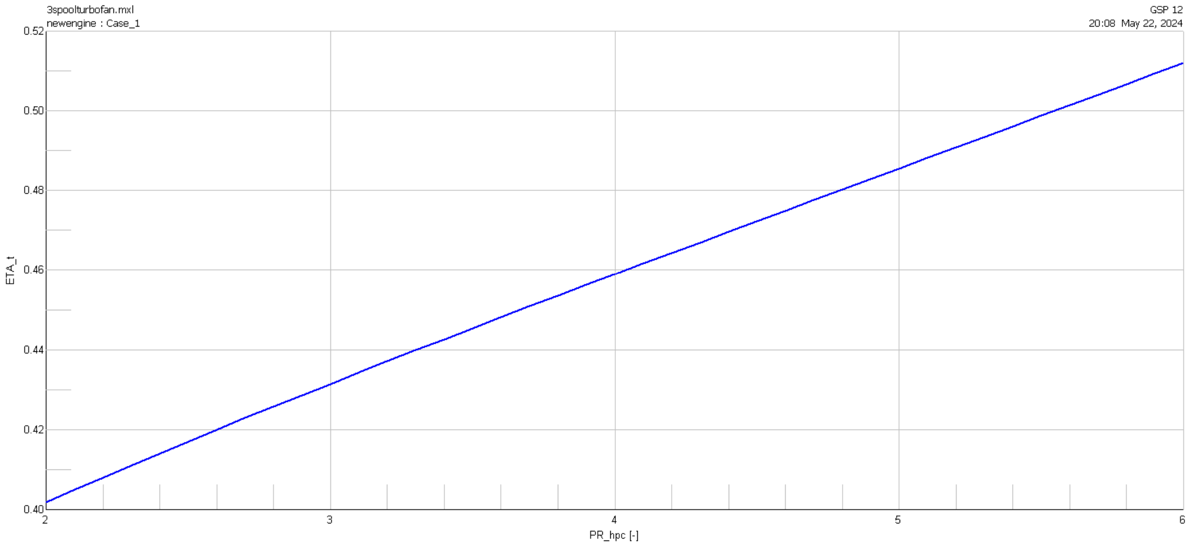

Figure 69: π_{HPC} vs ETA_t

π_{HPC} (High compressor pressure ratio) vs ETA_p(Propulsive efficiency)

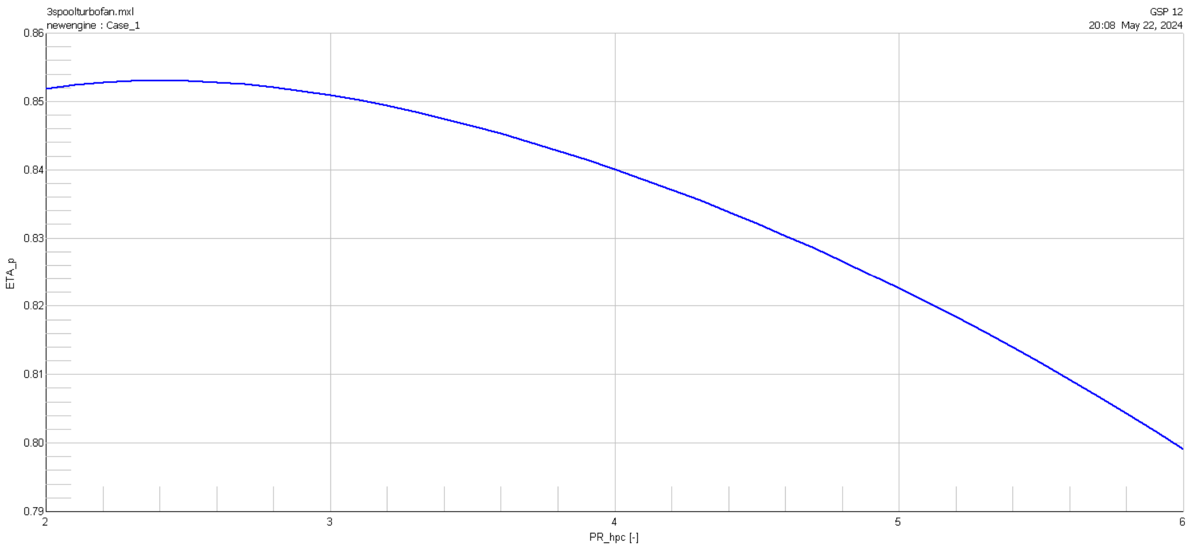

Figure 70: π_{HPC} vs ETA_p

π_{HPC} (High compressor pressure ratio) vs ETA_o(Overall efficiency)

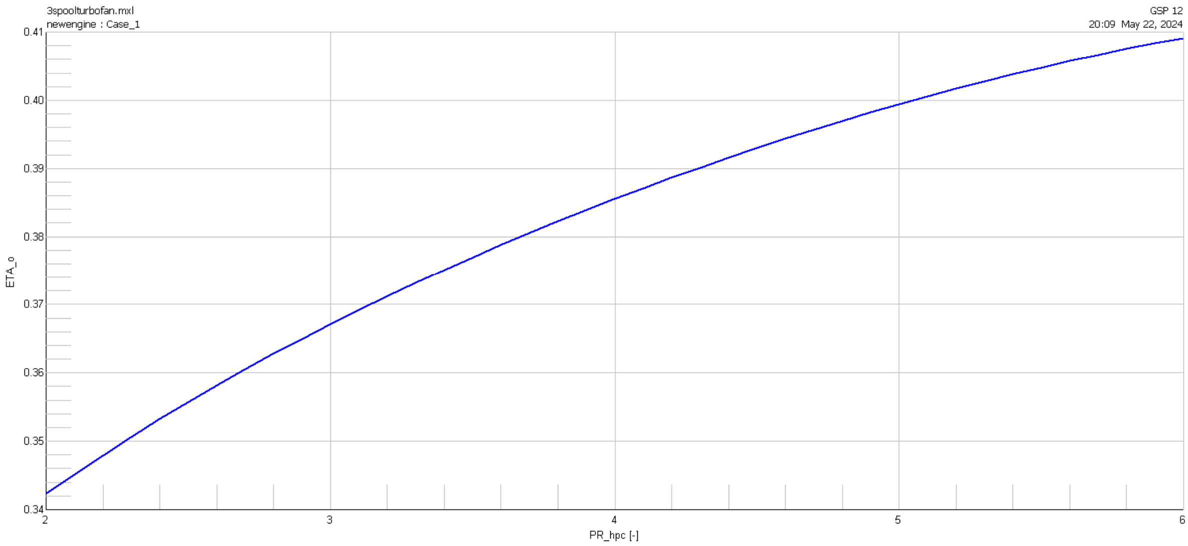

Figure 71: π_{HPC} vs ETA_o

π_{HPC} (High compressor pressure ratio) vs ETA_II(Second law efficiency)

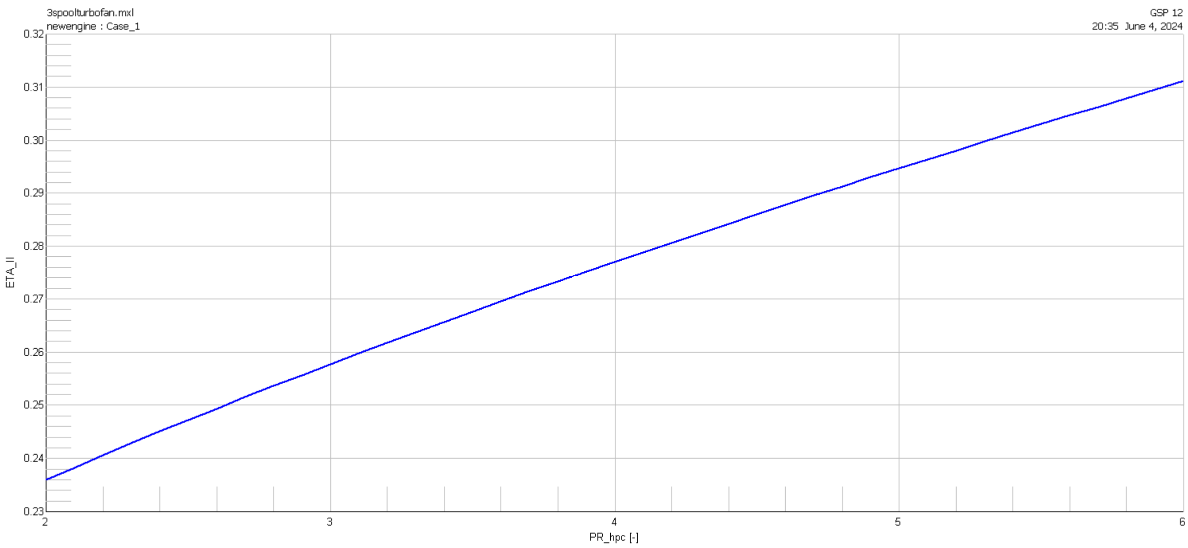

Figure 72: π_{HPC} vs ETA_II

4.9.4 Fan Pressure Ratio(π_{fan}) Effect

π_{fan} (Fan pressure ratio) vs FN(Thrust) vs TIT(Turbine inlet temperature)

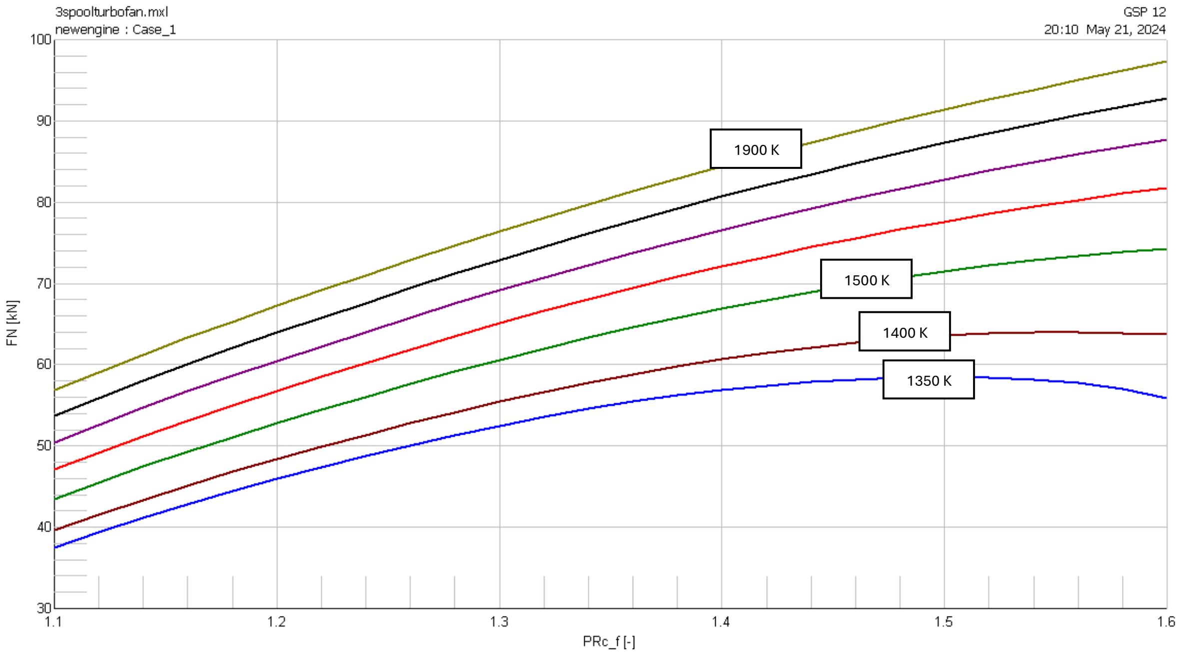

Figure 73: π_{fan} vs FN vs TIT

π_{fan} (Fan pressure ratio) vs TSFC(Thrust specific fuel consumption) vs TIT(Turbine inlet temperature)

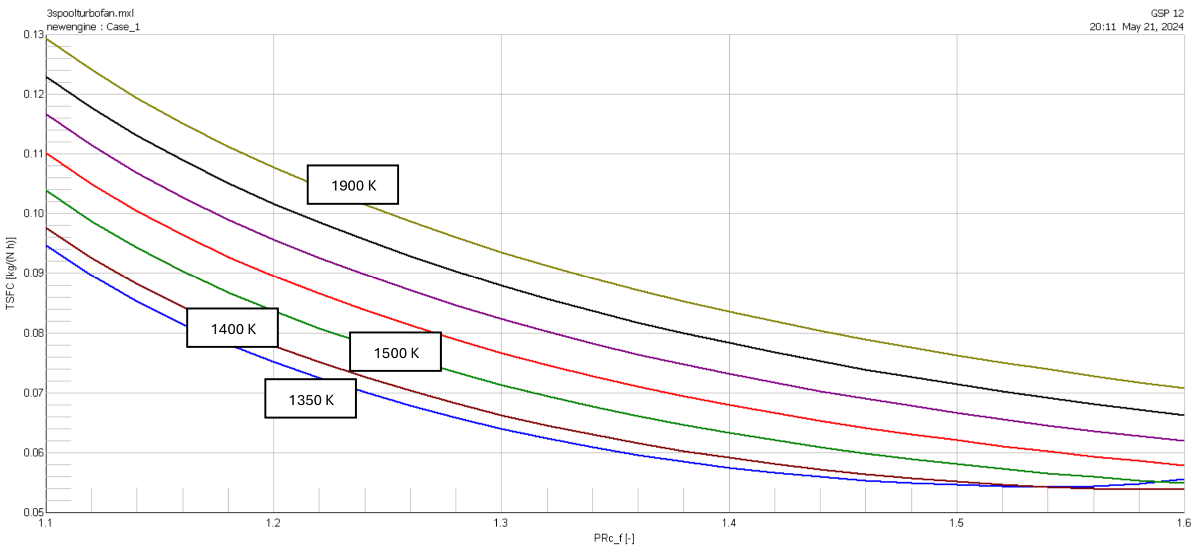

Figure 74: π_{fan} vs TSFC vs TIT

π_{fan} (Fan pressure ratio) vs ETA_t(Thermal efficiency) vs TIT(Turbine inlet temperature)

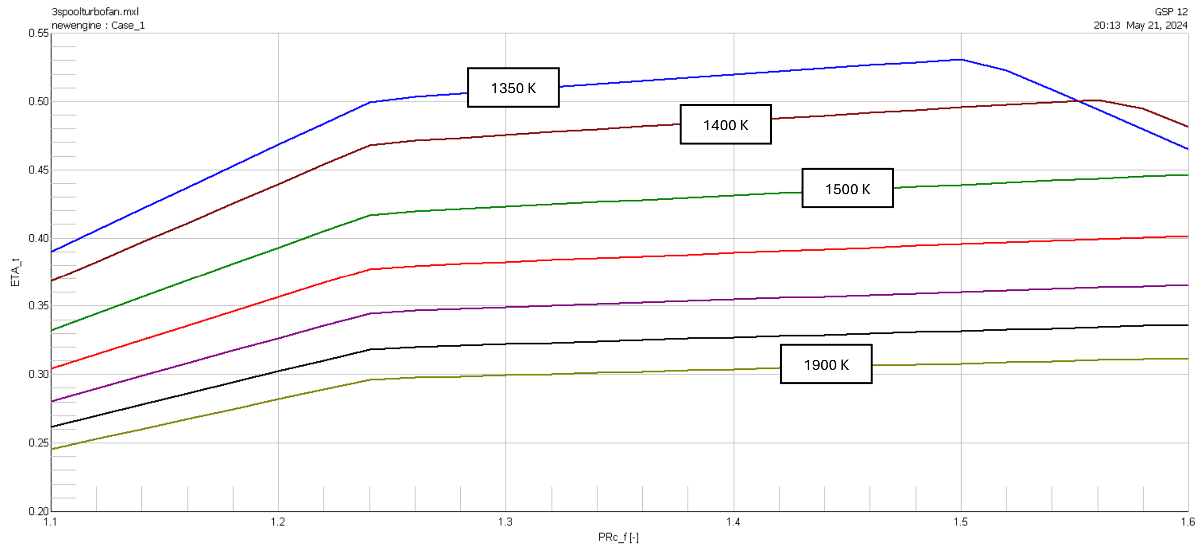

Figure 75: π_{fan} vs ETA_t vs TIT

π_{fan} (Fan pressure ratio) vs ETA_p(Propulsive efficiency) vs TIT(Turbine inlet temperature)

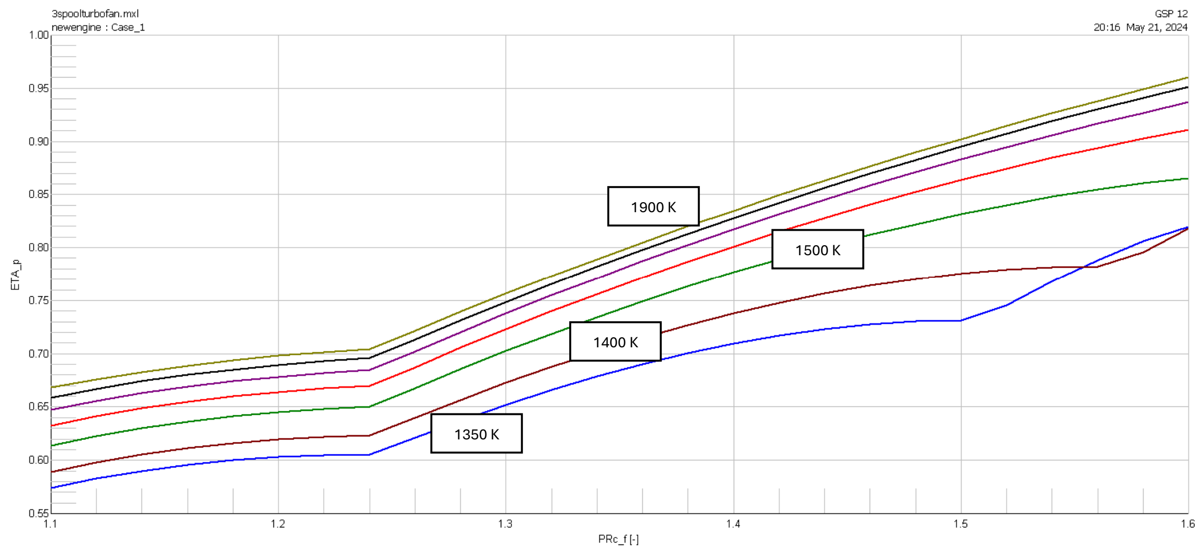

Figure 76: π_{fan} vs ETA_p vs TIT

π_{fan} (Fan pressure ratio) vs ETA_o(Overall efficiency) vs TIT(Turbine inlet temperature)

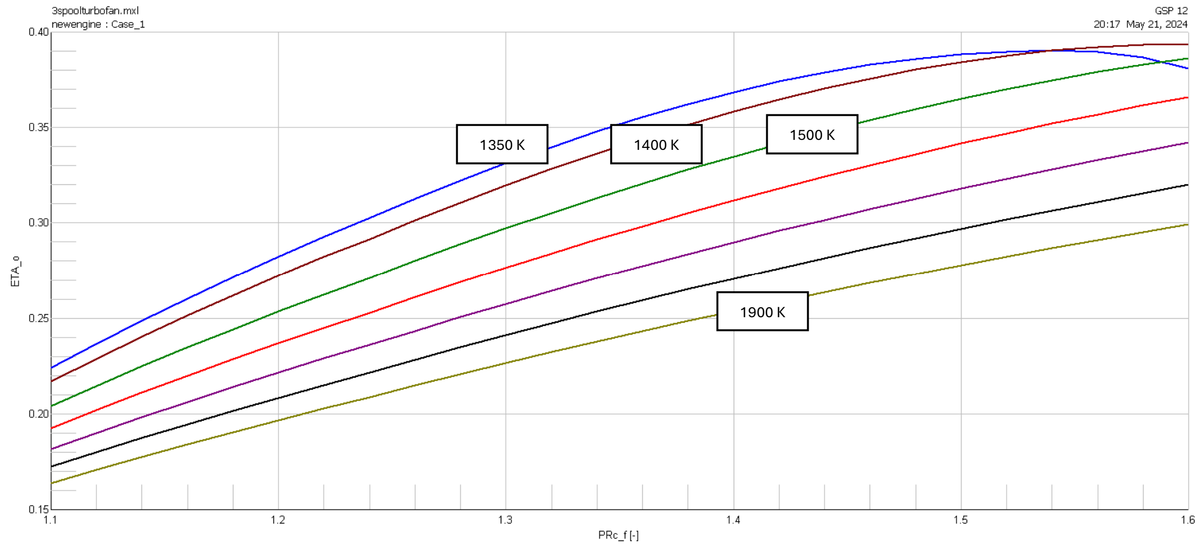

Figure 77: π_{fan} vs ETA_o vs TIT

π_{fan} (Fan pressure ratio) vs ETA_II(Second law efficiency) vs TIT(Turbine inlet temperature)

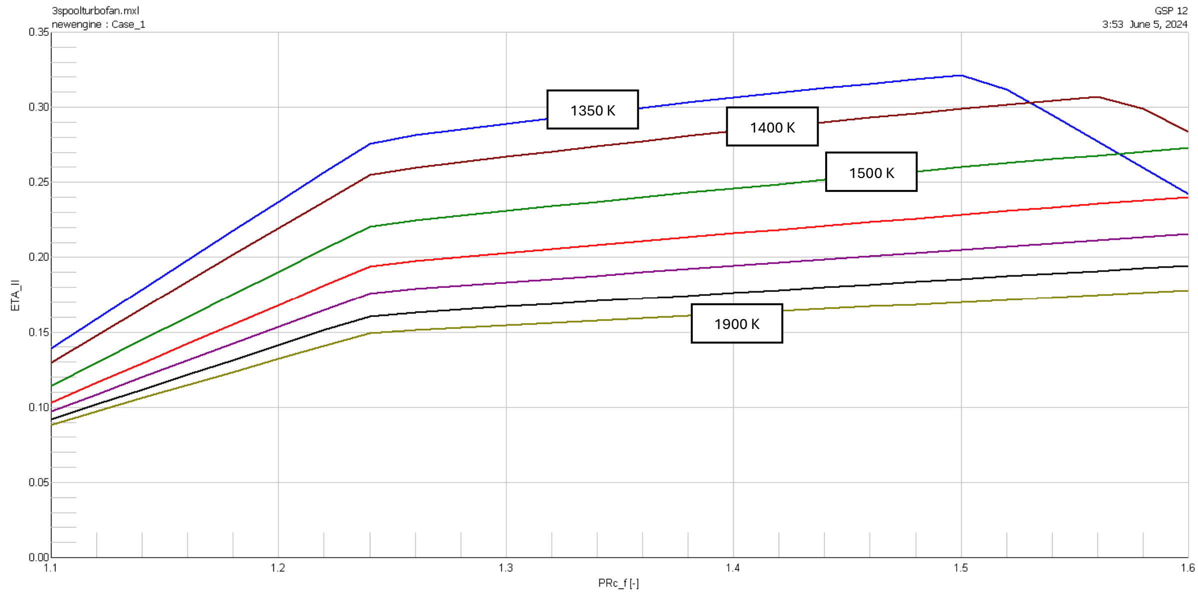

Figure 78: π_{fan} vs ETA_II vs TIT

4.9.5 OPR(Overall Pressure Ratio) Effect

OPR(Overall pressure ratio) vs SFN(Specific thrust)

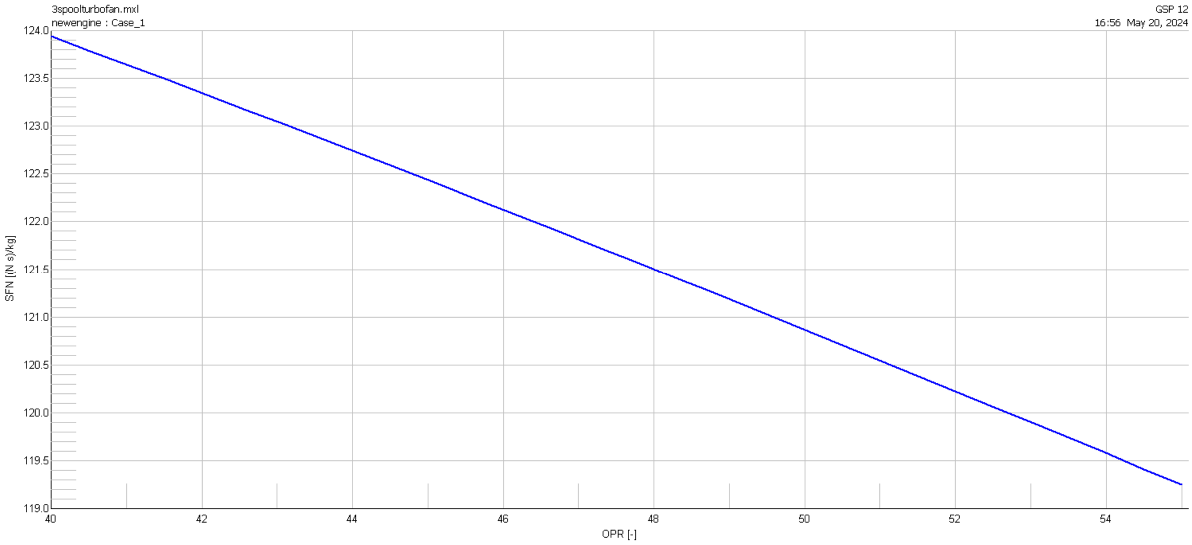

Figure 79:OPR vs SFN

OPR(Overall pressure ratio) vs TSFC(Thrust specific fuel consumption)

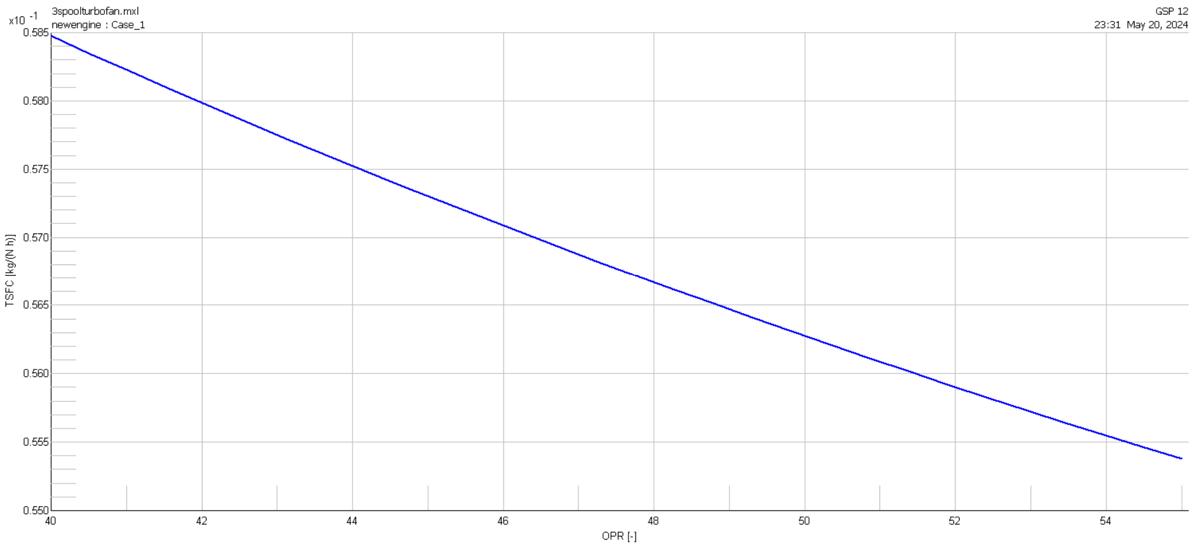

Figure 80:OPR vs TSFC

OPR(Overall pressure ratio) vs ETA_t(Thermal efficiency)

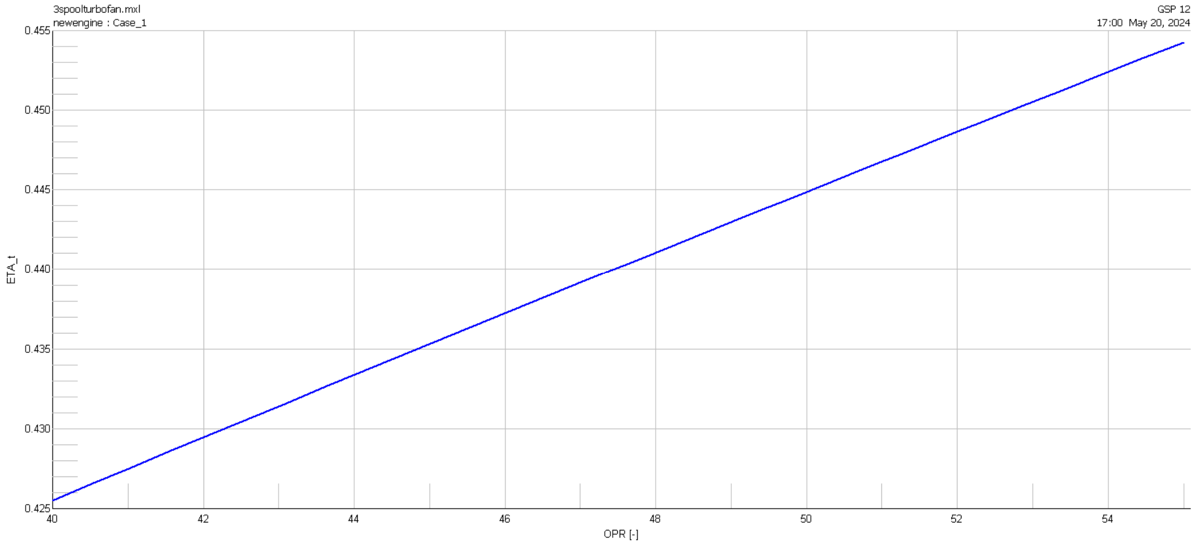

Figure 81:OPR vs ETA_t

OPR(Overall pressure ratio) vs ETA_p(Propulsive efficiency)

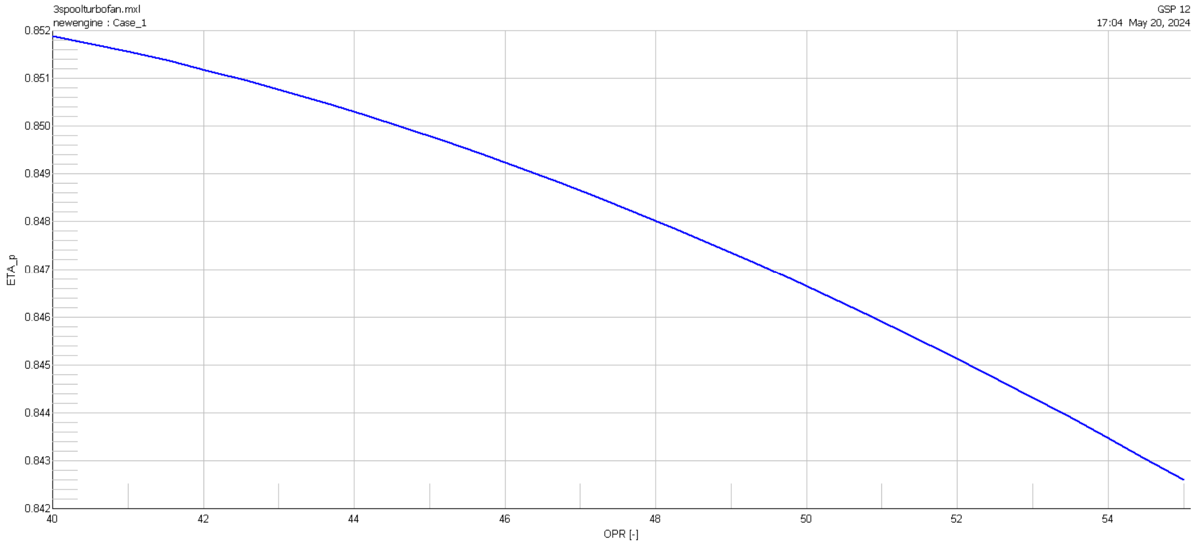

Figure 82:OPR vs ETA_p

OPR(Overall pressure ratio) vs ETA_o(Overall efficiency)

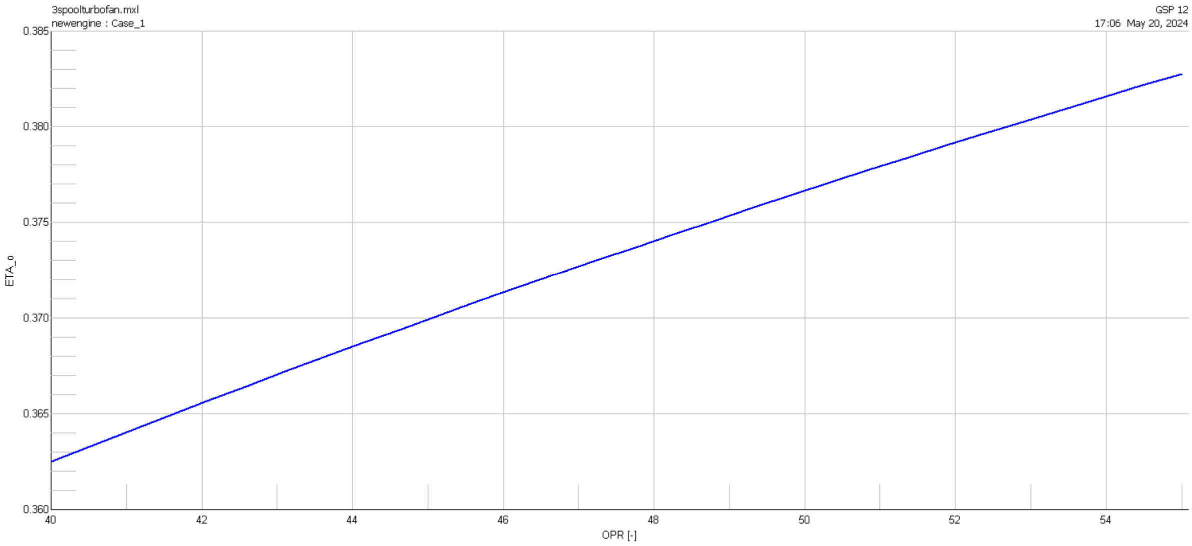

Figure 83:OPR vs ETA_o

OPR(Overall pressure ratio) vs ETA_II(Second law efficiency)

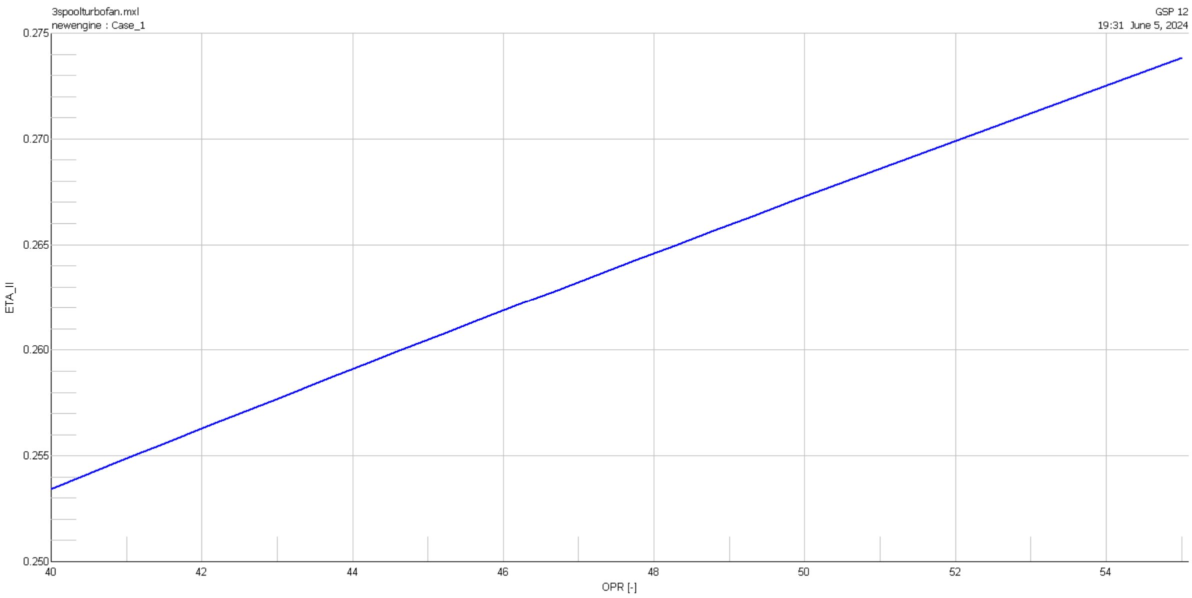

Figure 84: OPR vs ETA_II

4.9.6 BPR(Fan Bypass Ratio) Effect

BPR(Bypass ratio) vs SFN(Specific thrust)

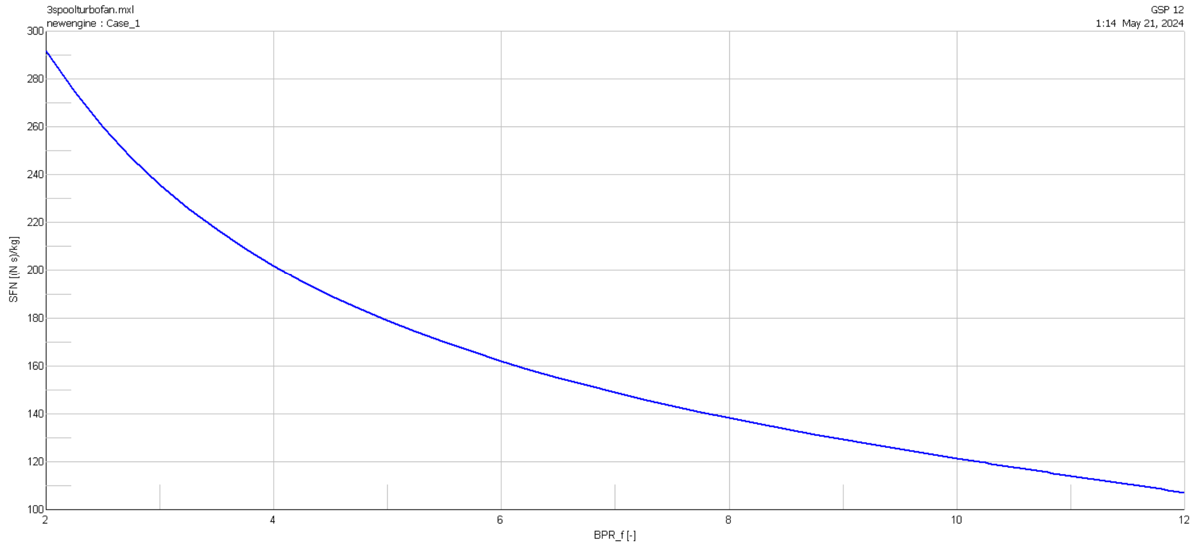

Figure 85:BPR vs Thrust

BPR(Bypass ratio) vs TSFC(Thrust specific fuel consumption)

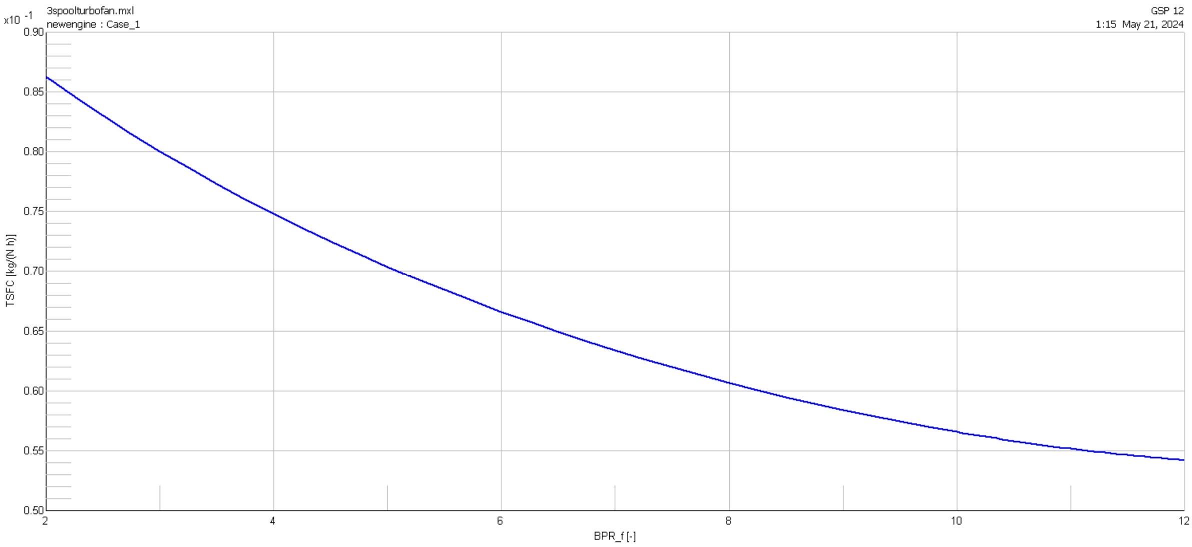

Figure 86:BPR vs TSFC

BPR(Bypass ratio) vs ETA_t(Thermal efficiency)

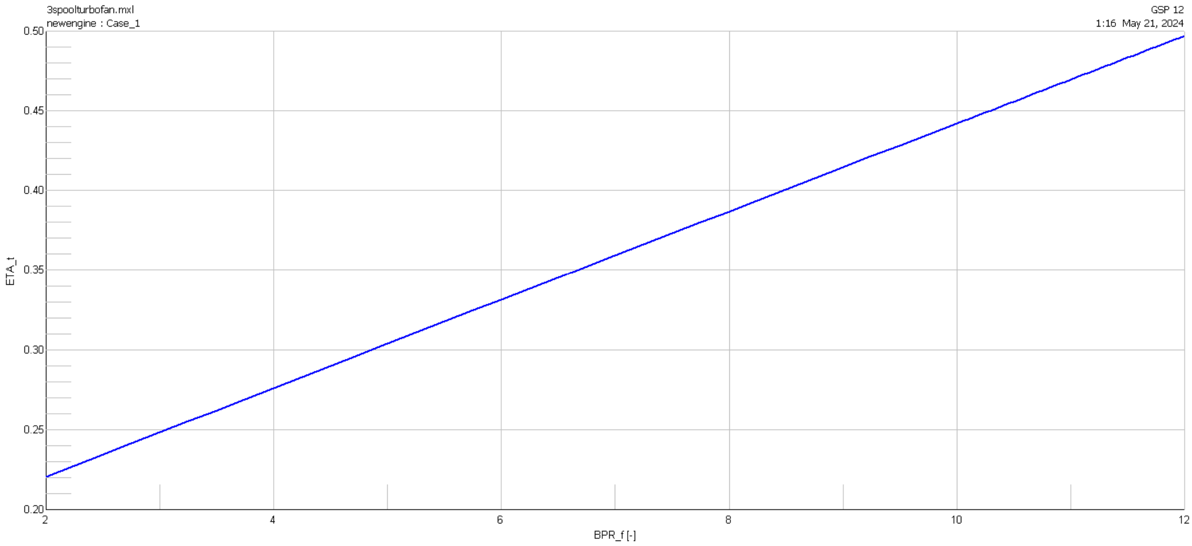

Figure 87:BPR vs ETA_t

BPR(Bypass ratio) vs ETA_p(Propulsive efficiency)

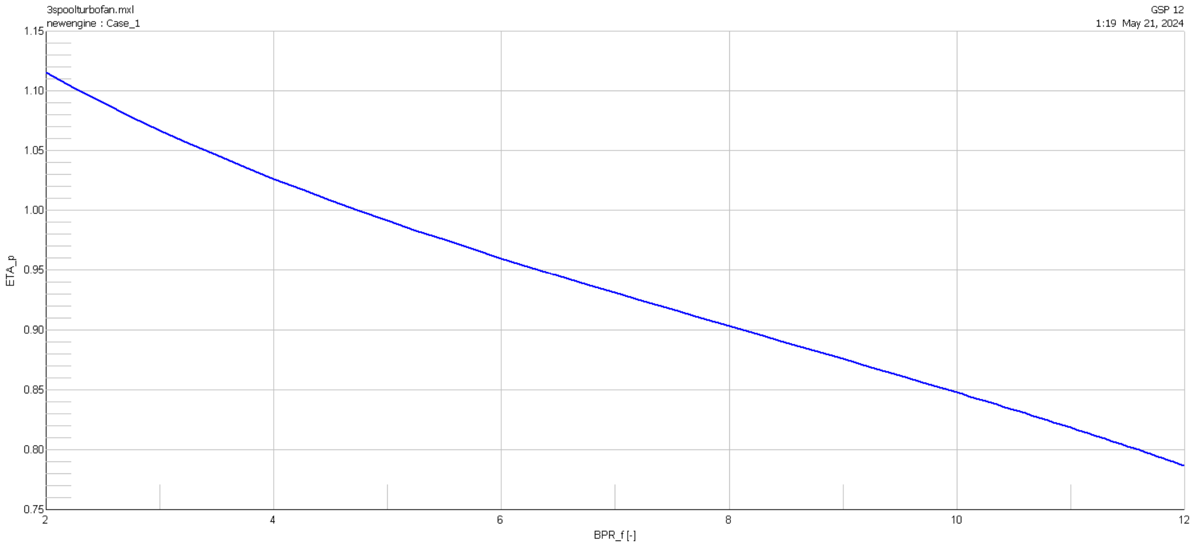

Figure 88:BPR vs ETA_p

BPR(Bypass ratio) vs ETA_o(Overall efficiency)

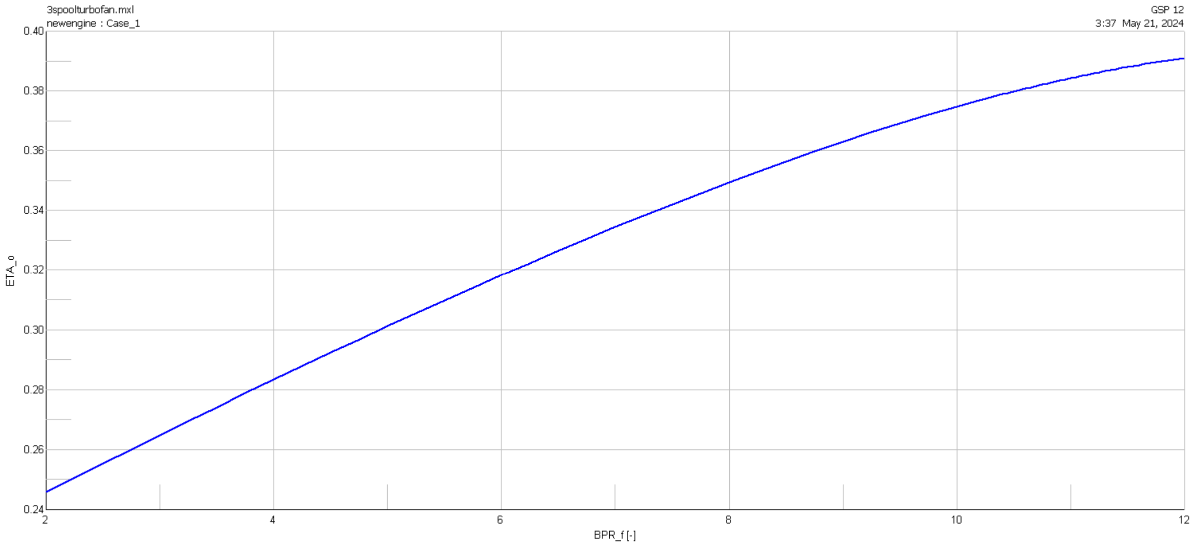

Figure 89:BPR vs ETA_o

BPR(Bypass ratio) vs ETA_II(Second law efficiency)

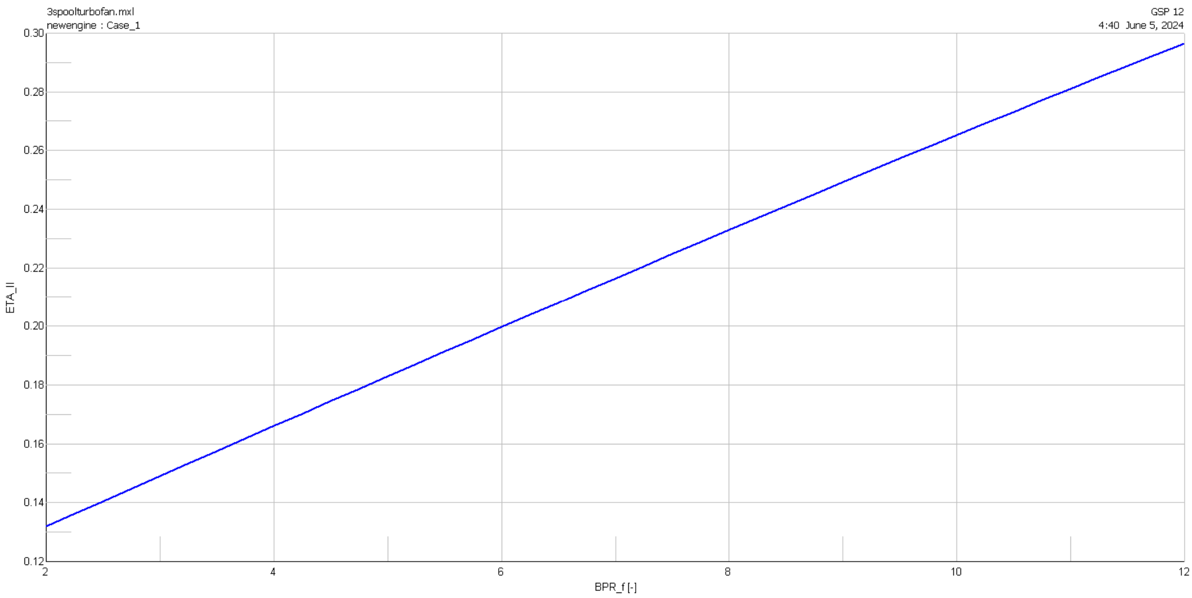

Figure 90:BPR vs ETA_II

4.9.7 Zp(Flight Altitude) Effect

Zp(Flight altitude) vs SFN(Specific thrust)

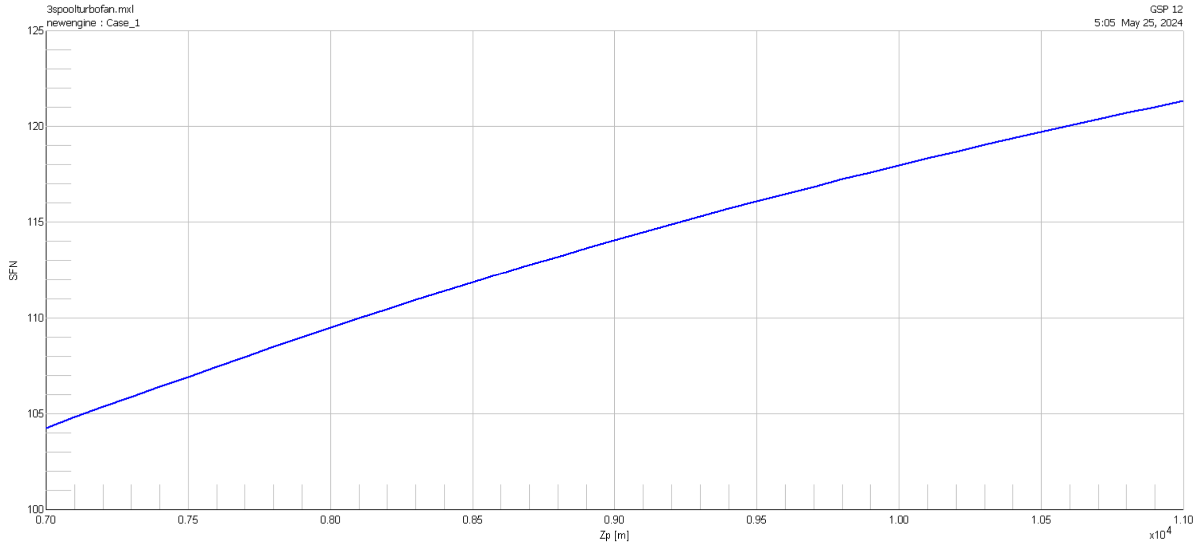

Figure 91:Zp vs SFN

Zp(Flight altitude) vs TSFC(Thrust specific fuel consumption)

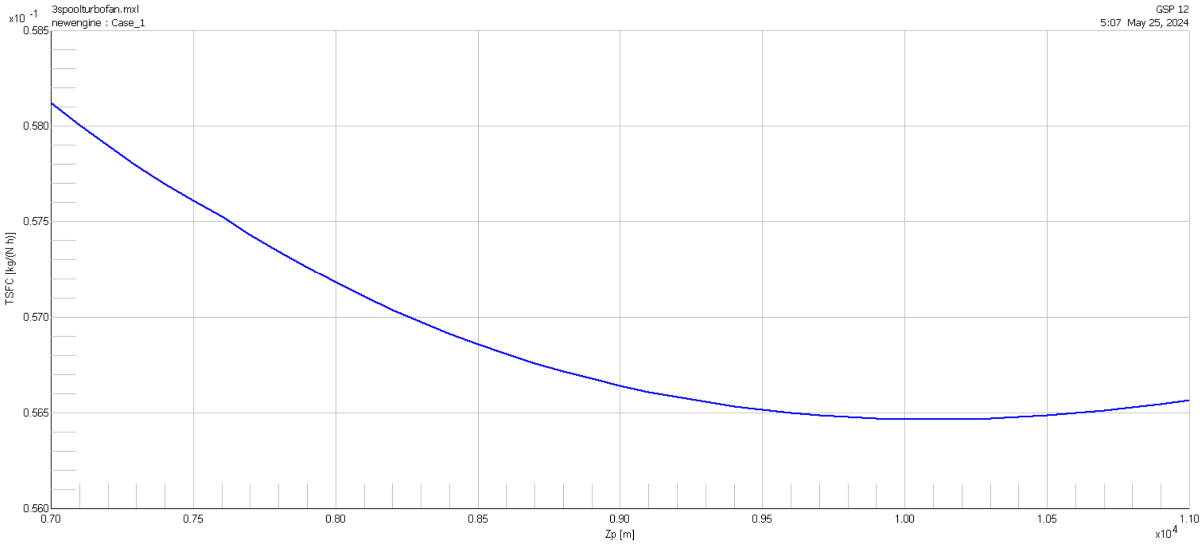

Figure 92:Zp vs TSFC

Zp(Flight altitude) vs ETA_t(Thermal efficiency)

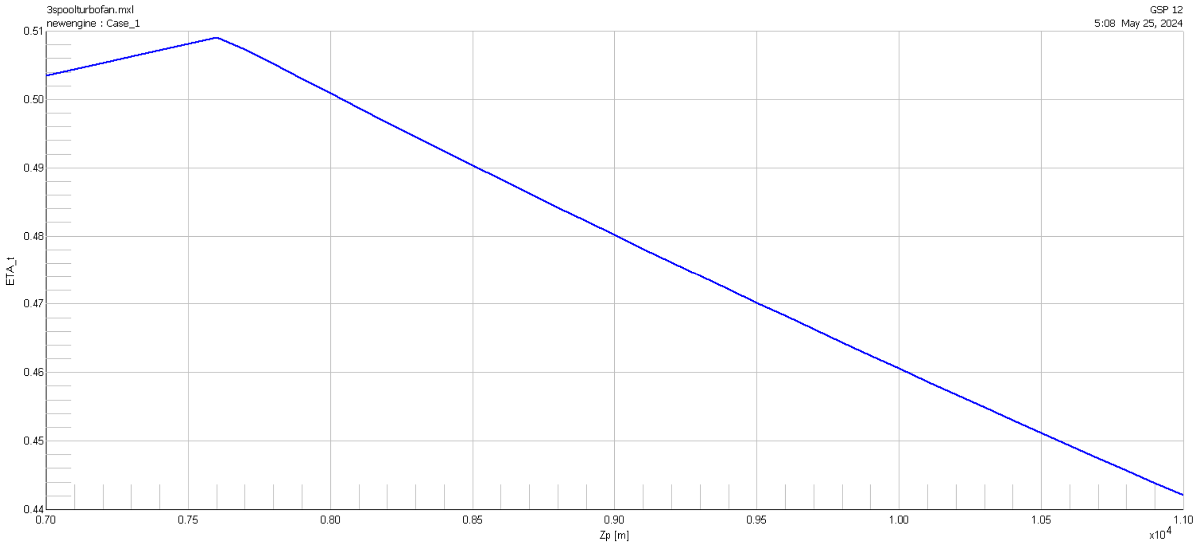

Figure 93:Zp vs ETA_t

Zp(Flight altitude) vs ETA_p(Propulsive efficiency)

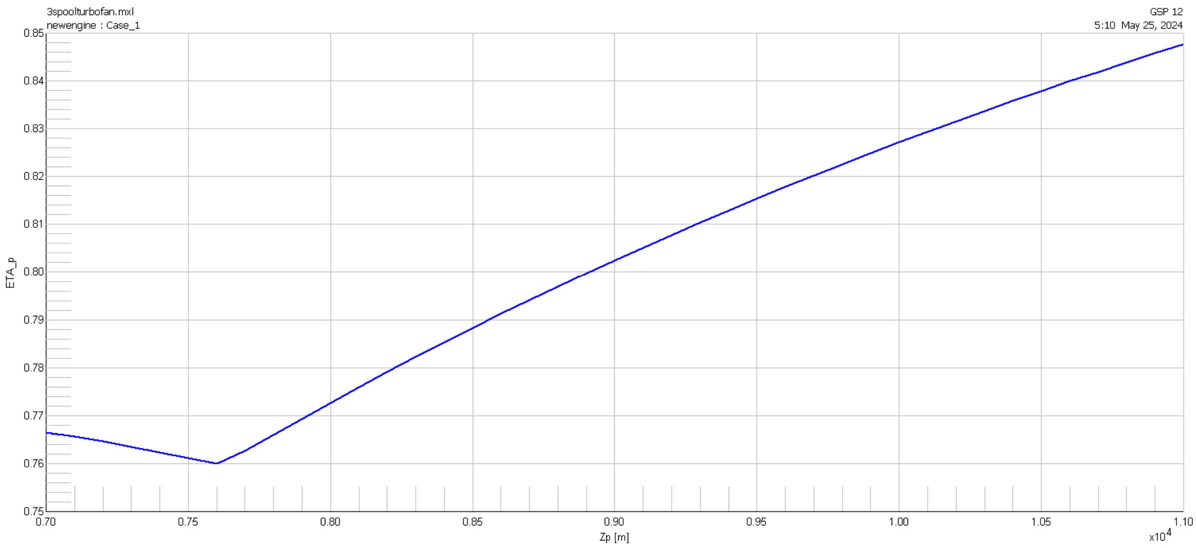

Figure 94:Zp vs ETA_p

Zp(Flight altitude) vs ETA_o(Overall efficiency)

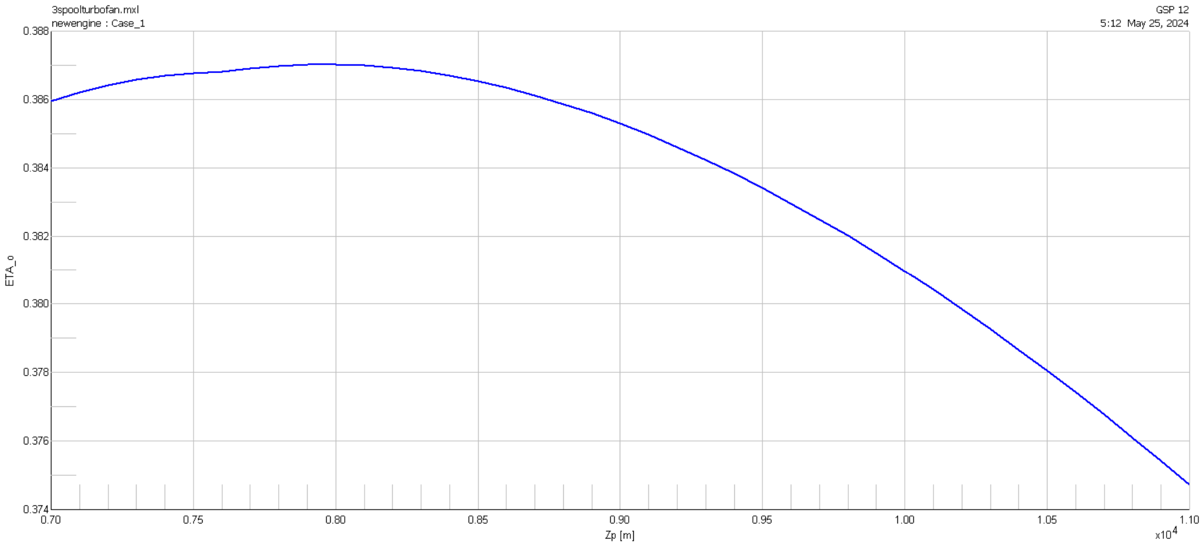

Figure 95:Zp vs ETA_o

Zp(Flight altitude) vs ETA_II(Second law efficiency)

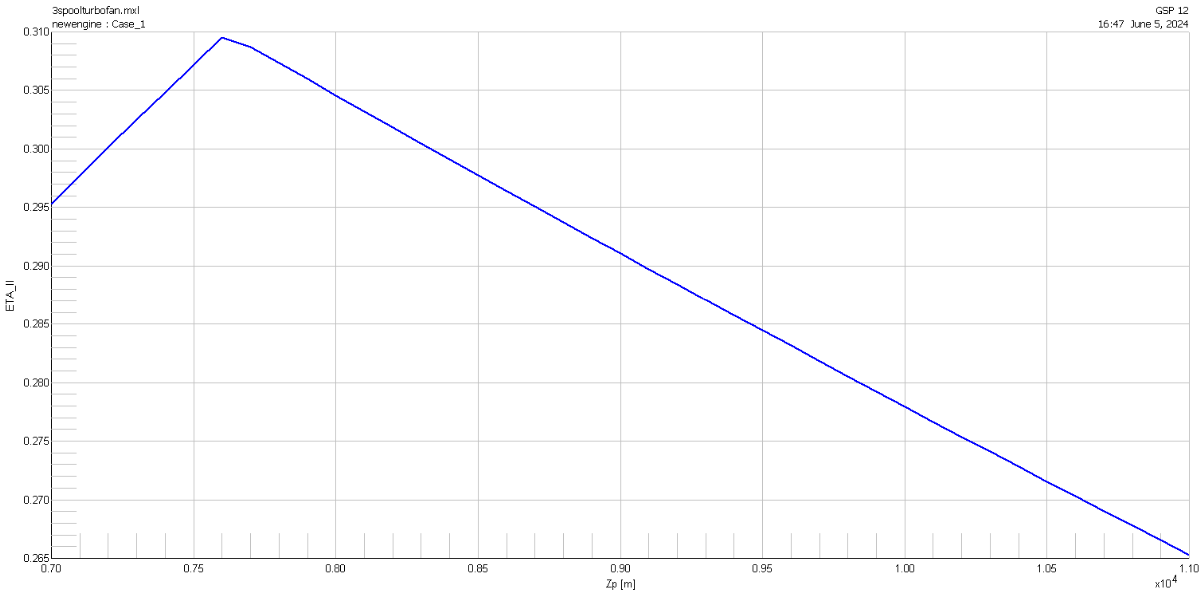

Figure 95:Zp vs ETA_II

4.9.8 Macha(Flight Mach Number) Effect

Macha(Flight mach number) vs SFN(Specific thrust)

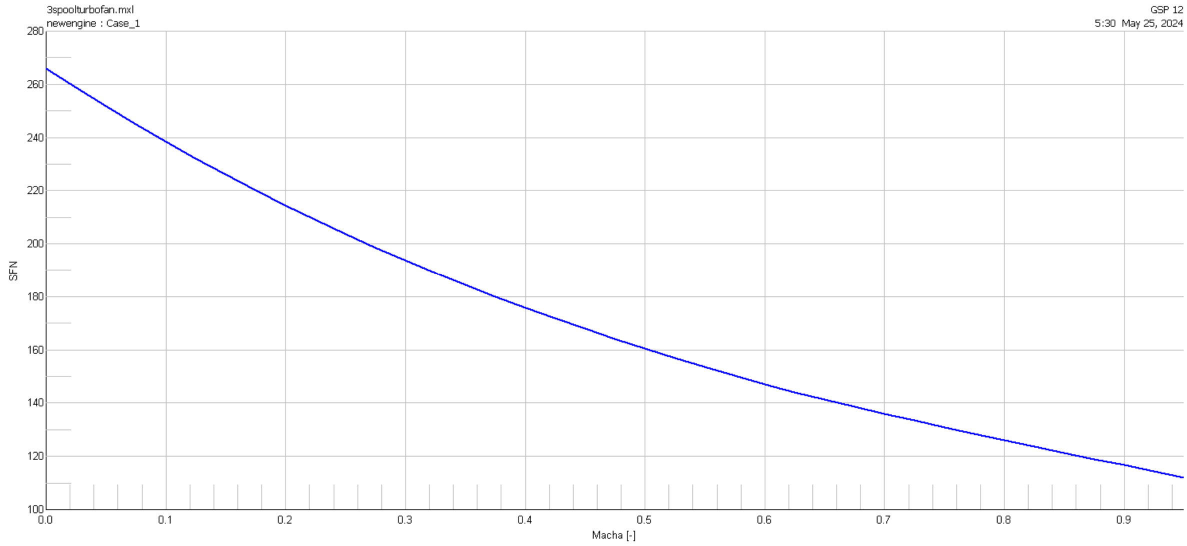

Figure 96:Macha vs SFN

Macha(Flight mach number) vs TSFC(Thrust specific fuel consumption)

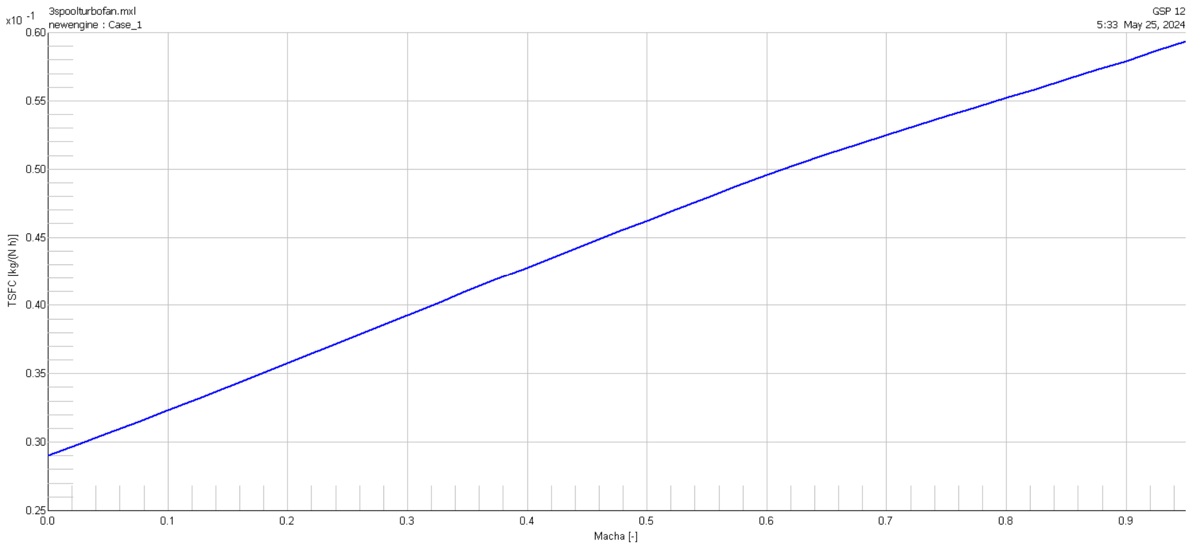

Figure 97:Macha vs TSFC

Macha(Flight mach number) vs ETA_t(Thermal efficiency)

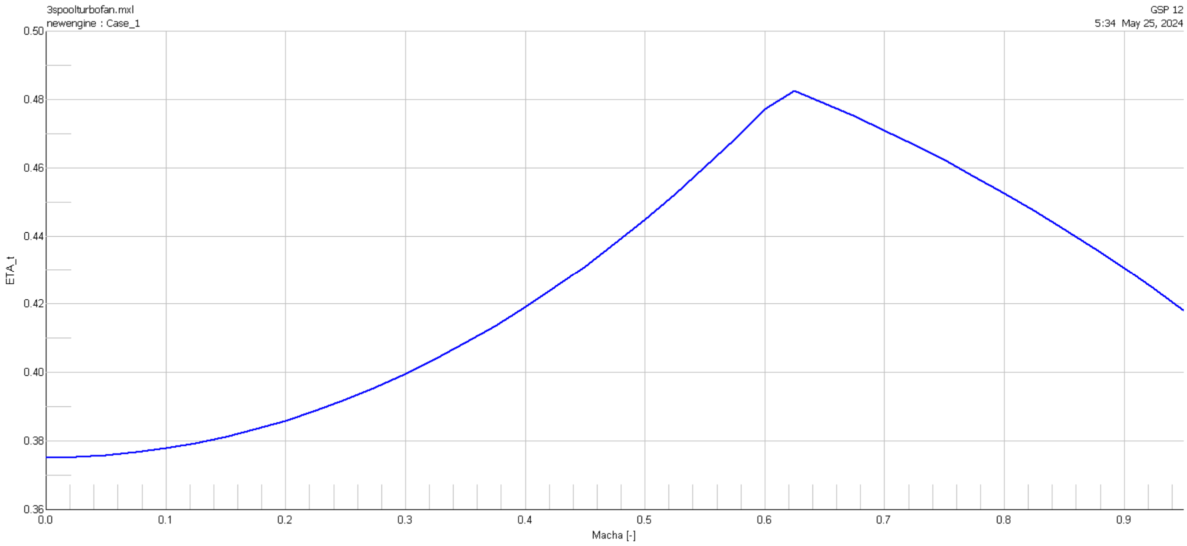

Figure 98:Macha vs ETA_t

Macha(Flight mach number) vs ETA_p(Propulsive efficiency)

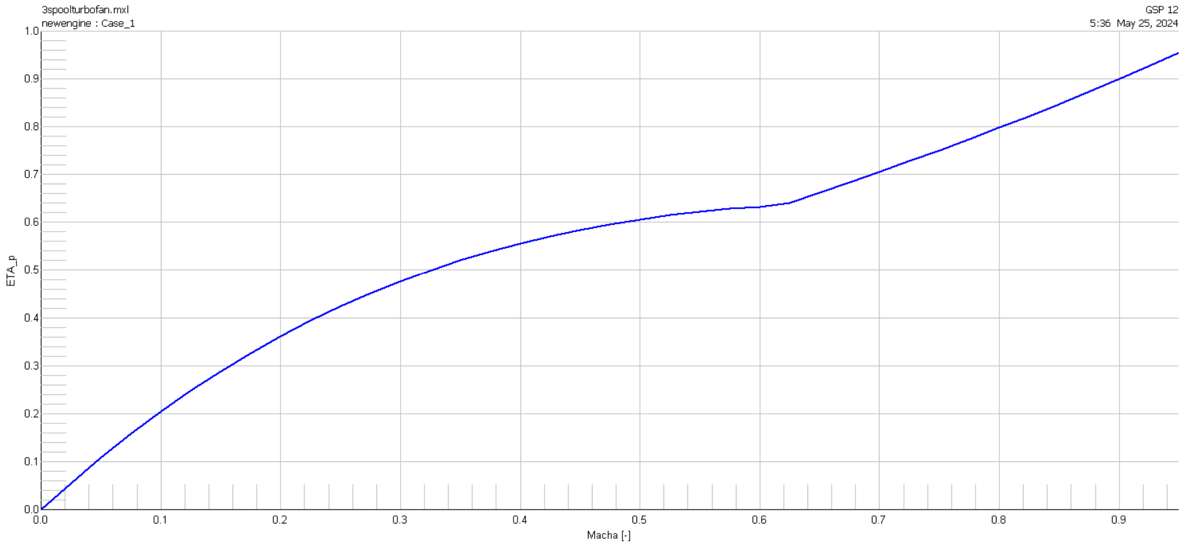

Figure 99:Macha vs ETA_p

Macha(Flight mach number) vs ETA_o(Overall efficiency)

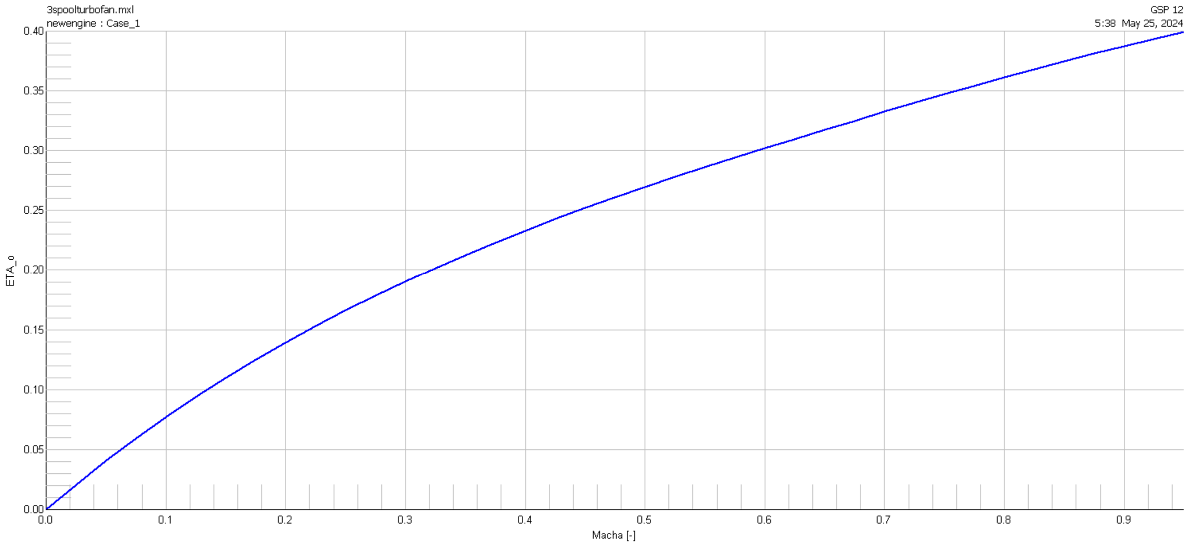

Figure 100:Macha vs ETA_o

Macha(Flight mach number) vs ETA_II(Second law efficiency)

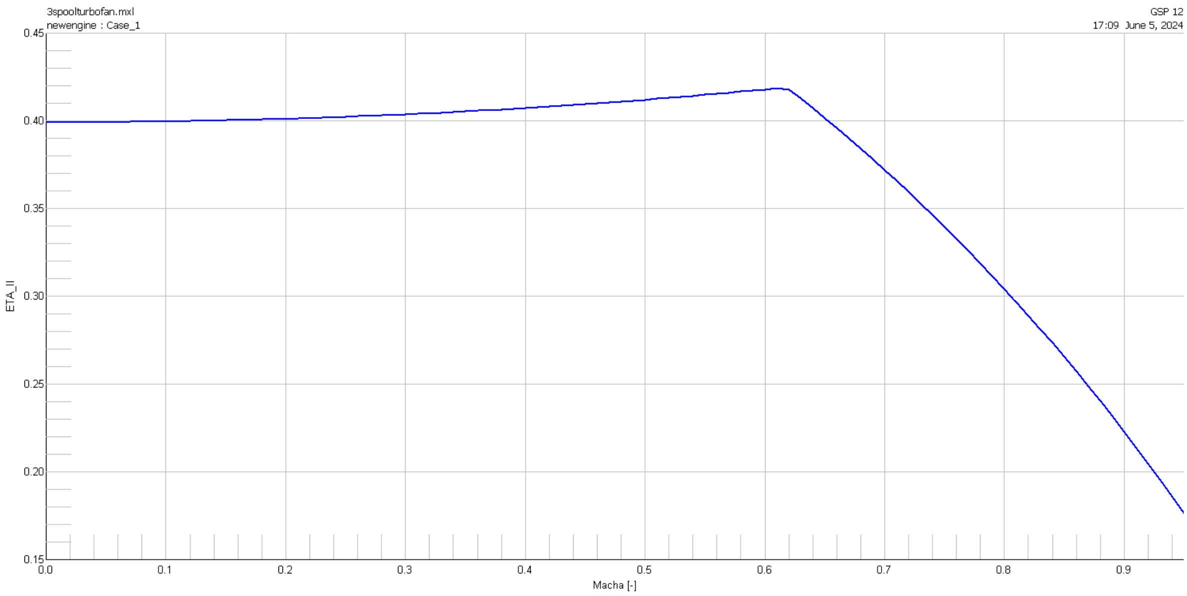

Figure 101: Macha vs ETA_II

4.10 Performance Analysis Report(Cruise)

4.10.1 TIT(Turbine Inlet Temperature)

The performance analysis was performed between temperatures of **1300K** and **1900K**. According to the results of the analysis,

-**FN(Thrust)** increases when **TIT** increases.

-**TSFC(Thrust specific fuel consumption)** decreases when **TIT** increases up to about **1375K**. After **1375K**, **TSFC** increases when **TIT** increases.

-$\boldsymbol{n_{thermal}}$**(Thermal efficiency)** increases when **TIT** increases up to about **1375K**. After **1375K**, $\boldsymbol{n_{thermal}}$ decreases when **TIT** increases.

-Changes in $\boldsymbol{n_{propulsive}}$**(Propulsive efficiency)** can be ignored in the increase of **TIT** up to 1375K. After **1375K**, $\boldsymbol{n_{propulsive}}$ increases in the increase of **TIT**.

-$\boldsymbol{n_{overall}}$**(Overall efficiency)** increases when **TIT** increases up to about **1375K**. After **1375K**, $\boldsymbol{n_{overall}}$ decreases when **TIT** increases.

-$\boldsymbol{n_{II}}$**(Second-law efficiency)** increases with increasing **TIT** up to about **1375K**. After **1375K**, $\boldsymbol{n_{II}}$ starts to decrease with increasing **TIT**.

4.10.2 π_{IPC}(Intermediate compressor pressure ratio)

The performance analysis was performed between pressure ratios of **6** and **15**. According to the results of the analysis,

-**FN(Thrust)** decreases when π_{IPC} increases.

-**TSFC(Thrust specific fuel consumption)** decreases when π_{IPC} increases.

-$\boldsymbol{n_{thermal}}$**(Thermal efficiency)** increases when π_{IPC} increases.

-$\boldsymbol{n_{propulsive}}$**(Propulsive efficiency)** decreases when π_{IPC} increases.

-$\boldsymbol{n_{overall}}$**(Overall efficiency)** increases when π_{IPC} increases.

-$\boldsymbol{n_{II}}$**(Second-law efficiency)** increases when π_{IPC} increases.

4.10.3 π_{HPC}(High compressor pressure ratio)

The performance analysis was performed between pressure ratios of **2** and **6**. According to the results of the analysis,

-**FN(Thrust)** decreases when π_{HPC} increases.

-**TSFC(Thrust specific fuel consumption)** decreases when π_{HPC} increases.

-$\boldsymbol{n_{thermal}}$**(Thermal efficiency)** increases when π_{HPC} increases.

-$\boldsymbol{n_{propulsive}}$**(Propulsive efficiency)** decreases when π_{HPC} increases.

-$n_{overall}$**(Overall efficiency)** increases when π_{HPC} increases.

-n_{II}**(Second-law efficiency)** increases when π_{HPC} increases.

4.10.4 π_{fan}(Fan pressure ratio)

The performance analysis was performed between pressure ratios of **1.1** and **1.6** with **7** different **TIT(Turbine inlet temperature)** values of **1350K 1400K 1500K 1600K 1700K 1800K 1900K**.According to the results of the analysis,

-**FN(Thrust)** increases when π_{fan} increases. **FN** is highest when **TIT is 1900K**

-**TSFC(Thrust specific fuel consumption)** decreases when π_{fan} increases. **TSFC** is lowest when **TIT** is **1400K**.

-For all **TIT** values, $n_{thermal}$**(Thermal efficiency)** increases as π_{fan} increases up to about **1.24**.After **1.24**, $n_{thermal}$ increases slowly as π_{fan} increases for all **TIT** values.When **TIT** is **1350K** and π_{fan} increases beyond about **1.5**, $n_{thermal}$ starts to decrease.At higher **TIT** values, this point is at higher π_{fan} values.However, the highest $n_{thermal}$ values are when **TIT** is **1350K**.

-The variation and characteristic of $n_{propulsive}$**(Propulsive efficiency)** with increasing π_{fan} for each **TIT** value is somewhat complex, but generally speaking, $n_{propulsive}$ increases with increasing π_{fan} for each **TIT** value up to about **1.24**. After **1.24**, $n_{propulsive}$ tends to increase with different curve characteristics. $n_{propulsive}$ is highest when **TIT** is **1900K**.

-For each **TIT** value, $n_{overall}$**(Overall efficiency)** increases as π_{fan} increases. $n_{overall}$ is highest when **TIT** is **1400K**.

-For all **TIT** values, n_{II}**(Second-law efficiency)** increases as π_{fan} increases up to about **1.24**.After **1.24**, n_{II} increases slowly as π_{fan} increases for all **TIT** values.When **TIT** is **1350K** and π_{fan} increases beyond about **1.5**, n_{II} starts to decrease.At higher **TIT** values, this point is at higher π_{fan} values.However, the highest n_{II} values are when **TIT** is **1350K**.

4.10.5 OPR(Overall pressure ratio)

The performance analysis was performed between pressure ratios of about **40** and **55**. According to the results of the analysis,

-**SFN(Specific thrust)** decreases when **OPR** increases.

-**TSFC(Thrust specific fuel consumption)** decreases when **OPR** increases.

-$n_{thermal}$**(Thermal efficiency)** increases when **OPR** increases.

-The change in $n_{propulsive}$**(Propulsive efficiency)** due to the increase in **OPR** is quite small; it is almost constant. Nevertheless, if we examine it, $n_{propulsive}$**(Propulsive efficiency)** decreases when **OPR** increases.

-$n_{overall}$**(Overall efficiency)** increases when **OPR** increases.

-$\boldsymbol{n_{II}}$**(Second-law efficiency)** increases when **OPR** increases.

4.10.6 BPR(Bypass ratio)

The performance analysis was performed between bypass ratios of **2** and **12**. According to the results of the analysis,

-**SFN(Specific thrust)** decreases when **BPR** increases.

-**TSFC(Thrust specific fuel consumption)** decreases when **BPR** increases.

-$\boldsymbol{n_{thermal}}$**(Thermal efficiency)** increases when **BPR** increases.

-$\boldsymbol{n_{propulsive}}$**(Propulsive efficiency)** decreases when **BPR** increases.

-$\boldsymbol{n_{overall}}$**(Overall efficiency)** increases when **BPR** increases.

-$\boldsymbol{n_{II}}$**(Second-law efficiency)** increases when **BPR** increases.

4.10.7 Zp(Flight altitude)

The performance analysis was performed between altitudes of **7000m** and **11000m**. According to the results of the analysis,

-**SFN(Specific thrust)** increases when **Zp** increases.

-**TSFC(Thrust specific fuel consumption)** decreases when **Zp** increases up to about **10000m**. After **10000m TSFC** starts to increase as **Zp** increases.

-As **Zp** increases up to about **7600m**, $\boldsymbol{n_{thermal}}$**(Thermal efficiency)** increases. After **7600m**, $\boldsymbol{n_{thermal}}$ decreases as **Zp** increases.

-As **Zp** increases up to about **7600m**, $\boldsymbol{n_{propulsive}}$**(Propulsive efficiency)** increases. After **7600m**, $\boldsymbol{n_{propulsive}}$ decreases as **Zp** increases.

-As **Zp** increases up to about **8000m**, $\boldsymbol{n_{overall}}$**(Overall efficiency)** increases. After **8000m**, $\boldsymbol{n_{overall}}$ decreases as **Zp** increases.

-As **Zp** increases up to about **7600m**, $\boldsymbol{n_{II}}$**(Second-law efficiency)** increases. After **7600m**, $\boldsymbol{n_{II}}$ decreases as **Zp** increases.

4.10.8 Macha(Flight mach number)

The performance analysis was performed between mach numbers of **0M** and **0.95M**. According to the results of the analysis,

-**SFN(Specific thrust)** decreases when **Macha** increases.

-**TSFC(Thrust specific fuel consumption)** increases when **Macha** increases.

-Until **Macha** about **0.63M**, $\boldsymbol{n_{thermal}}$**(Thermal efficiency)** increases with increasing **Macha**. After **0.63M**, $\boldsymbol{n_{thermal}}$ decreases with increasing **Macha**.

-$\boldsymbol{n_{propulsive}}$**(Propulsive efficiency)** increases with increasing **Macha**.

-$\boldsymbol{n_{overall}}$**(Overall efficiency)** increases with increasing **Macha**.

-Up to about **0.63M**, the change of $\boldsymbol{n_{II}}$**(Second-law efficiency)** with increasing **Macha** is quite small; it can be considered constant. After **0.63M**, $\boldsymbol{n_{II}}$ decreases with increasing **Macha**.

4.11 Maps of Design Conditions

4.11.1 SFN vs TSFC(By varying BPR and TIT)

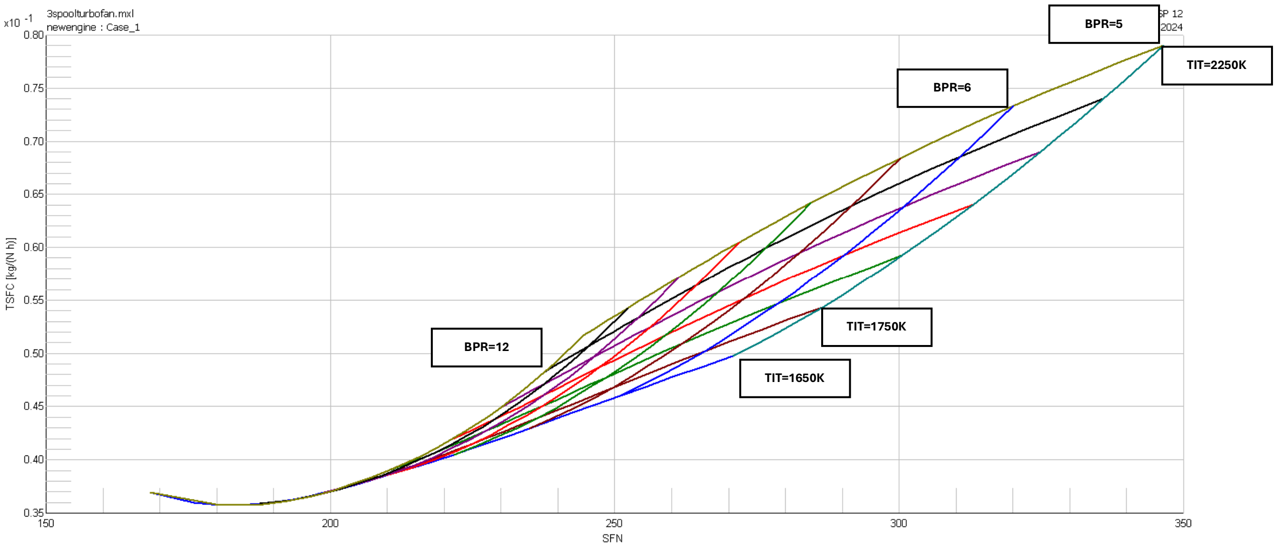

Figure 102:Take-off SFN vs TSFC with control variables BPR and TIT

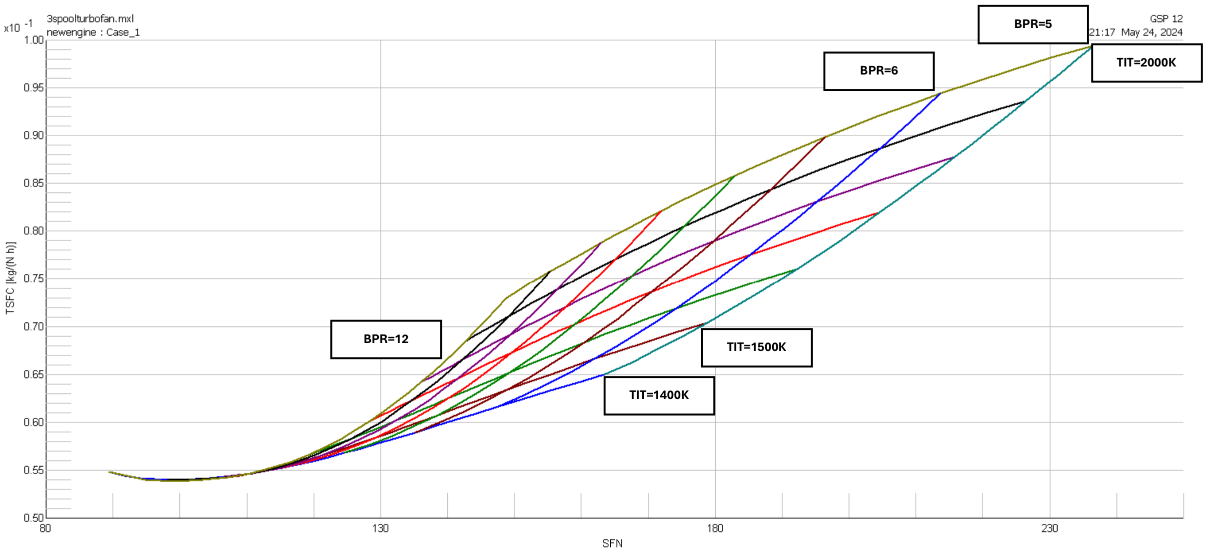

Figure 103:Cruise SFN vs TSFC with control variables BPR and TIT

4.11.2 FN vs ETA_o(By varying BPR and TIT)

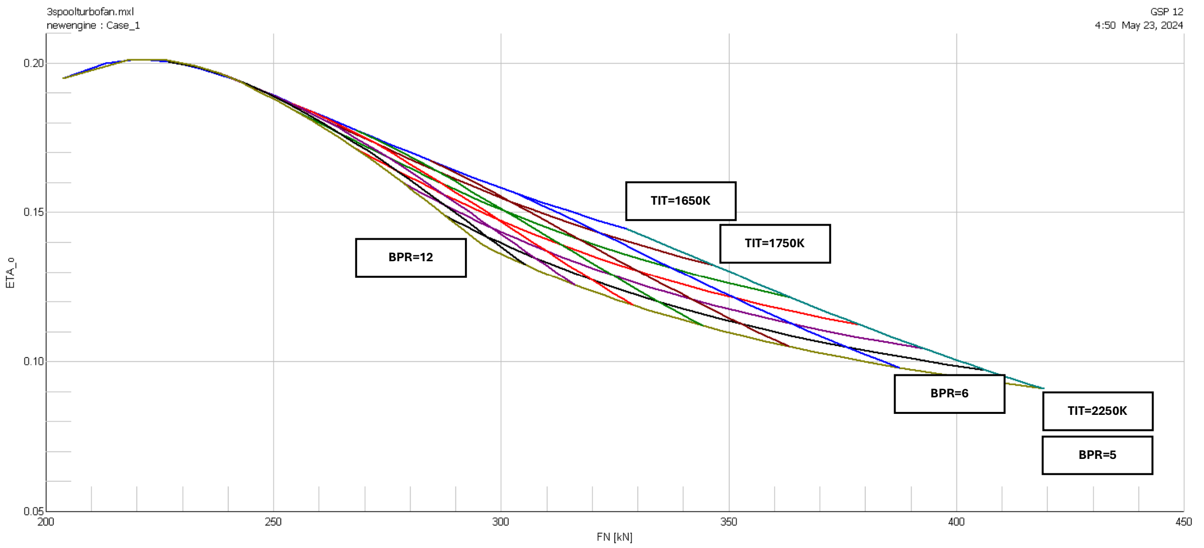

Figure 104:Take-off FN vs ETA_o with control variables BPR and TIT

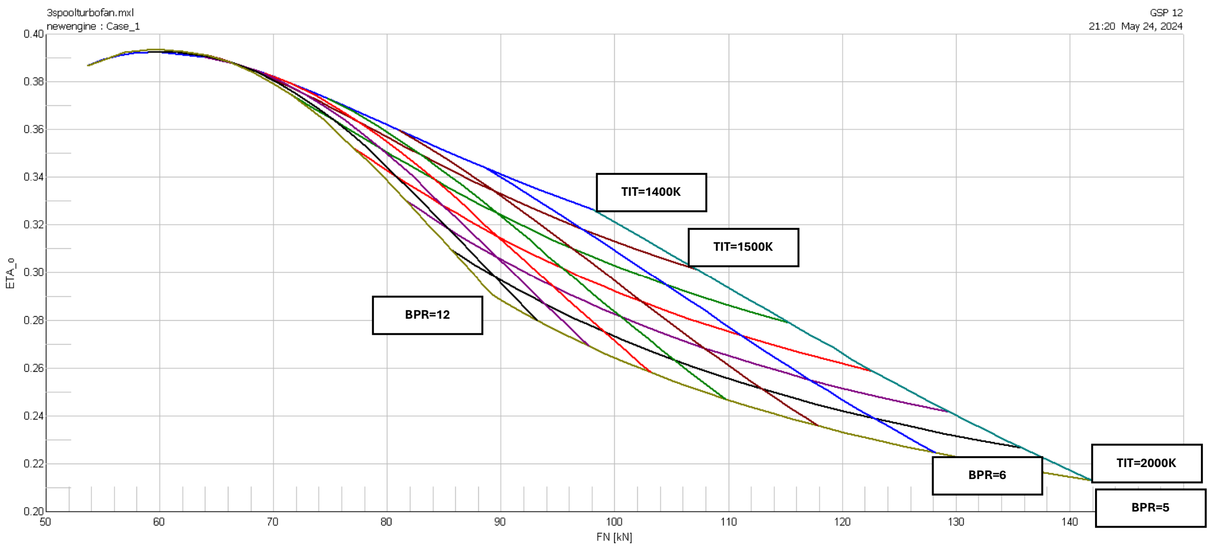

Figure 105:Cruise FN vs ETA_o with control variables BPR and TIT

4.11.3 SFN vs TSFC(By varying FPR and TIT)

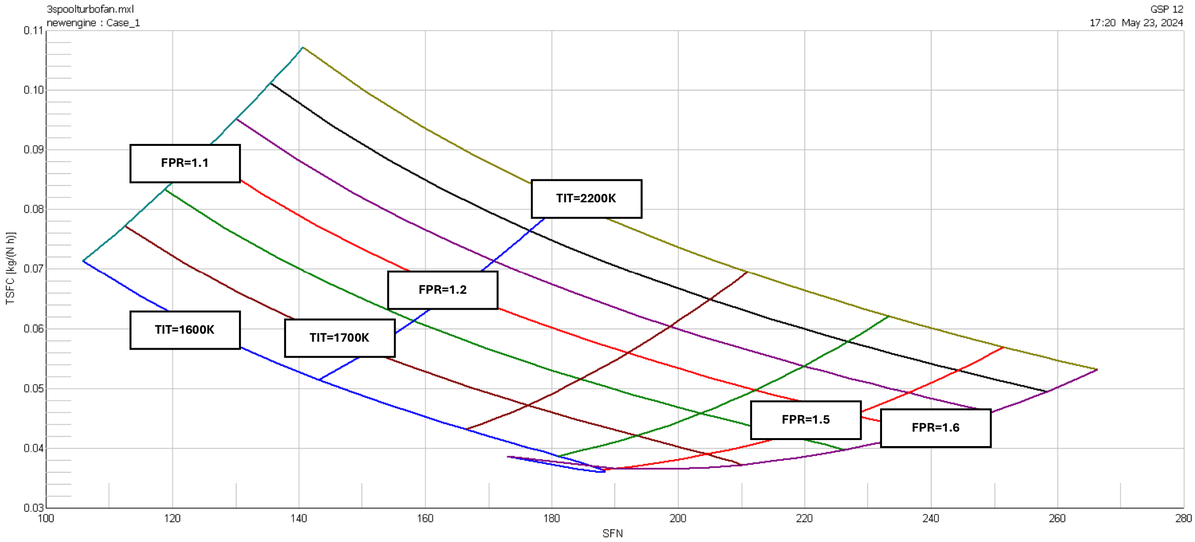

Figure 106:Take-off SFN vs TSFC with control variables FPR and TIT

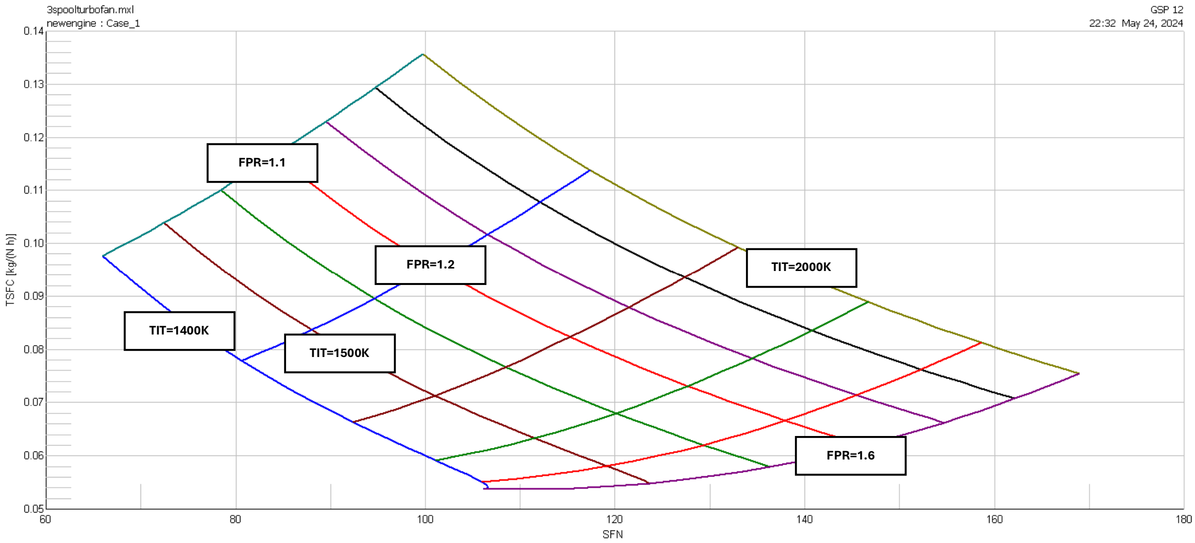

Figure 107:Cruise SFN vs TSFC with control variables FPR and TIT

4.11.4 FN vs ETA_o(By varying FPR and TIT)

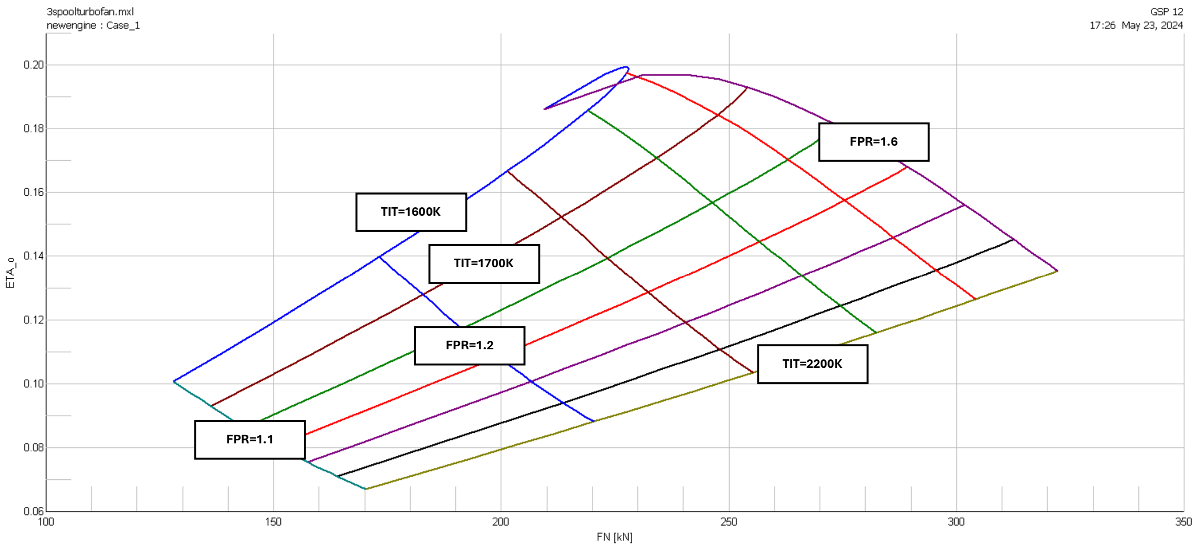

Figure 108:Take-off FN vs ETA_o with control variables FPR and TIT

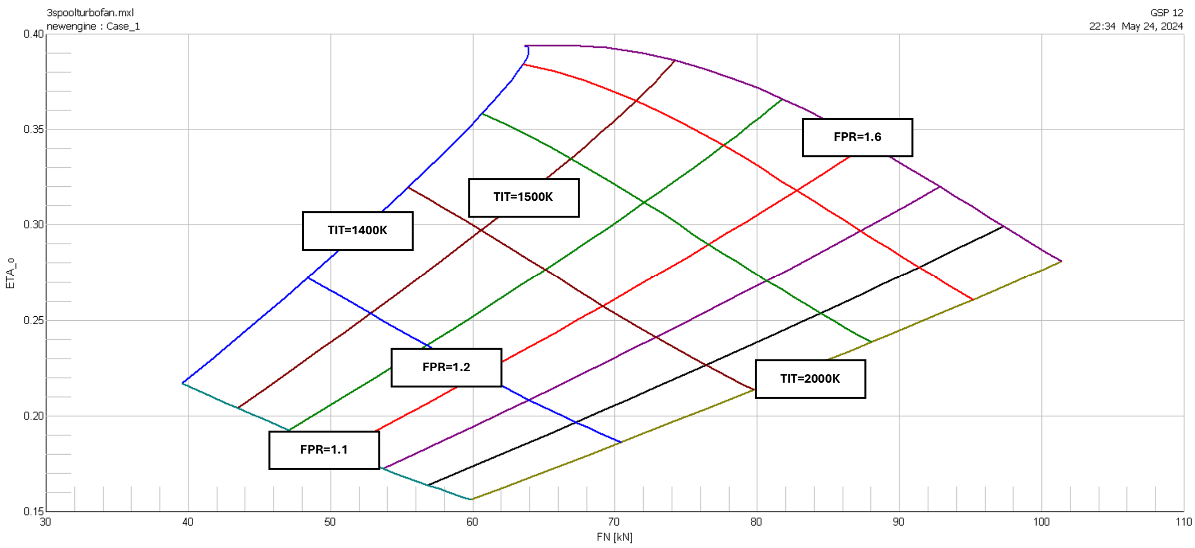

Figure 109:Cruise FN vs ETA_o with control variables FPR and TIT

4.11.5 SFN vs TSFC(By varying BPR and OPR)

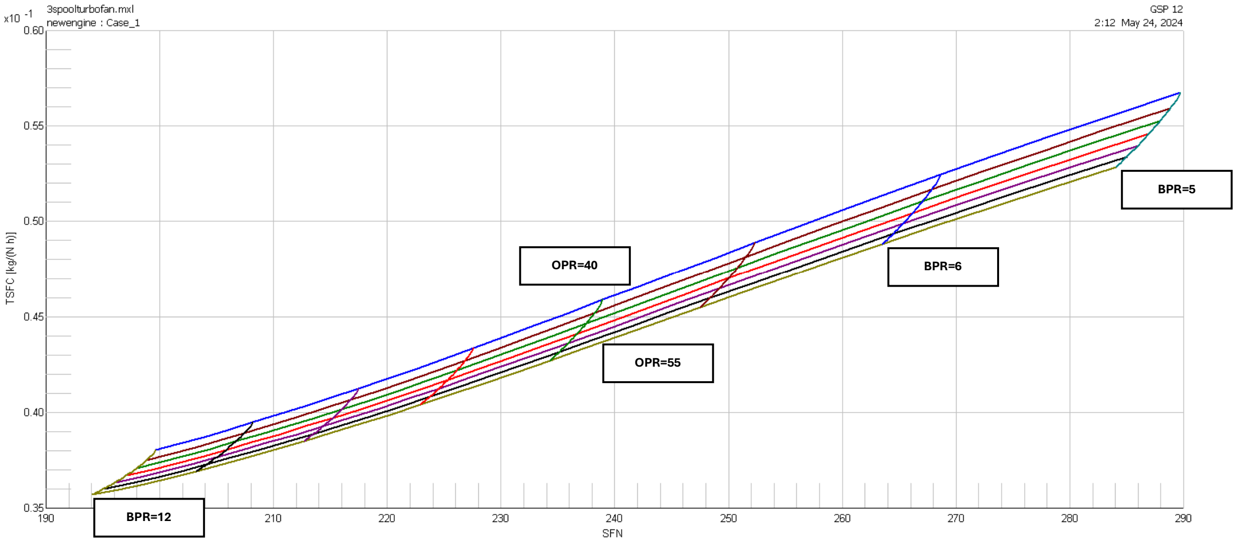

Figure 110:Take-off SFN vs TSFC with control variables BPR and OPR

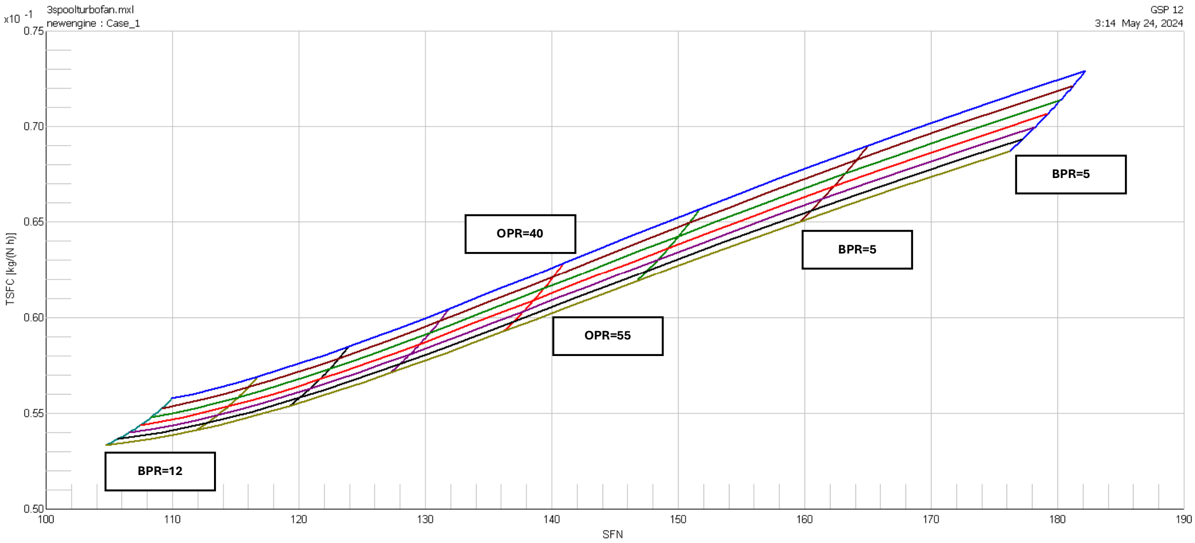

Figure 111:Cruise SFN vs TSFC with control variables BPR and OPR

4.11.6 FN vs ETA_o(By varying BPR and OPR)

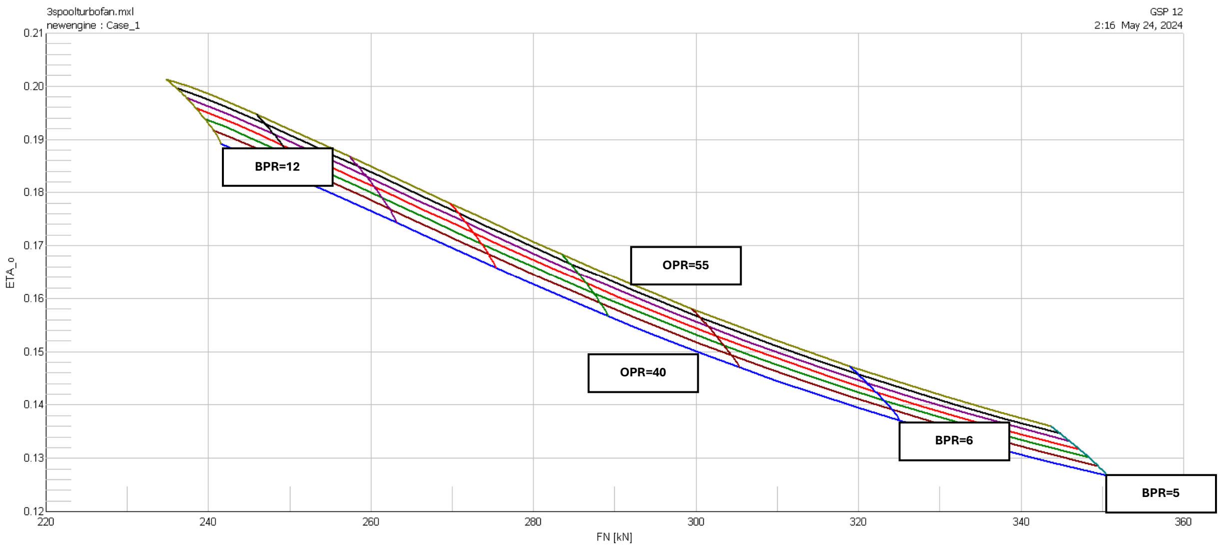

Figure 112:Take-off FN vs ETA_o with control variables BPR and OPR

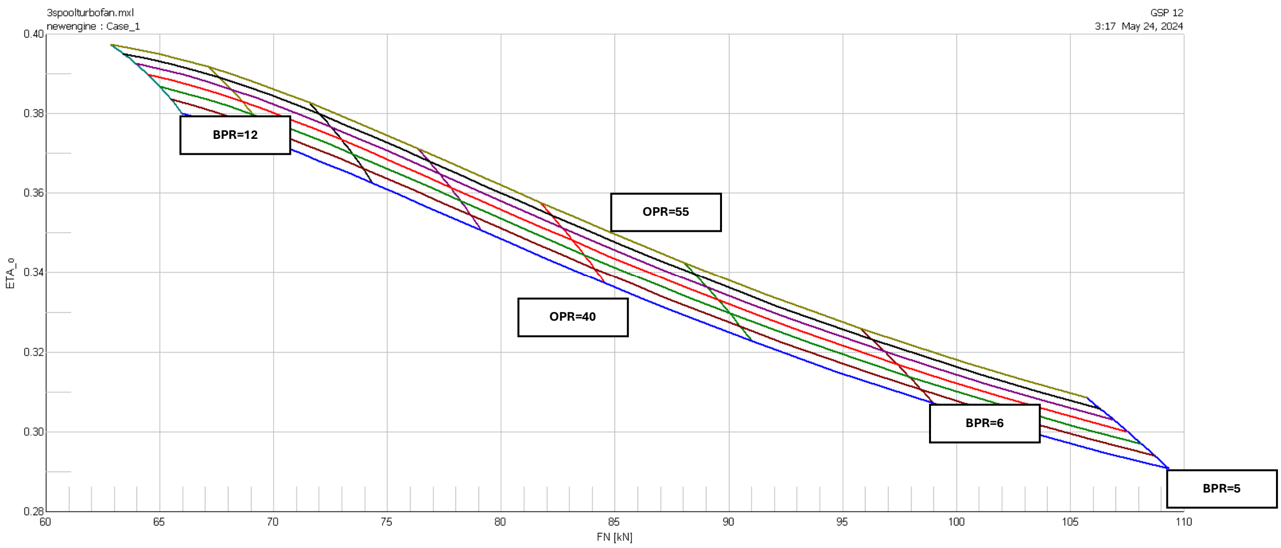

Figure 113:Cruise FN vs ETA_o with control variables BPR and OPR

4.11.7 SFN vs TSFC(By varying BPR and FPR)

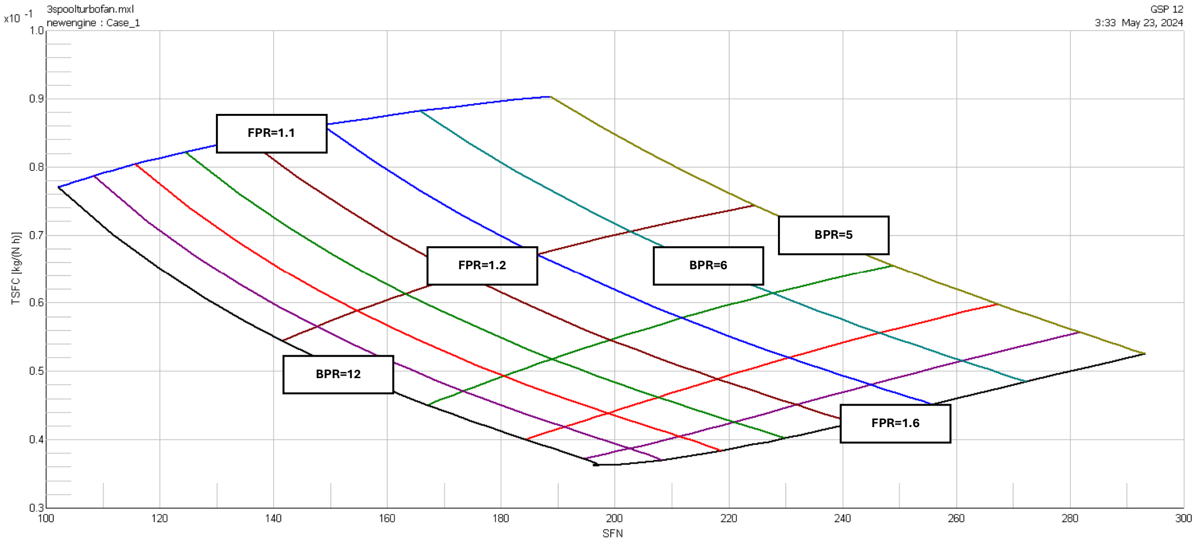

Figure 114:Take-off SFN vs TSFC with control variables BPR and FPR

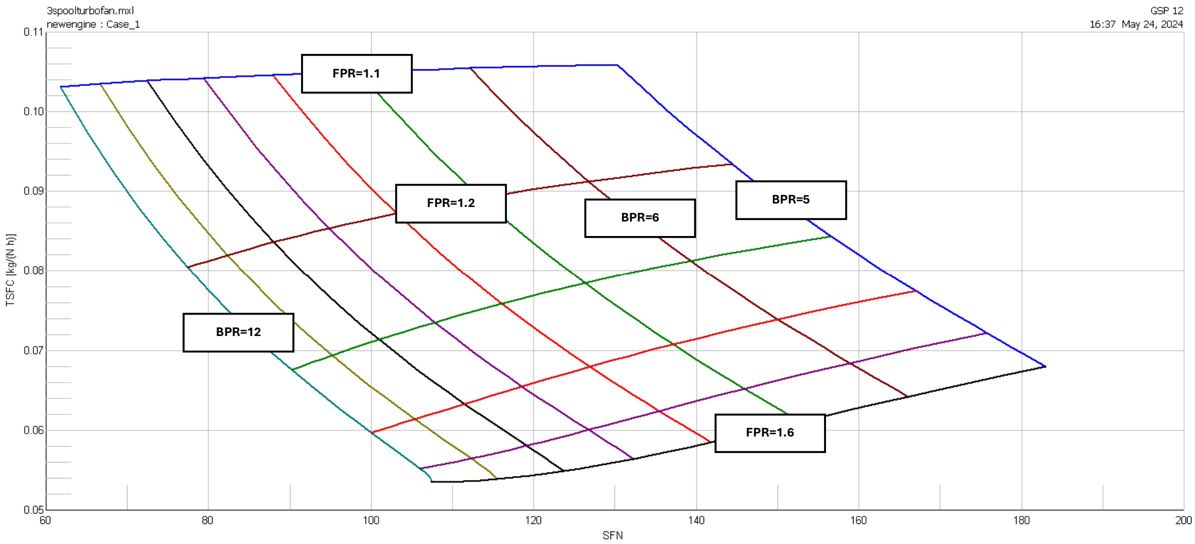

Figure 115:Cruise SFN vs TSFC with control variables BPR and FPR

4.11.8 FN vs ETA_o(By varying BPR and FPR)

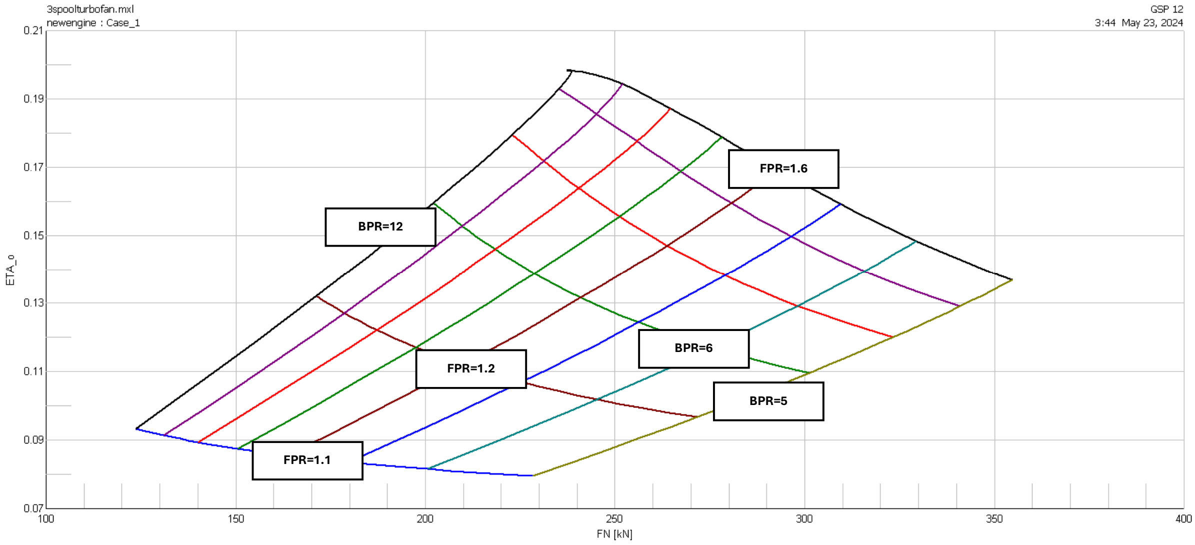

Figure 116:Take-off FN vs ETA_o with control variables BPR and FPR

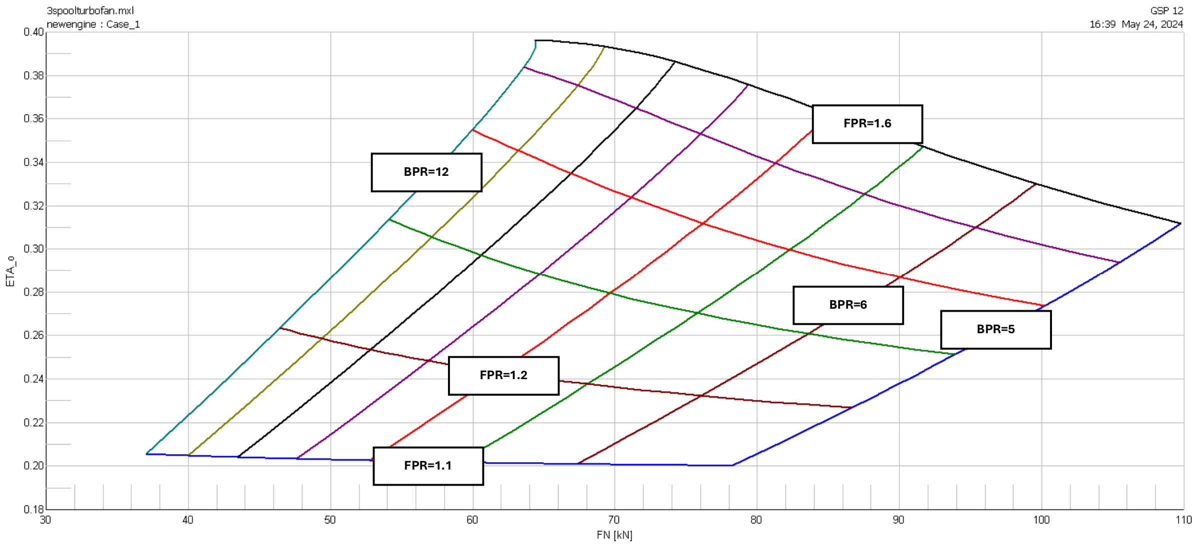

Figure 117:Cruise FN vs ETA_o with control variables BPR and FPR

4.12 Performance Maps Report(Take-off)

4.12.1 BPR,TIT(Take-off)

In this performance map, **BPR(Bypass ratio)** and **TIT(Turbine inlet temperature)** are chosen as control variables. The map has **BPR** curves increasing from **5** to **12** with each increment of **1** and **TIT** curves increasing from **1650K** to **2250K** with each increment of **100K**.The output variables to be analyzed are **FN(Thrust)**,**SFN(Specific thrust)**,**TSFC(Thrust specific fuel consumption)** and $\boldsymbol{n_{overall}}$**(Overall efficiency)**.

SFN vs TSFC(By varying BPR and TIT)

-While **TIT** is constant, **SFN** tends to decrease when **BPR** increases.

-While **TIT** is constant, **TSFC** tends to decrease when **BPR** increases.

-While **BPR** is constant, **SFN** tends to increase when **TIT** increases.

-While **BPR** is constant, **TSFC** tends to increase when **TIT** increases.

-**The highest SFN** occurs when **BPR** is equal to **5** and **TIT** is equal to **2250K**.

-**The lowest TSFC** occurs when **BPR** is equal to **12** and **TIT** is equal to **1650K**.

FN vs $\boldsymbol{n_{overall}}$**(By varying BPR and TIT)**

-While **TIT** is constant, **FN** tends to decrease when **BPR** increases.

-While **TIT** is constant, $\boldsymbol{n_{overall}}$ tends to increase when **BPR** increases.

-While **BPR** is constant, **FN** tends to increase when **TIT** increases.

-While **BPR** is constant, $\boldsymbol{n_{overall}}$ tends to decrease when **TIT** increases.

-**The highest FN** occurs when **BPR** is equal to **5** and **TIT** is equal to **2250K**.

-**The highest** $\boldsymbol{n_{overall}}$ occurs when **BPR** is equal to **12** and **TIT** is equal to **1650K**.

4.12.2 BPR,FPR(Take-off)

In this performance map, **BPR(Bypass ratio)** and **FPR(Fan pressure ratio)** are chosen as control variables. The map has **BPR** curves increasing from **5** to **12** with each increment of **1** and **FPR** curves increasing from **1.1** to **1.6** with each increment of **0.1**.The output variables to be analyzed are **FN(Thrust)**,**SFN(Specific thrust)**,**TSFC(Thrust specific fuel consumption)** and $\boldsymbol{n_{overall}}$**(Overall efficiency)**.

SFN vs TSFC(By varying BPR and FPR)

-While **FPR** is constant, **SFN** tends to decrease when **BPR** increases.

-While **FPR** is constant, **TSFC** tends to decrease when **BPR** increases.

-While **BPR** is constant, **SFN** tends to increase when **FPR** increases.

-While **BPR** is constant, **TSFC** tends to decrease when **FPR** increases.

-**The highest SFN** occurs when **BPR** is equal to **5** and **FPR** is equal to **1.6**.

-**The lowest TSFC** occurs when **BPR** is equal to **12** and **FPR** is equal to **1.6**.

FN vs $n_{overall}$ (By varying BPR and FPR)

-While **FPR** is constant, **FN** tends to decrease when **BPR** increases.

-While **FPR** is constant, $n_{overall}$ tends to increase when **BPR** increases.

-While **BPR** is constant, **FN** tends to increase when **FPR** increases.

-While **BPR** is constant, $n_{overall}$ tends to increase when **FPR** increases.

-**The highest FN** occurs when **BPR** is equal to **5** and **FPR** is equal to **1.6**.

-**The highest $n_{overall}$** occurs when **BPR** is equal to **12** and **FPR** is equal to **1.6**.

4.12.3 BPR,OPR(Take-off)

In this performance map, **BPR(Bypass ratio)** and **OPR(Overall pressure ratio)** are chosen as control variables. The map has **BPR** curves increasing from **5** to **12** with each increment of **1** and **OPR** curves increasing from **40** to **55** with each increment of **2.5**.The output variables to be analyzed are **FN(Thrust)**,**SFN(Specific thrust)**,**TSFC(Thrust specific fuel consumption)** and $n_{overall}$(**Overall efficiency**).

SFN vs TSFC(By varying BPR and FPR)

-While **OPR** is constant, **SFN** tends to decrease when **BPR** increases.

-While **OPR** is constant, **TSFC** tends to decrease when **BPR** increases.

-While **BPR** is constant, **SFN** tends to decrease when **OPR** increases.

-While **BPR** is constant, **TSFC** tends to decrease when **OPR** increases.

-**The highest SFN** occurs when **BPR** is equal to **5** and **OPR** is equal to **40**.

-**The lowest TSFC** occurs when **BPR** is equal to **12** and **OPR** is equal to **55**.

FN vs $n_{overall}$ (By varying BPR and FPR)

-While **OPR** is constant, **FN** tends to decrease when **BPR** increases.

-While **OPR** is constant, $n_{overall}$ tends to increase when **BPR** increases.

-While **BPR** is constant, **FN** tends to decrease when **OPR** increases.

-While **BPR** is constant, $n_{overall}$ tends to increase when **OPR** increases.

-**The highest FN** occurs when **BPR** is equal to **5** and **OPR** is equal to **40**.

-**The highest $n_{overall}$** occurs when **BPR** is equal to **12** and **OPR** is equal to **55**.

4.12.4 FPR,TIT(Take-off)

In this performance map, **FPR(Fan pressure ratio)** and **TIT(Turbine inlet temperature)** are chosen as control variables. The map has **FPR** curves increasing from **1.1** to **1.6** with each increment of **0.1** and **TIT** curves increasing from **1600K** to **2200K** with each increment of **100K**.The output variables to be analyzed are **FN(Thrust)**,**SFN(Specific thrust)**,**TSFC(Thrust specific fuel consumption)** and $n_{overall}$**(Overall efficiency)**.

SFN vs TSFC(By varying FPR and TIT)

-While **TIT** is constant, **SFN** tends to increase when **FPR** increases.

-While **TIT** is constant, **TSFC** tends to decrease when **FPR** increases.

-While **FPR** is constant, **SFN** tends to increase when **TIT** increases.

-While **FPR** is constant, **TSFC** tends to increase when **TIT** increases.

-**The highest SFN** occurs when **FPR** is equal to **1.6** and **TIT** is equal to **2200K**.

-**The lowest TSFC** occurs when **FPR** is equal to **1.6** and **TIT** is equal to **1600K**.

FN vs $n_{overall}$(By varying FPR and TIT)

-While **TIT** is constant, **FN** tends to increase when **FPR** increases.

-While **TIT** is constant, $n_{overall}$ tends to increase when **FPR** increases.

-While **FPR** is constant, **FN** tends to increase when **TIT** increases.

-While **FPR** is constant, $n_{overall}$ tends to decrease when **TIT** increases.

-**The highest FN** occurs when **FPR** is equal to **1.6** and **TIT** is equal to **2200K**.

-**The highest $n_{overall}$** occurs when **BPR** is equal to **1.6** and **TIT** is equal to **1600K**.

4.13 Performance Maps Report(Cruise)

4.13.1 BPR,TIT(Cruise)

In this performance map, **BPR(Bypass ratio)** and **TIT(Turbine inlet temperature)** are chosen as control variables. The map has **BPR** curves increasing from **5** to **12** with each increment of **1** and **TIT** curves increasing from **1400K** to **2000K** with each increment of **100K**.The output variables to be analyzed are **FN(Thrust)**,**SFN(Specific thrust)**,**TSFC(Thrust specific fuel consumption)** and $n_{overall}$**(Overall efficiency)**.

SFN vs TSFC(By varying BPR and TIT)

-While **TIT** is constant, **SFN** tends to decrease when **BPR** increases.

-While **TIT** is constant, **TSFC** tends to decrease when **BPR** increases.

-While **BPR** is constant, **SFN** tends to increase when **TIT** increases.

-While **BPR** is constant, **TSFC** tends to increase when **TIT** increases.

-**The highest SFN** occurs when **BPR** is equal to **5** and **TIT** is equal to **2000K**.

-**The lowest TSFC** occurs when **BPR** is equal to **12** and **TIT** is equal to **1400K**.

FN vs $n_{overall}$(By varying BPR and TIT)

-While **TIT** is constant, **FN** tends to decrease when **BPR** increases.

-While **TIT** is constant, $n_{overall}$ tends to increase when **BPR** increases.

-While **BPR** is constant, **FN** tends to increase when **TIT** increases.

-While **BPR** is constant, $n_{overall}$ tends to decrease when **TIT** increases.

-**The highest FN** occurs when **BPR** is equal to **5** and **TIT** is equal to **2000K**.

-**The highest** $n_{overall}$ occurs when **BPR** is equal to **12** and **TIT** is equal to **1400K**.

4.13.2 BPR,FPR(Cruise)

In this performance map, **BPR(Bypass ratio)** and **FPR(Fan pressure ratio)** are chosen as control variables. The map has **BPR** curves increasing from **5** to **12** with each increment of **1** and **FPR** curves increasing from **1.1** to **1.6** with each increment of **0.1**.The output variables to be analyzed are **FN(Thrust)**,**SFN(Specific thrust)**,**TSFC(Thrust specific fuel consumption)** and $n_{overall}$**(Overall efficiency)**.

SFN vs TSFC(By varying BPR and FPR)

-While **FPR** is constant, **SFN** tends to decrease when **BPR** increases.

-While **FPR** is constant, **TSFC** tends to decrease when **BPR** increases.

-While **BPR** is constant, **SFN** tends to increase when **FPR** increases.

-While **BPR** is constant, **TSFC** tends to decrease when **FPR** increases.

-**The highest SFN** occurs when **BPR** is equal to **5** and **FPR** is equal to **1.6**.

-**The lowest TSFC** occurs when **BPR** is equal to **12** and **FPR** is equal to **1.6**.

FN vs $n_{overall}$ (By varying BPR and FPR)

-While **FPR** is constant, **FN** tends to decrease when **BPR** increases.

-While **FPR** is constant, $n_{overall}$ tends to increase when **BPR** increases.

-While **BPR** is constant, **FN** tends to increase when **FPR** increases.

-While **BPR** is constant, $n_{overall}$ tends to increase when **FPR** increases.

-**The highest FN** occurs when **BPR** is equal to **5** and **FPR** is equal to **1.6**.

-**The highest $n_{overall}$** occurs when **BPR** is equal to **12** and **FPR** is equal to **1.6**.

4.13.3 BPR,OPR(Cruise)

In this performance map, **BPR(Bypass ratio)** and **OPR(Overall pressure ratio)** are chosen as control variables. The map has **BPR** curves increasing from **5** to **12** with each increment of **1** and **OPR** curves increasing from **40** to **55** with each increment of **2.5**.The output variables to be analyzed are **FN(Thrust)**,**SFN(Specific thrust)**,**TSFC(Thrust specific fuel consumption)** and $n_{overall}$**(Overall efficiency**).

SFN vs TSFC(By varying BPR and FPR)

-While **OPR** is constant, **SFN** tends to decrease when **BPR** increases.

-While **OPR** is constant, **TSFC** tends to decrease when **BPR** increases.

-While **BPR** is constant, **SFN** tends to decrease when **OPR** increases.

-While **BPR** is constant, **TSFC** tends to decrease when **OPR** increases.

-**The highest SFN** occurs when **BPR** is equal to **5** and **OPR** is equal to **40**.

-**The lowest TSFC** occurs when **BPR** is equal to **12** and **OPR** is equal to **55**.

FN vs $n_{overall}$ (By varying BPR and FPR)

-While **OPR** is constant, **FN** tends to decrease when **BPR** increases.

-While **OPR** is constant, $n_{overall}$ tends to increase when **BPR** increases.

-While **BPR** is constant, **FN** tends to decrease when **OPR** increases.

-While **BPR** is constant, $n_{overall}$ tends to increase when **OPR** increases.

-**The highest FN** occurs when **BPR** is equal to **5** and **OPR** is equal to **40**.

-**The highest $n_{overall}$** occurs when **BPR** is equal to **12** and **OPR** is equal to **55**.

4.13.4 FPR,TIT(Cruise)

In this performance map, **FPR(Fan pressure ratio)** and **TIT(Turbine inlet temperature)** are chosen as control variables. The map has **FPR** curves increasing from **1.1** to **1.6** with each increment of **0.1** and **TIT** curves increasing from **1400K** to **2000K** with each increment of **100K**.The output variables to be analyzed are **FN(Thrust)**,**SFN(Specific thrust)**,**TSFC(Thrust specific fuel consumption)** and $n_{overall}$(**Overall efficiency**).

SFN vs TSFC(By varying FPR and TIT)

-While **TIT** is constant, **SFN** tends to increase when **FPR** increases.

-While **TIT** is constant, **TSFC** tends to decrease when **FPR** increases.

-While **FPR** is constant, **SFN** tends to increase when **TIT** increases.

-While **FPR** is constant, **TSFC** tends to increase when **TIT** increases.

-**The highest SFN** occurs when **FPR** is equal to **1.6** and **TIT** is equal to **2000K**.

-**The lowest TSFC** occurs when **FPR** is equal to **1.6** and **TIT** is equal to **1400K**.

FN vs $n_{overall}$(By varying FPR and TIT)

-While **TIT** is constant, **FN** tends to increase when **FPR** increases.

-While **TIT** is constant, $n_{overall}$ tends to increase when **FPR** increases.

-While **FPR** is constant, **FN** tends to increase when **TIT** increases.

-While **FPR** is constant, $n_{overall}$ tends to decrease when **TIT** increases.

-**The highest FN** occurs when **FPR** is equal to **1.6** and **TIT** is equal to **2000K**.

-**The highest $n_{overall}$** occurs when **BPR** is equal to **1.6** and **TIT** is equal to **1400K**.

4.14 Cost Analysis

4.14.1 Fuel Costs at Design Conditions

The fuel to be used in the turbofan engine is **JP-8**. The unit price and properties of the fuel are given below:

$$Fuel\colon Jet\ A/A_1, JP-8, Avtur$$

$$\rho_{avg} = 0.8075\ \frac{kg}{L}$$

$$Unit\ cost = 90.04968\ \frac{dollars}{barrel}$$

So,the unit cost in the unit mass basis is

$$c_F = \left(90.04968\ \frac{dollars}{barrel}\right) * \left(\frac{1\ barrel}{159\ L}\right) * \rho_{avg}\left(\frac{kg}{L}\right)$$

$$c_F = 0.7013624628\ \frac{dollars}{kg}$$

Recalling that the fuel flow rates at the design conditions are

$$WF_{take-off} = 2.855\ \frac{kg}{s}$$

$$WF_{cruise} = 1.1439\ \frac{kg}{s}$$

Therefore,the fuels costs rates at the design condions are

$$\dot{C}_F = c_F * WF$$

$$\dot{C}_{F,take-off} = \left(0.7013624628\ \frac{dollars}{kg}\right) * \left(2.855\ \frac{kg}{s}\right) \cong 2.00239\ \frac{dollars}{s}$$

$$\dot{C}_{F,take-off} = 2.00239\ \frac{dollars}{s} = 7208.60\frac{dollars}{h}$$

$$\dot{C}_{F,cruise} = \left(0.7013624628\ \frac{dollars}{kg}\right) * \left(1.1439\ \frac{kg}{s}\right) \cong 0.802288\ \frac{dollars}{s}$$

$$\dot{C}_{F,cruise} = 0.802288\ \frac{dollars}{s} = 2888.24\ \frac{dollars}{h}$$

4.14.2 Fuel Cost Performance Analysis

4.14.2.1 Turbine Inlet Temperature(TIT) Effect

Take-off TIT(Turbine inlet temperature) vs WF(Fuel flow)

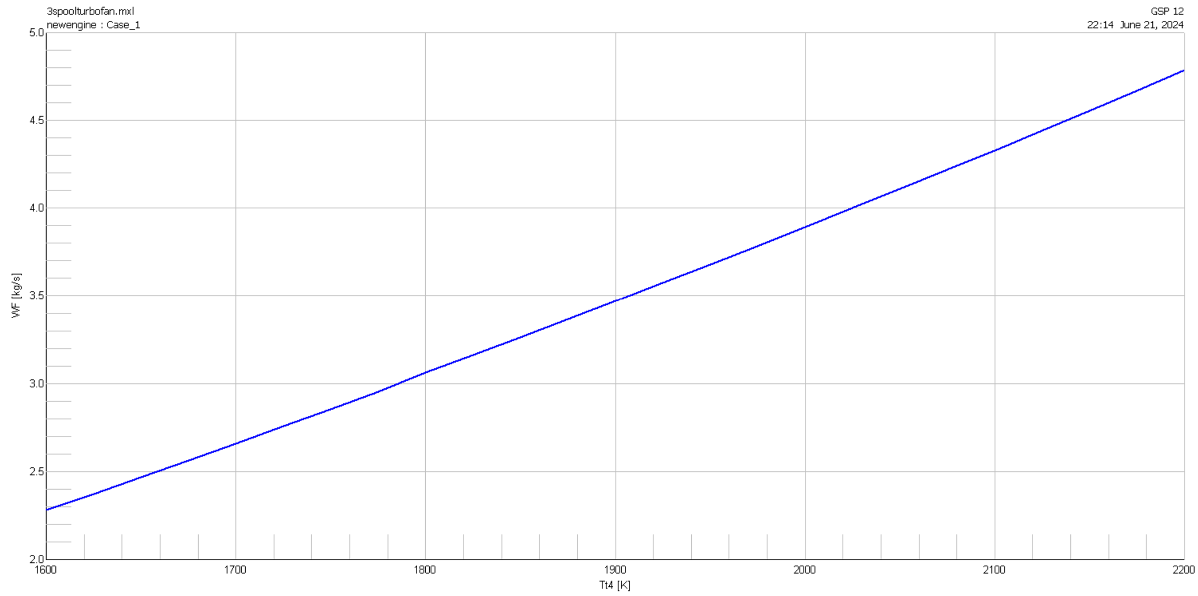

Figure 118:Take-off TIT vs WF

Take-off TIT(Turbine inlet temperature) vs CF(Fuel cost)

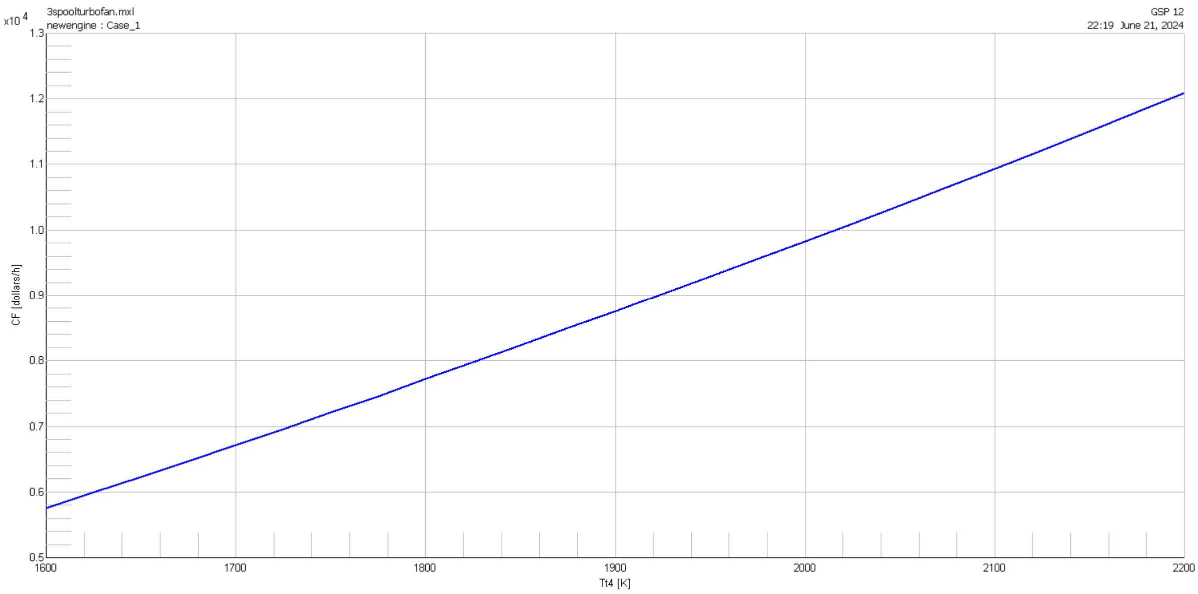

Figure 119:Take-off TIT vs CF

Cruise TIT(Turbine inlet temperature) vs WF(Fuel flow)

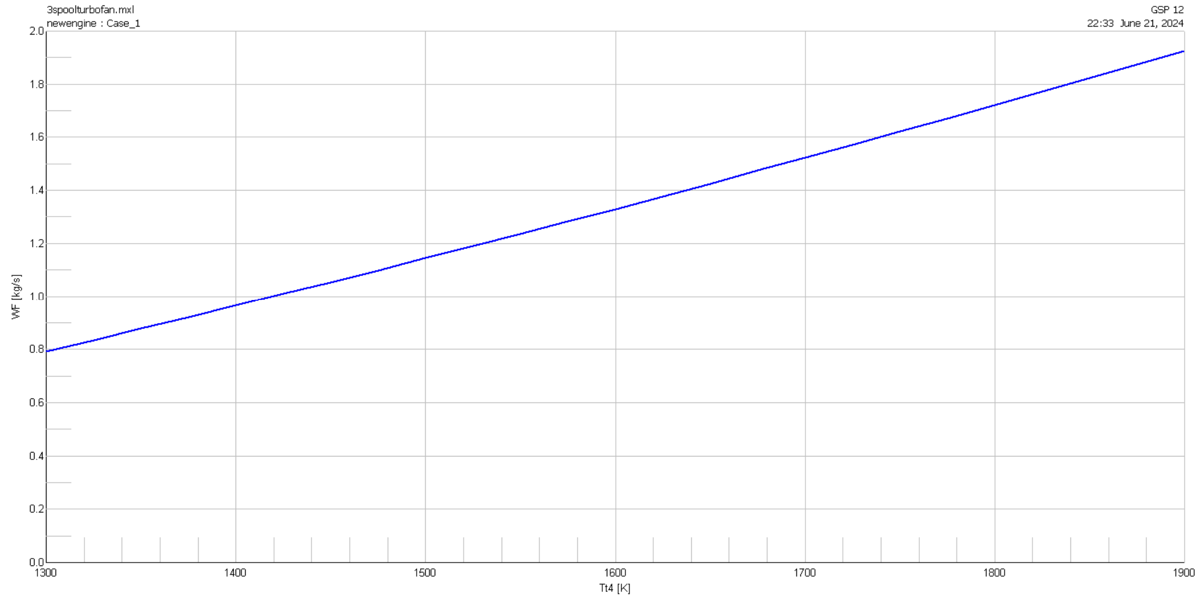

Figure 120:Cruise TIT vs WF

Cruise TIT(Turbine inlet temperature) vs CF(Fuel cost)

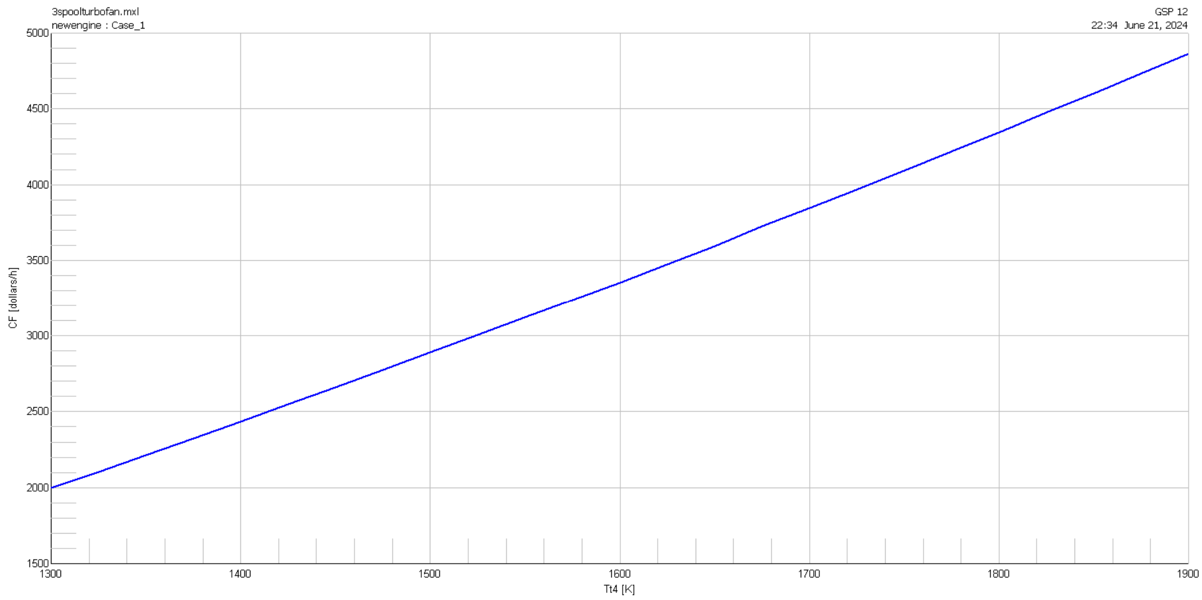

Figure 121:Cruise TIT vs CF

4.14.2.2 Fan Pressure Ratio(π_{fan}) Effect

Take-off π_{fan} (Fan pressure ratio) vs WF(Fuel flow) vs TIT(Turbine inlet temperature)

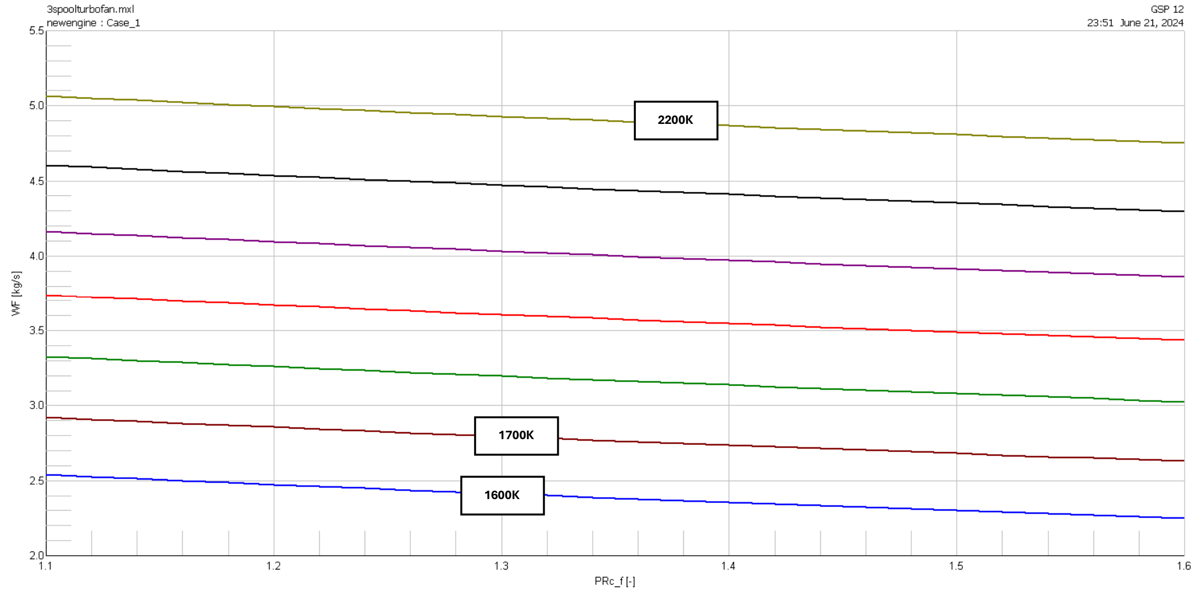

Figure 122:Take-off π_{fan} vs WF vs TIT

Take-off π_{fan} (Fan pressure ratio) vs CF(Fuel cost) vs TIT(Turbine inlet temperature)

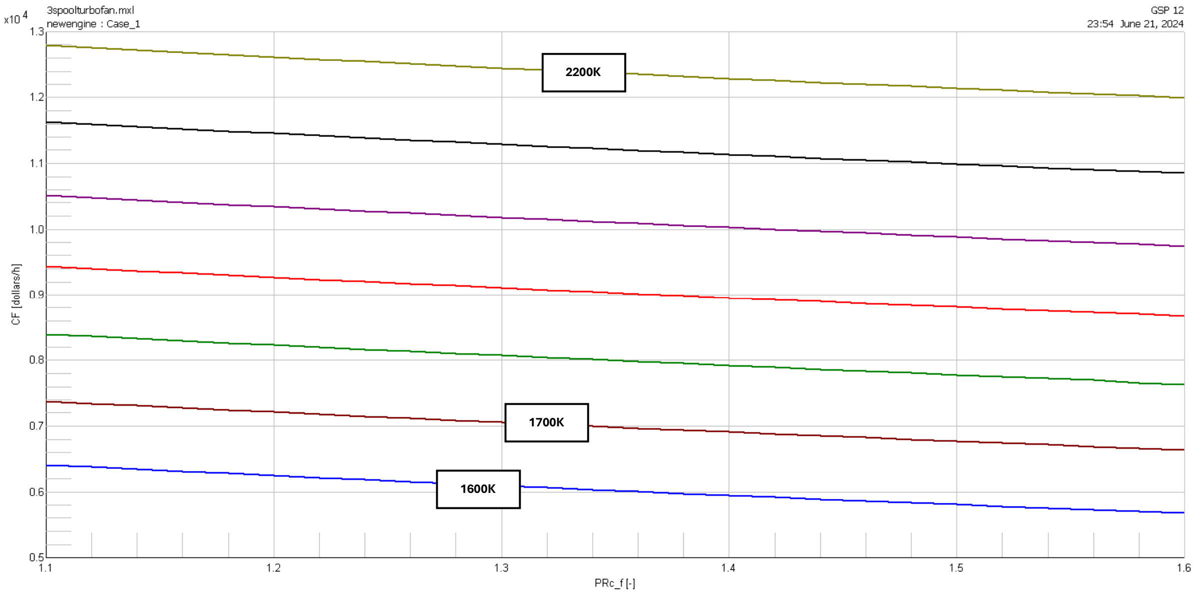

Figure 123:Take-off π_{fan} vs CF vs TIT

Cruise π_{fan} (Fan pressure ratio) vs WF(Fuel flow) vs TIT(Turbine inlet temperature)

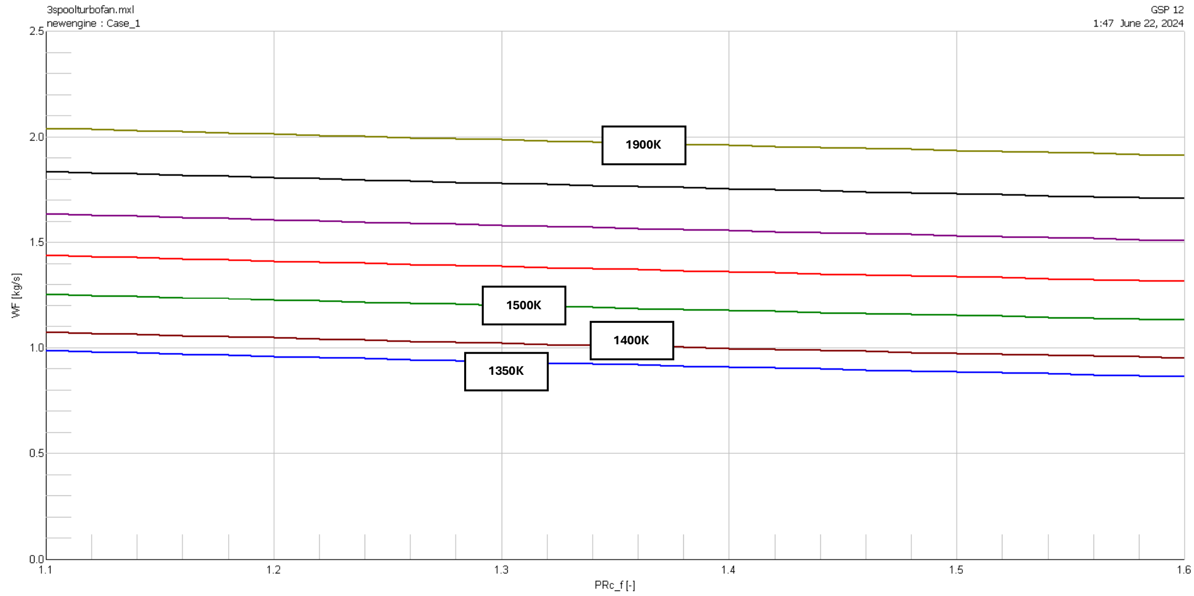

Figure 124:Cruise π_{fan} vs WF vs TIT

Cruise π_{fan} (Fan pressure ratio) vs CF(Fuel cost) vs TIT(Turbine inlet temperature)

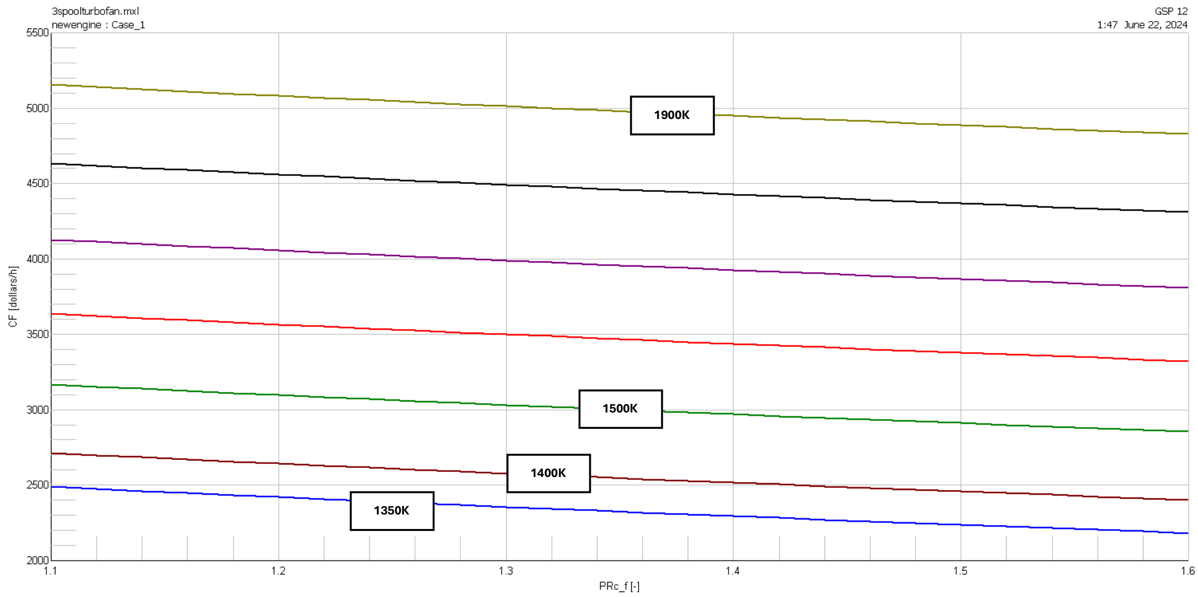

Figure 125: Cruise π_{fan} vs CF vs TIT

4.14.2.3 Overall Pressure Ratio(OPR) Effect

Take-off OPR(Overall pressure ratio) vs WF(Fuel flow)

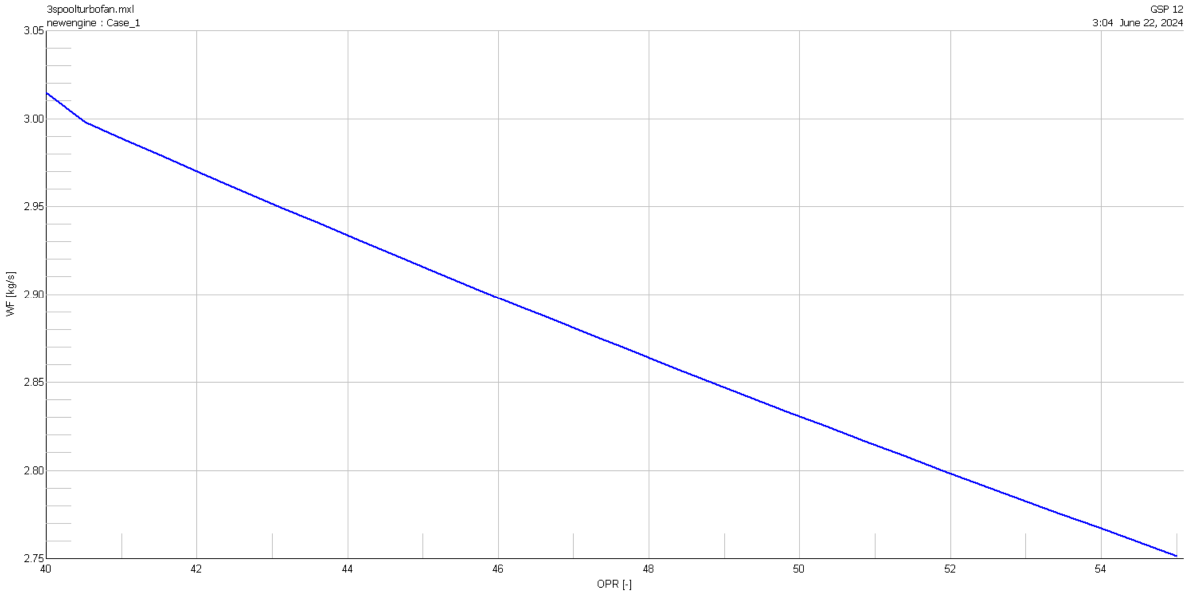

Figure 126:Take-off OPR vs WF

Take-off OPR(Overall pressure ratio) vs CF(Fuel cost)

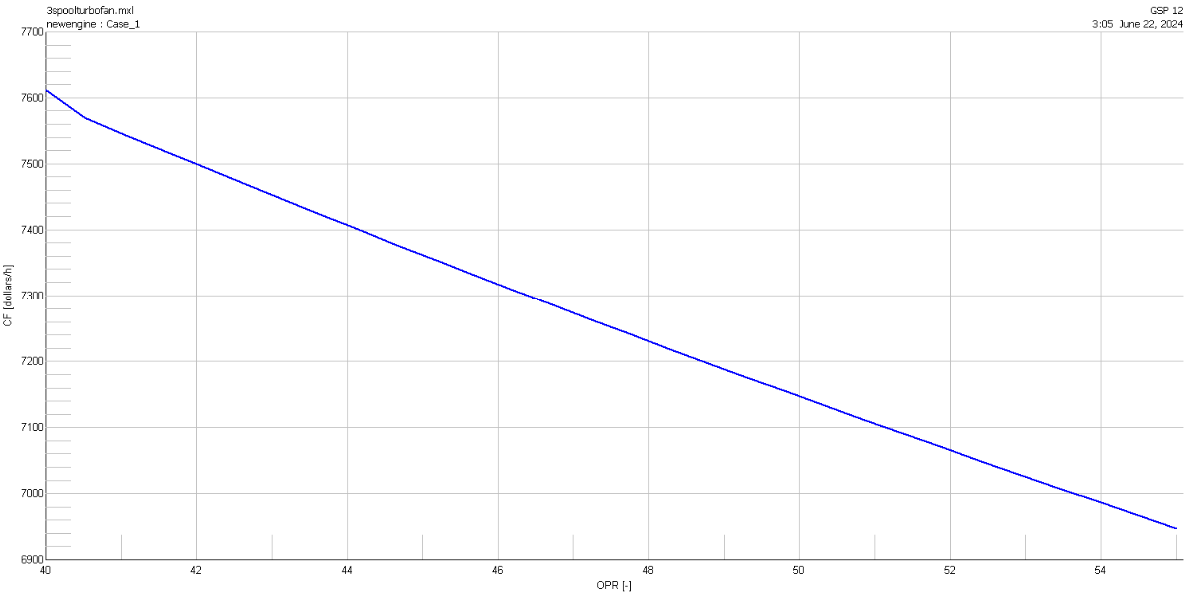

Figure 127:Take-off OPR vs CF

Cruise OPR(Overall pressure ratio) vs WF(Fuel flow)

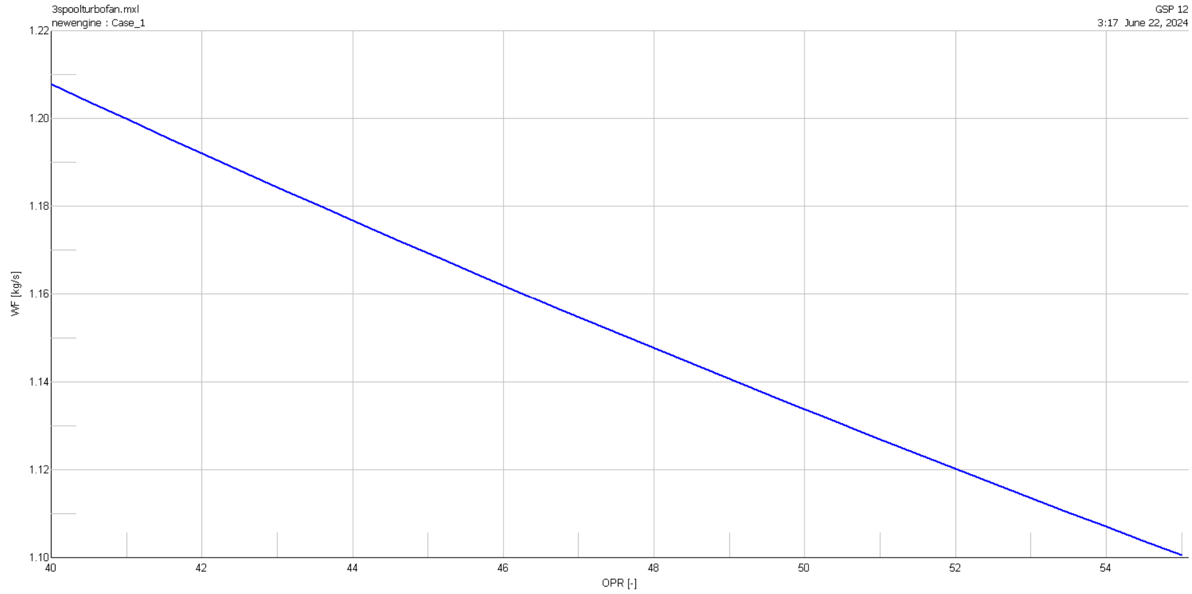

Figure 128:Cruise OPR vs WF

Cruise OPR(Overall pressure ratio) vs CF(Fuel cost)

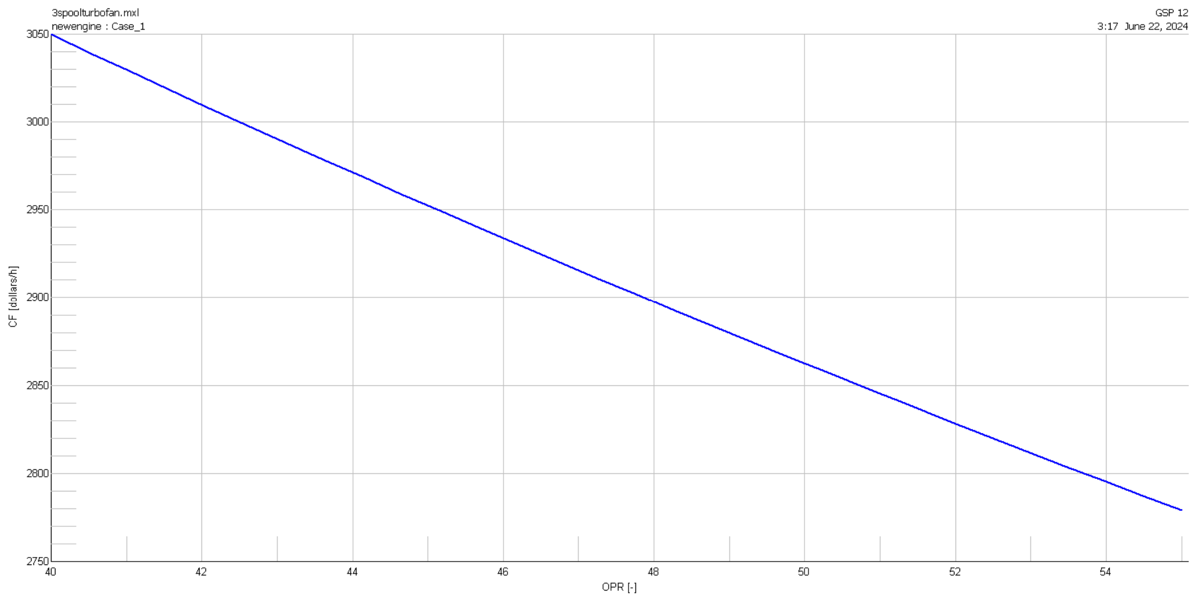

Figure 129:Cruise OPR vs CF

4.14.2.4 Bypass Ratio(BPR) Effect

Take-off BPR(Bypass ratio) vs WF(Fuel flow)

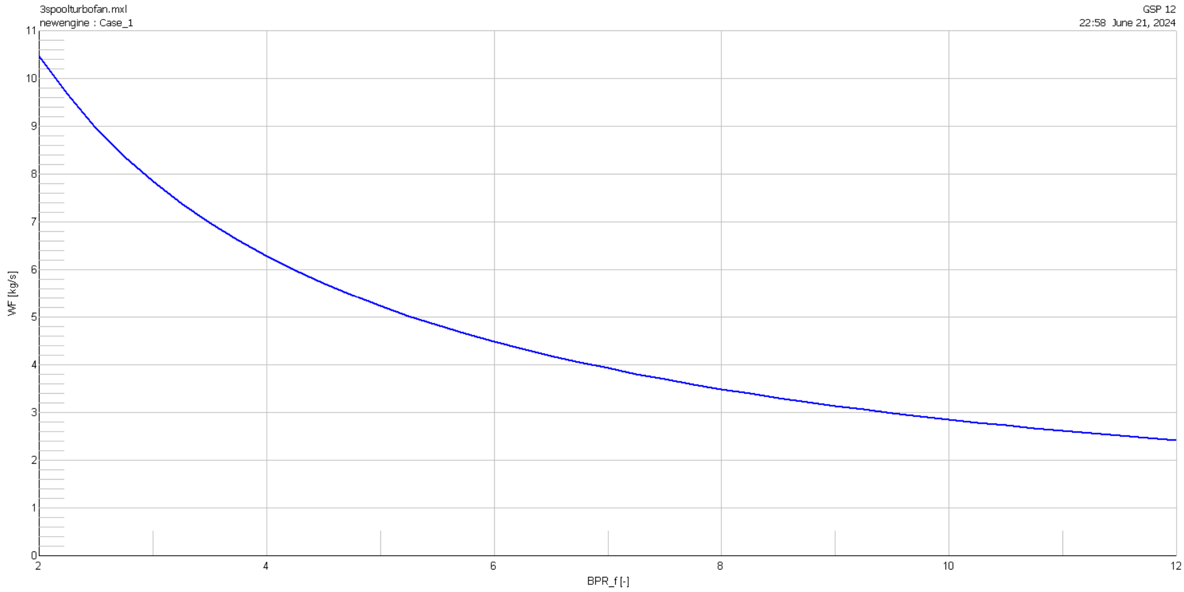

Figure 130:Take-off BPR vs WF

Take-off BPR(Bypass ratio) vs CF(Fuel cost)

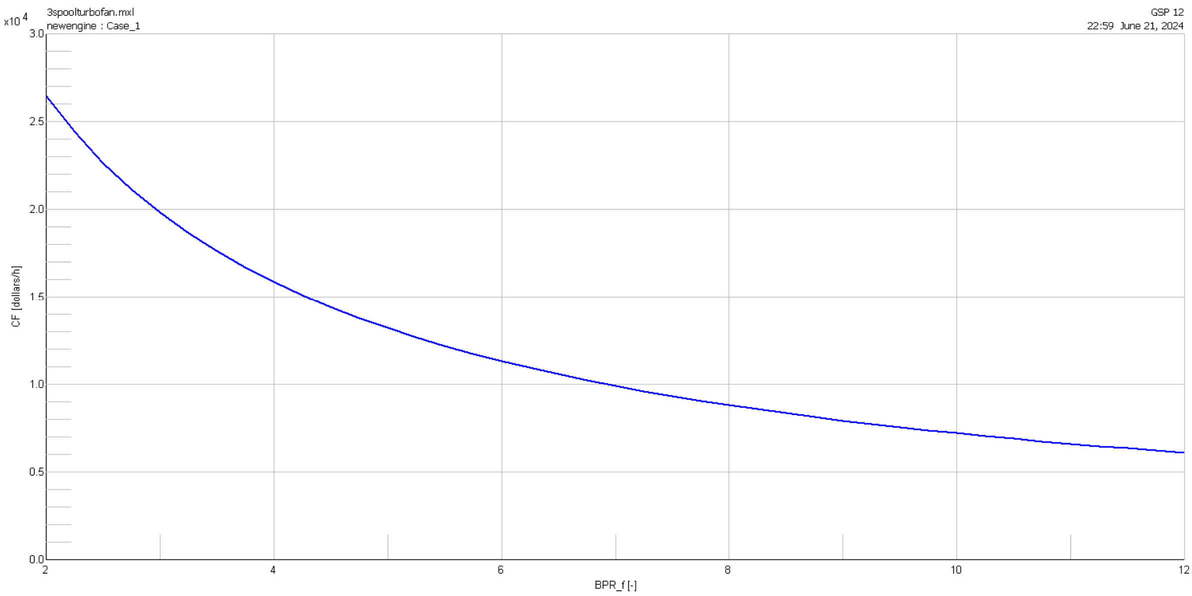

Figure 131:Take-off BPR vs CF

Cruise BPR(Bypass ratio) vs WF(Fuel flow)

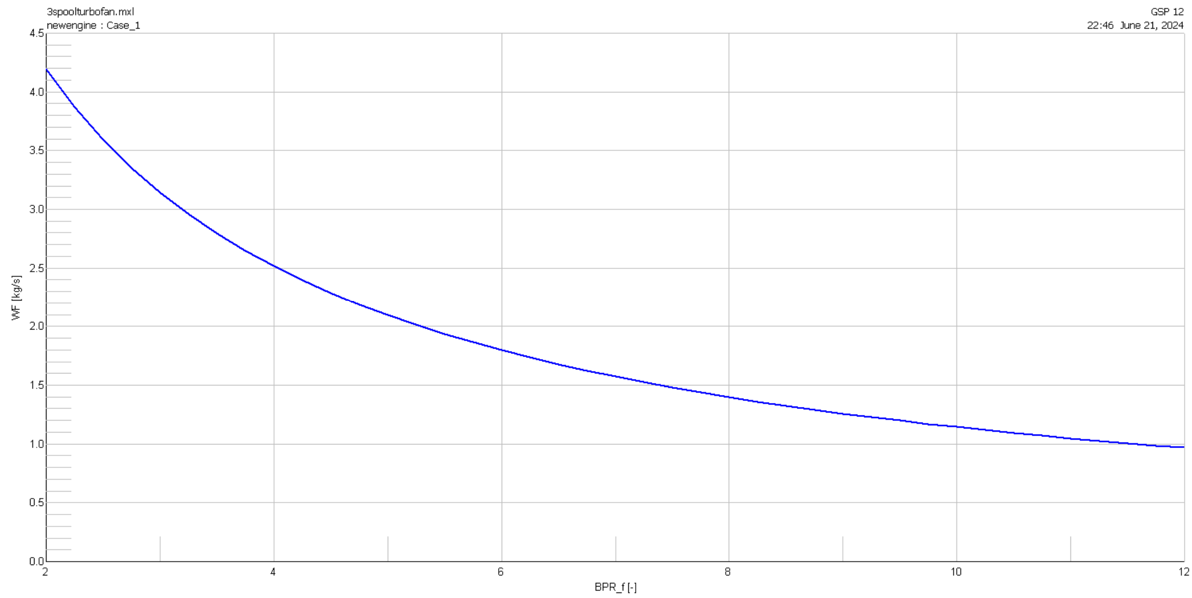

Figure 132:Cruise BPR vs WF

Cruise BPR(Bypass ratio) vs CF(Fuel cost)

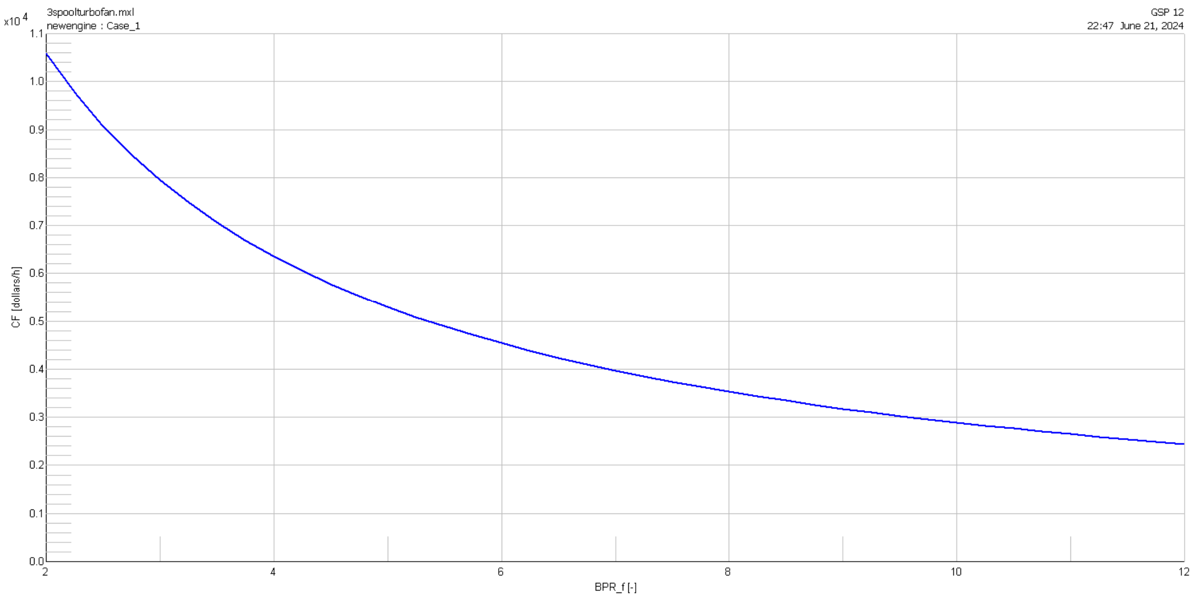

Figure 133:Cruise BPR vs CF

According to the results of the analysis for fuel cost C_F,

-C_F(**Fuel cost per hour**) increases when **TIT** increases.

-C_F remains nearly constant when π_{fan} increases.

-C_F decreases when **OPR** increases.

-C_F decreases when **BPR** increases.

4.14.3 Turbine Blade Material

As a consequence of the **high Overall Pressure Ratio(OPR)**, the **Turbine Inlet Temperature (TIT)** must also be increased to achieve an **optimal Brayton cycle**;that has been shown in the performance analysis for both **take-off and cruise conditions**.However,after reaching **optimum TIT**, the **Thrust specific fuel consumption(TSFC)** starts to increase and **the thermal, the overall and the second law efficiencies** start to drop very quicly. **Figure x** illustrates the historical progression of **TIT** and the advancements in the maximum **permissible metal operating temperature**.

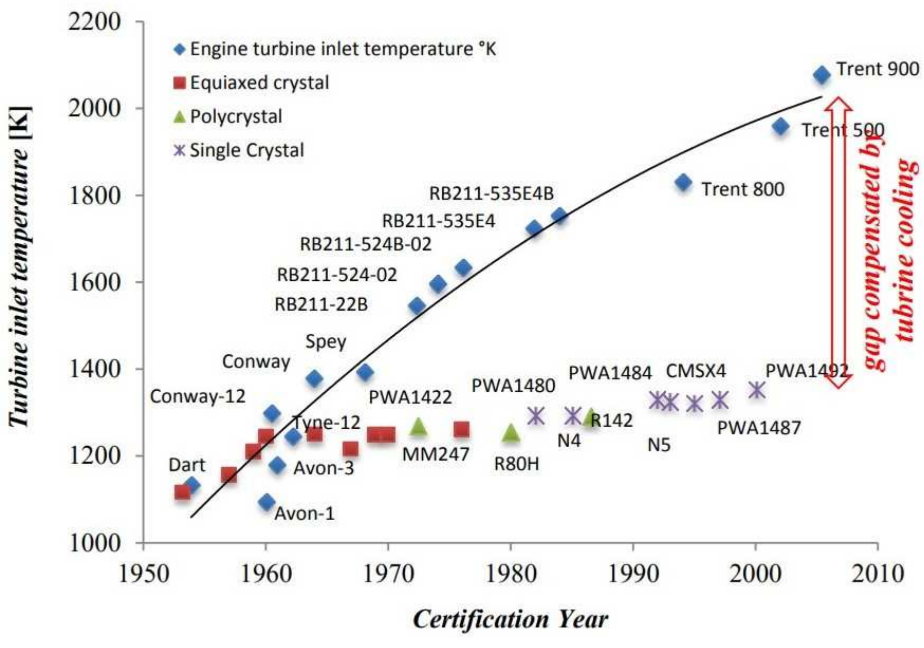

Figure 134:Evolution of turbine inlet temperature and metal operating temperature over the years(from Rolls-Royce jet engine)

The average increase in **TIT** has been about **19 K per year**, which is much higher than the increase in metal operating temperature of around **5 K per year**. Advanced cooling techniques help to manage this difference. When the **TIT** goes much higher than the allowed metal operating temperature, a lot of bleed air is needed to cool the turbine stage, and more expensive materials are needed for turbine blades. Therefore, **TIT** should be **as low as possible** to **reduce material costs**.

5 Conclusions

This project presents a conceptual design for an High Bypass Turbofan Engine. The performance of the turbofan engine is evaluated to determine the optimal conditions for takeoff and cruise. Accurate design is ensured by making appropriate assumptions.

The performance analysis is performed by varying fan,ipc(intermediate pressure compressor) hpc(high pressure compressor) and overall pressure ratios, Altitude, BPR(Bypass ratio), Mach number, Ambient temperature, Ambient pressure, TIT(Turbine inlet temperature) to get better thrust or specific thrust,thrust specific fuel consumption, thermal efficiency, propulsive efficiency,the overall efficiency,and second law efficiency.

From our study, we concluded that the turbofan engine has a high thrust capability with low fuel consumption and high overall efficiency. According to the parametric study, when TIT (Turbine Inlet Temperature) increases, FN(Thrust) and TSFC(Thrust Specific Fuel Consumption) tend to increase, while overall and second law efficiencies tend to decrease. When BPR(Bypass Ratio) increases, SFN(Specific Thrust) and TSFC tend to decrease, while overall and second law efficiencies tend to increase. When FPR(Fan Pressure Ratio) increases, FN and both overall and second law efficiencies tend to increase, and TSFC tends to decrease; however, only a certain range of FPR values are suitable for the engine. When OPR(Overall Pressure Ratio) increases, SFN and TSFC tend to decrease, while overall and second law efficiencies tend to increase. C_F(Fuel cost rate) tends to decrease with increasing BPR, FPR, and OPR, but C_F tends to increase with increasing TIT.

Increases in BPR, FPR, and OPR generally increase the efficiency of the system, but each increase in these parameters increases the amount of shaft work required to operate the system; therefore, for maximum efficiency, TIT should be at the optimum value, but an increase in TIT after the optimum value will cause the efficiency of the system to decrease again. In addition, a high TIT value will increase the production cost of the engine, as it will require turbine blades made of superalloys that can withstand these values, as well as using a lot of fuel.

REFERENCES

[1] Yunus A. Çengel, Michael A. Boles, *Thermodynamics An Engineering Approach Eight Edition*

[2] John D. Anderson Jr., *Modern Compressible Flow with Historical Perspective*

[3] Trent 1000 Poster. Available: https://www.rolls-royce.com/

[4] Trent 900 Poster. Available: https://www.rolls-royce.com/

[5] Trent XWB Poster. Available: : https://www.rolls-royce.com/

[6] https://en.wikipedia.org/wiki/Rolls-Royce_Trent_1000

[7] MATLAB. Available: https://mathworks.com

[8] GSP. Available: https://www.gspteam.com

[9] A. Dik, N. Biten, V. Zaccaria, I. Aslanidou, K.G. Kyprianidis, *Conceptual Design of a 3-Shaft Turbofan Engine with Reduced Fuel Consumption for 2025*

[10] Ahmed El-Sayed, Islam Mohamed Zaid, Mohamed Ehab, Abdullah M. Mahrous, *Performance Analysis of High Bypass Turbofan Engine Trent 1000-A**

[11] Ahmed El-Sayed, Mohamed S Emeara, Mohamed A. El Habet, *Performance Analysis of High Bypass Ratio Turbofan Aeroengine*

[12] T.Grönstedt, *Conceptual Aero Engine Design Modeling, Engine Sizing*

[13] A. F. El Sayed, *Fundamentals of aircraft and rocket propulsion*

[14] Feijia Yin, Arvind Gangoli Rao, *Performance Analysis of an Aero Engine with Interstage Turbine Burner*

[15] https://jet-a1-fuel.com/

A MATLAB Scripts

A1 Regression

```
format long
%Regression analysis(Take-off)
T_take_off = [291.75; 332.91; 655.49; 926.62; 1750; 1525.52; 1268.08; ...
    900.42; 778.02; 296.78];
T_cruise = [247.96; 283.01; 561.23; 799.94; 1500; 1299.60; 1071.31; ...
    744.49; 638.41; 238.09];
gamma_take_off = [1.40014; 1.398817; 1.369393; 1.341981; 1.284516; ...
    1.290748; 1.301391; 1.326321; 1.338205; 1.40012];
gamma_cruise = [1.400917; 1.40034; 1.380114; 1.353659; 1.295557; ...
    1.303199; 1.316155; 1.344988; 1.357087; 1.40267];
T_take_off = sort(T_take_off);
T_cruise = sort(T_cruise);
gamma_take_off = sort(gamma_take_off,'descend');
gamma_cruise = sort(gamma_cruise,'descend');

figure(1)
plot(T_take_off,gamma_take_off,'*')
title('take-off')
xlabel('temperature[K]')
ylabel('specific heat ratio')
grid on

figure(2)
plot(T_cruise,gamma_cruise,'*')
title('cruise')
xlabel('temperature[K]')
ylabel('specific heat ratio')
grid on
```

A2 Specific Heat Ratio Functions

```
function cp = cp_take_off(T)
%take-off specific heat function
%determine specific heat ratio
gamma_take_off = (-8.630329896*10^-5).*T + 1.42046792;
R = 0.28705; %kJ/kg*K,ideal gas constant of air
%determine specific heat
cp = (R*gamma_take_off)./(gamma_take_off - 1);
end

function cp = cp_cruise(T)
%cruise specific heat function
%determine specific heat ratio
gamma_cruise = (-9.122439091*10^-5).*T + 1.422829055;
R = 0.28705; %kJ/kg*K,ideal gas constant of air
%determine specific heat
cp = (R*gamma_cruise)./(gamma_cruise - 1);
end
```

A3 Second-Law Analysis Take-off

```
%Take-off second law analysis
%Ambient conditions
T0 = 288.15; %K
s0 = 6.82989; %kJ/kg*K
z = 0; %m,altitude
g = 9.81; %m/s^2,gravity
%Total temperatures of states(K)
T1 = 291.75; T2 = 291.75; T3 = 332.91; T4 = 332.91; T5 = 655.49;
T6 = 926.62; T7 = 1750.00; T8 = 1525.52; T9 = 1268.08; T10 = 900.42;
T11 = 900.42; T12 = 900.42; T13 = 332.91; T14 = 332.91;
%Temperature vector(K)
T = [T1 T2 T3 T4 T5 T6 T7 T8 T9 T10 T11 T12 T13 T14];
T = T';
%Entropies of states(kJ/kg*K)
s1 = 6.82989; s2 = 6.83568; s3 = 6.84441; s4 = 6.85316;
s5 = 6.89982; s6 = 6.92907; s7 = 7.83872; s8 = 7.85311;
s9 = 7.87250; s10 = 7.91018; s11 = 7.91598; s12 = 7.91018;
s13 = 6.85316; s14 = 6.84441;
%Entropy vector(kJ/kg*K)
s = [s1 s2 s3 s4 s5 s6 s7 s8 s9 s10 s11 s12 s13 s14];
s = s';
%exergies of fluid stream at sections
Tavg = (T+T0)/2; %mean temperature vector(K)
psi = cp_take_off(Tavg).*(T-T0) - T0.*(s-s0) + g*z/1000;
psi1 = psi(1); psi2 = psi(2); psi3 = psi(3); psi4 = psi(4);
psi5 = psi(5); psi6 = psi(6); psi7 = psi(7); psi8 = psi(8);
psi9 = psi(9); psi10 = psi(10); psi11 = psi(11); psi12 = psi(12);
psi13 = psi(13); psi14 = psi(14);
%second law efficiencies of the components
%inlet
```

```
eta_inlet = psi2./psi1;
%fan
m0_dot = 1210; %kg/s,total mass flow rate
W_fan_dot = 50071.76; %kJ/s,shaft work by fan
w_fan = W_fan_dot./m0_dot; %kJ/kg,shaft work by fan
eta_fan = (psi3 - psi2)./w_fan;
%cold core duct
eta_ccd = psi4./psi3; %efficiency of ccd
%ipc
bpr = 10; %bypass ratio
mc_dot = m0_dot./(bpr+1); %kg/s,core mass flow rate
mb_dot = bpr.*mc_dot; %kg/s,bypass mass flow rate
W_ipc_dot = 36576.83; %kJ/s,shaft work by ipc
w_ipc = W_ipc_dot./mc_dot; %kJ/kg,shaft work by ipc
eta_ipc = (psi5 - psi4)./w_ipc; %efficiency of ipc
%hpc
W_hpc_dot = 32693.42; %kJ/s,shaft work by hpc
w_hpc = W_hpc_dot./mc_dot; %kJ/kg,shaft work by hpc
eta_hpc = (psi6 - psi5)./w_hpc; %efficiency of hpc
%combustor
mf_dot = 2.855; %kg/s,fuel flow rate
LHV = 43031; %kJ/kg,lower heating value of fuel
eta_c = 0.99; %combustion efficiency
eta_cb = (mc_dot.*(psi7 - psi6))./(mf_dot.*eta_c.*LHV); %efficiency of cb
%hpt
W_hpt_dot = 32726.12; %kJ/s,shaft work to hpt
w_hpt = W_hpt_dot./mc_dot; %kJ/kg,shaft work to hpt
eta_hpt = 1 - T0.*(s8 - s7)./(psi7 - psi8); %efficiency of hpt
%ipt
W_ipt_dot = 36613.44; %kJ/s,shaft work to ipt
w_ipt = W_ipt_dot./mc_dot; %kJ/kg,shaft work to ipt
eta_ipt = 1 - T0.*(s9 - s8)./(psi8 - psi9); %efficiency of ipt
%lpt
W_lpt_dot = 50121.86; %kJ/s,shaft work to lpt
w_lpt = W_lpt_dot./mc_dot; %kJ/kg,shaft work to ipt
eta_lpt = 1 - T0.*(s10 - s9)./(psi9 - psi10); %efficiency of lpt
%hot core duct
eta_hcd = psi11./psi10; %efficiency of hcd
%hot nozzle
T_hn = 778.02; %K,static nozzle exit temperature
V_hn = 531.1; %m/s,hot nozzle velocity
eta_hn = (1/2000).*(V_hn.^2)./psi12; %efficiency of hn
%bypass duct
eta_bd = psi13./psi3; %efficiency of bd
%cold nozzle
T_cn = 296.78; %K,static nozzle exit temperature
V_cn = 269.5; %m/s,cold nozzle velocity
eta_cn = (1/2000).*(V_cn.^2)./psi14; %efficiency of cn
```

A4 Second-Law Analysis Cruise

```
%Cruise second law analysis
%Ambient conditions
T0 = 216.65; %K
s0 = 7.01927; %kJ/kg*K
z = 12000; %m,altitude
g = 9.81; %m/s^2,gravity
%Total temperatures of states(K)
T1 = 247.96; T2 = 247.96; T3 = 283.01; T4 = 283.01; T5 = 561.23;
T6 = 799.94; T7 = 1500; T8 = 1299.60; T9 = 1071.31; T10 = 744.49;
T11 = 744.49; T12 = 744.49; T13 = 283.01; T14 = 283.01;
%Temperature vector(K)
T = [T1 T2 T3 T4 T5 T6 T7 T8 T9 T10 T11 T12 T13 T14];
T = T';
%Entropies of states(kJ/kg*K)
s1 = 7.01927; s2 = 7.02486; s3 = 7.03360; s4 = 7.04234;
s5 = 7.08881; s6 = 7.11794; s7 = 7.96966; s8 = 7.98425;
s9 = 8.00391; s10 = 8.04289; s11 = 8.04870; s12 = 8.04289;
s13 = 7.04234; s14 = 7.03360;
%Entropy vector(kJ/kg*K)
s = [s1 s2 s3 s4 s5 s6 s7 s8 s9 s10 s11 s12 s13 s14];
s = s';
%exergies of fluid stream at sections
Tavg = (T+T0)/2; %mean temperature vector(K)
psi = cp_cruise(Tavg).*(T-T0) - T0.*(s-s0) + g*z/1000;
psi1 = psi(1); psi2 = psi(2); psi3 = psi(3); psi4 = psi(4);
psi5 = psi(5); psi6 = psi(6); psi7 = psi(7); psi8 = psi(8);
psi9 = psi(9); psi10 = psi(10); psi11 = psi(11); psi12 = psi(12);
psi13 = psi(13); psi14 = psi(14);
%second law efficiencies of the components
%inlet
eta_inlet = psi2./psi1;
%fan
m0_dot = 600; %kg/s,total mass flow rate
W_fan_dot = 21104.12; %kJ/s,shaft work by fan
w_fan = W_fan_dot./m0_dot; %kJ/kg,shaft work by fan
eta_fan = (psi3 - psi2)./w_fan;
%cold core duct
eta_ccd = psi4./psi3; %efficiency of ccd
%ipc
bpr = 10; %bypass ratio
mc_dot = m0_dot./(bpr+1); %kg/s,core mass flow rate
mb_dot = bpr.*mc_dot; %kg/s,bypass mass flow rate
W_ipc_dot = 15459.55; %kJ/s,shaft work by ipc
w_ipc = W_ipc_dot./mc_dot; %kJ/kg,shaft work by ipc
eta_ipc = (psi5 - psi4)./w_ipc; %efficiency of ipc
%hpc
W_hpc_dot = 13935.63; %kJ/s,shaft work by hpc
w_hpc = W_hpc_dot./mc_dot; %kJ/kg,shaft work by hpc
eta_hpc = (psi6 - psi5)./w_hpc; %efficiency of hpc
%combustor
mf_dot = 1.1439; %kg/s,fuel flow rate
LHV = 43031; %kJ/kg,lower heating value of fuel
```

```
eta_c = 0.99; %combustion efficiency
eta_cb = (mc_dot.*(psi7 - psi6))./(mf_dot.*eta_c.*LHV); %efficiency of cb
%hpt
W_hpt_dot = 13949.57; %kJ/s,shaft work to hpt
w_hpt = W_hpt_dot./mc_dot; %kJ/kg,shaft work to hpt
eta_hpt = 1 - T0.*(s8 - s7)./(psi7 - psi8); %efficiency of hpt
%ipt
W_ipt_dot = 15475.02; %kJ/s,shaft work to ipt
w_ipt = W_ipt_dot./mc_dot; %kJ/kg,shaft work to ipt
eta_ipt = 1 - T0.*(s9 - s8)./(psi8 - psi9); %efficiency of ipt
%lpt
W_lpt_dot = 21125.23; %kJ/s,shaft work to lpt
w_lpt = W_lpt_dot./mc_dot; %kJ/kg,shaft work to ipt
eta_lpt = 1 - T0.*(s10 - s9)./(psi9 - psi10); %efficiency of lpt
%hot core duct
eta_hcd = psi11./psi10; %efficiency of hcd
%hot nozzle
T_hn = 638.41; %K,static nozzle exit temperature
V_hn = 484.3; %m/s,hot nozzle velocity
eta_hn = (1/2000).*(V_hn.^2)./psi12; %efficiency of hn
%bypass duct
eta_bd = psi13./psi3; %efficiency of bd
%cold nozzle
T_cn = 238.09; %K,static nozzle exit temperature
V_cn = 300.2; %m/s,cold nozzle velocity
eta_cn = (1/2000).*(V_cn.^2)./psi14; %efficiency of cn
```

A5 Brayton Cycle T-s Diagram

```
%T-s diagram
%Take-off Total temperatures of states(K)
T1_take_off = 291.75; T2_take_off = 291.75; T3_take_off = 332.91;
T4_take_off = 332.91; T5_take_off = 655.49; T6_take_off = 926.62;
T7_take_off = 1750.00; T8_take_off = 1525.52; T9_take_off = 1268.08;
T10_take_off = 900.42; T11_take_off = 900.42; T12_take_off = 900.42;
%Cruise Total temperatures of states(K)
T1_cruise = 247.96; T2_cruise = 247.96; T3_cruise = 283.01;
T4_cruise = 283.01; T5_cruise = 561.23; T6_cruise = 799.94;
T7_cruise = 1500; T8_cruise = 1299.60; T9_cruise = 1071.31;
T10_cruise = 744.49; T11_cruise = 744.49; T12_cruise = 744.49;
%Take-off Temperature vector(K)
T_take_off = [T1_take_off T2_take_off T3_take_off T4_take_off ...
    T5_take_off T6_take_off T7_take_off T8_take_off T9_take_off ...
    T10_take_off T11_take_off T12_take_off];
T_take_off = T_take_off';
%Cruise Temperature vector(K)
T_cruise = [T1_cruise T2_cruise T3_cruise T4_cruise T5_cruise ...
   T6_cruise T7_cruise T8_cruise T9_cruise T10_cruise T11_cruise ...
   T12_cruise];
%Take-off Entropies of states(kJ/kg*K)
s1_take_off = 6.82989; s2_take_off = 6.83568; s3_take_off = 6.84441;
s4_take_off = 6.85316; s5_take_off = 6.89982; s6_take_off = 6.92907;
s7_take_off = 7.83872; s8_take_off = 7.85311; s9_take_off = 7.87250;
```

```
s10_take_off = 7.91018; s11_take_off = 7.91598; s12_take_off = 7.91018;
%Take-off Entropy vector(kJ/kg*K)
s_take_off = [s1_take_off s2_take_off s3_take_off s4_take_off ...
    s5_take_off s6_take_off s7_take_off s8_take_off s9_take_off ...
    s10_take_off s11_take_off s12_take_off];
s_take_off = s_take_off';
%Cruise Entropies of states(kJ/kg*K)
s1_cruise = 7.01927; s2_cruise = 7.02486; s3_cruise = 7.03360;
s4_cruise = 7.04234; s5_cruise = 7.08881; s6_cruise = 7.11794;
s7_cruise = 7.96966; s8_cruise = 7.98425; s9_cruise = 8.00391;
s10_cruise = 8.04289; s11_cruise = 8.04870; s12_cruise = 8.04289;
%Cruise Entropy vector(kJ/kg*K)
s_cruise = [s1_cruise s2_cruise s3_cruise s4_cruise s5_cruise ...
    s6_cruise s7_cruise s8_cruise s9_cruise s10_cruise s11_cruise ...
    s12_cruise];
%Plot take-off T-s diagram
figure(1)
plot(s_take_off,T_take_off,'*-')
title('take-off')
xlabel('entropy(kJ/kg*K)')
ylabel('temperature(K)')
grid on
%Plot cruise T-s diagram
figure(2)
plot(s_cruise,T_cruise,'*-')
title('cruise')
xlabel('entropy(kJ/kg*K)')
ylabel('temperature(K)')
grid on
```